



5-2000

An investigation of the melt blown web defect known as "shot" using metallocene and ziegler-natta based polypropylene resins

Imad M. Qashou

Follow this and additional works at: https://trace.tennessee.edu/utk_gradthes

Recommended Citation

Qashou, Imad M., "An investigation of the melt blown web defect known as "shot" using metallocene and ziegler-natta based polypropylene resins. " Master's Thesis, University of Tennessee, 2000.
https://trace.tennessee.edu/utk_gradthes/9471

This Thesis is brought to you for free and open access by the Graduate School at TRACE: Tennessee Research and Creative Exchange. It has been accepted for inclusion in Masters Theses by an authorized administrator of TRACE: Tennessee Research and Creative Exchange. For more information, please contact trace@utk.edu.

To the Graduate Council:

I am submitting herewith a thesis written by Imad M. Qashou entitled "An investigation of the melt blown web defect known as "shot" using metallocene and ziegler-natta based polypropylene resins." I have examined the final electronic copy of this thesis for form and content and recommend that it be accepted in partial fulfillment of the requirements for the degree of Master of Science, with a major in Polymer Engineering.

J. E. Spruiell, Major Professor

We have read this thesis and recommend its acceptance:

Robert Beson, Paul Phillips

Accepted for the Council:

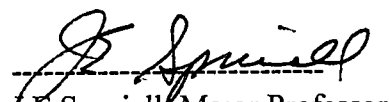
Carolyn R. Hodges

Vice Provost and Dean of the Graduate School

(Original signatures are on file with official student records.)

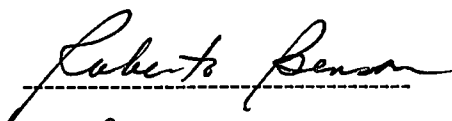
To the Graduate Council:

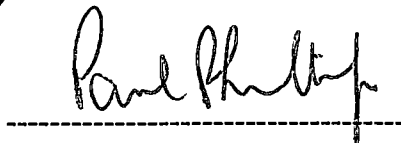
I am submitting herewith a thesis written by IMAD M. QASHOU entitled "AN INVESTIGATION OF THE MELT BLOWN WEB DEFECT KNOWN AS "SHOT" USING METALLOCENE AND CATALYZED POLYPROPYLENE RESINS." I have examined the final copy of this thesis for form and content and recommend that it be accepted in partial fulfillment of the requirements for the degree of Master of Science, with a major in Polymer Engineering.




J.E. Spruiell, Major Professor

We have read this thesis
and recommend its acceptance





Accepted for the Council



Associate Vice Chancellor
And Dean of the Graduate School

**AN INVESTIGATION OF THE MELT BLOWN WEB
DEFECT KNOWN AS "SHOT" USING METALLOCENE
AND ZIEGLER-NATTA BASED POLYPROPYLENE
RESINS**

**A THESIS PRESENTED FOR THE
MASTER OF SCIENCE
DEGREE
THE UNIVERSITY OF TENNESSEE, KNOXVILLE**

**IMAD M. QASHOU
MAY 2000**

*To my parents,
my brothers and sisters.
To Nadia*

ACKNOWLEDGEMENTS

I would like to express my sincere and deepest gratitude to my major professor Dr. J. E. Spruiell for his guidance, advice, help and continuous encouragement throughout the project.

I am indebted to Exxon Mobil Chemical Company for funding this project and supplying the resins and resin characteristics. I am particularly indebted to Dr. C.Y. Cheng, the project director, for his insight, helpful suggestions, and rapid response when inquiries were made. He also arranged for the GPC measurements on the webs that are reported in the thesis.

I am also grateful to Dr. M.W. Milligan for allowing me to use the melt blowing line in his laboratory to process the different resins used in this thesis. His suggestions about the different techniques of shot analysis, fiber diameter measurements and discussions of shot formation processes were invaluable. I am particularly grateful to Mr. Todd W. Taylor for helping me get up to speed in the melt blown area, for help in using the WebPro system, and in fiber diameter measurement techniques. He also helped with processing the resins studied in this thesis.

Sincere thanks are also extended to professors P.J. Phillips and R.A. Benson for serving on my committee and providing suggestions and insightful discussions. The help and aid provided by other faculty members and by my fellow graduate students, over the period of my study, is highly appreciated.

ABSTRACT

An extensive experimental investigation was undertaken to study the influence of processing parameters and resin type on the production of shot in the melt blowing process. Both early generation commercial metallocene and conventional Ziegler-Natta based polypropylene resins were used in this investigation.

In addition to the base metallocene and Ziegler-Natta resins, the effect of blending these resins together was studied. Finally, the effect of adding nucleating agents to the base metallocene resin on shot production was investigated.

The study showed that the early generation commercial metallocene resin used in this research produced more shot than conventional resins with all other processing conditions being equal. Die air pressure had a strong effect on the shot production; an increase in die air pressure produced more shot in the web sample. Processing temperature produced a similar trend; an increase in process temperature produced more shot in the web sample. Blending Ziegler-Natta polypropylene into a metallocene based polypropylene tended to decrease the shot formation in proportion to the percentage of the conventional resin.

Examination of the crystallization kinetics of the base resin indicated that the Ziegler-Natta base resin crystallized faster under quiescent conditions than the metallocene base resin. Similarly, measurements on the blends indicated a gradual

increase of crystallization kinetics from that of the metallocene resin to that of the Ziegler-Natta resin.

In order to investigate whether the differences in crystallization kinetics were responsible for the differences in shot production, nucleating agents were added to a base resin to increase the rate of base resin crystallization. Nucleating agents had very little effect on the production of shot. Laboratory tests indicated that these additives did provide the accelerated crystallization kinetics in quiescent conditions, however, this did not produce the desired reduction in shot formation.

TABLE OF CONTENTS

CHAPTER	PAGE
1. INTRODUCTION.....	1
2. BACKGROUND AND LITERATURE REVIEW.....	8
2.1 Nonwoven Classification and Technology.....	8
2.2 Development and Description of the Melt Blowing Process.....	11
2.2.1 Historical Perspective.....	12
2.2.2 Process Description.....	15
2.3 Polypropylenes for the Melt Blowing Process.....	17
2.3.1 Basic Structure of Polypropylene.....	17
2.3.2 Requirements for Melt Blowing.....	19
2.3.3 Comparison of Conventional Ziegler-Natta and Metallocene Polypropylene.....	20
2.3.4 Polypropylene Crystalline Forms.....	30
2.3.4.1 α -Monoclinic Form.....	32
2.3.4.2 β -Pseudohexagonal Form.....	33
2.3.4.3 γ -Orthorhombic Form.....	34
2.3.4.4 Conformationally Disordered or Smectic Form.....	35
2.4 Properties of Melt Blown Webs.....	38
2.4.1 Factors Affecting the Physical Properties.....	39
2.4.2 Factors Affecting Shot Formation.....	52
3. EXPERIMENTAL APPARTUS AND PROCEDURES.....	62

3.1 Materials.....	62
3.1.1 First Part: Blends of Metallocene Catalyzed PP and Conventional Ziegler-Natta PP.....	62
3.1.2 Second Part: Nucleated Resins.....	63
3.2 Fabric Processing.....	65
3.3 Processing Conditions.....	67
3.4 Melt-Blown Web Creation.....	69
3.5 Analysis of Web Samples.....	71
3.5.1 Average Fiber Diameter Determination.....	71
3.5.2 Number of Shot per Area Determination.....	77
3.5.3 Effect of Processing Parameters on WebPro Shot Detection.....	85
3.6 Thermal Analysis.....	86
3.7 Orientation.....	88
3.8 Wide Angle X-ray Scattering (WAXS).....	90
3.9 Melt Flow Rate.....	91
4. RESULTS AND DISCUSSION.....	92
4.1 Investigation of the Effect of Blending Metallocene and Ziegler-Natta Catalyzed Resins on Shot Production.....	94
4.2 Investigation of the Effect of Nucleating Agents on Shot Production.....	110
4.3 Molecular Weights and Polydispersity Results.....	124
4.4 Molecular Orientation of the Fibers.....	129

5. CONCLUSIONS AND FUTURE WORK.....	133
5.1 Conclusions.....	133
5.2 Future Work.....	136
REFERENCES.....	138
APPENDIX SEM Images Of Shot Particles and Melt Blown Fibers.....	144
VITA.....	150

LIST OF FIGURES

FIGURE	PAGE
1.1 Schematic of the Melt Blowing Process.	2
1.2 SEM Image of a Shot Particle.....	4
2.1 Flow Diagram of Classification of Nonwoven Fabric Formation Techniques...	9
2.2 Comparison of Conventional and Metallocene Catalyst.....	21
2.3 Comparison of Conventional and Metallocene Polypropylene Fibers at Different Relative Draw Force.....	27
2.4 Comparison of Conventional and Metallocene Polypropylene at Different Levels of Hydrohead and Air Permeability.....	29
2.5 Crystal Structures of Isotactic Polypropylene.....	31
2.6 Comparison of α -iPP, aPP and the Smectic iPP Structure.....	36
3.1 Schematic of the Melt Blowing Facility at the University of Tennessee.....	66
3.2 Experimental Melt Blowing Die Nosepiece Configuration.....	68
3.3 Cross-sectional View of the Single Screw Extruder and the Die Test Section.....	70
3.4 Methodology Used to Determine the Average Fiber Diameter for previous and Current Investigations..	72
3.5 Drawing of View Through the Microscope During Diameter Analysis.....	74
3.6 Schematic Showing Fiber Diameter Measurement.	76
3.7 Hardware Configuration for Shot Analysis.....	79
3.8 WebPro Image Before Scanning Process.....	80
3.9 WebPro Image After Scanning Process.....	80
3.10 WebPro Shot Analysis Output-Shot Diameter Distribution.....	82

3.11 WebPro Shot Analysis Output-Shot Orientation Distribution.....	83
3.12 WebPro Shot Analysis Output-Shot Aspect Ratio Distribution.....	84
4.1 Number of Shot per cm ² vs. Processing Conditions of the Blend Resins.....	95
4.2 Number of Shot per cm ² vs. DCD of the Blend Resins @500°F.....	97
4.3 Number of Shot per cm ² vs. DCD of the Blend Resins@475°F.....	98
4.4 Number of Shot per cm ² vs. DCD of the Blend Resins@450°F.....	99
4.5 (a) DSC Heating and Cooling Curves of the B1 Resin.....	102
4.5 (b) DSC Heating and Cooling Curves of the B2 Resin.....	102
4.5 (c) DSC Heating and Cooling Curves of the B3 Resin.....	103
4.5 (d) DSC Heating and Cooling Curves of the B4 Resin.....	103
4.5 (e) DSC Heating and Cooling Curves of the B5 Resin.....	104
4.5 (f) DSC Heating and Cooling Curves of the B6 Resin.....	104
4.6 Half-time of Crystallization vs. Crystallization Temperature of the Blend Resin.	106
4.7 X-ray Diffraction Pattern of the Melt Blown Webs.....	108
4.8 X-ray Diffraction Pattern of the As-Blown Fibers.....	109
4.9 Number of Shot per in ² vs. Process Conditions of the Sodium Benzoate Nucleating Agent NR1 and NR2.....	113
4.10 Average Fiber Diameter vs. Process Conditions of the Sodium Benzoate Nucleating Agent NR1 and NR2.....	114
4.11 Number of Shot per in ² vs. Process Conditions of the Sodium Benzoate Nucleating Agent NR1, NR2, NR3 and NR4.....	116
4.12 Average Fiber Diameter vs. Process Conditions of the Sodium Benzoate Nucleating Agent NR1, NR2, NR3 and NR4..	117

4.13 Number of Shot per in ² vs. Process Conditions of the Millad Nucleating Agent NR5 and NR6.....	118
4.14 Average Fiber Diameter vs. Process Conditions of the Millad Nucleating Agent NR5 and NR6.....	119
4.15 Half-time vs. Crystallization Temperature of the Different Nucleated Resins....	121
4.16 Number Average Molecular Weight of the Different Webs.....	125
4.17 Weight Average Molecular Weight of the Different Webs.....	127
4 18 Polydispersity of the Different Webs.....	128
4.19 Birefringence vs. Fiber Diameter of the Melt Blown Fibers.....	130

LIST OF TABLES

TABLE	PAGE
2.1 Effect of Processing Conditions on Shot Production for the >1000 MFR Resins in Jana's Study [22].....	60
2.2 Effect of Processing Conditions on Shot Production for the <1000 MFR Resins in Jana's Study [22].....	61
3.1 Blend Ratios of the Different Blend Resins.....	63
3.2 First Kind of Nucleated Resins (sodium benzoate Nucleating Agent).....	64
3.3 Second Kind of Nucleated Resins (Millad Nucleating Agent).....	64
4.1 Non-isothermal Thermal Characterization of the Metallocene-ZN Different Blend Resins.....	101
4.2 Non-isothermal Thermal Characterization of the Different Nucleated Resins.....	122

CHAPTER ONE

INTRODUCTION

The melt blowing process falls under the general classification of polymer laid nonwoven fabrics. In recent years there has been considerable interest in this process from both commercial and scientific points of view [1]. **Figure 1.1** shows a schematic of the melt blowing process. The melt blowing process is defined as follows [2]:

“It is a process in which usually a thermoplastic, fiber forming polymer is extruded through a linear die containing several hundred small orifices. Convergent streams of hot air (exiting from the top and bottom sides of the die nosepiece) rapidly attenuate the extruded polymer streams to form extremely fine diameter fibers (1-5 μ m). The attenuated fibers subsequently get blown by high velocity air onto a collector screen-thus forming a fine fibered self-bonded nonwoven melt blown web.”

Nonwoven melt blown fabrics are used for many applications including filtration media, protective apparel for use in the health care profession, surgical supplies, and liquid wipes. Examples of melt blown products in either the pure or the composite form are oil spill sorbents, wipes, surgical gowns, surgical face masks, liquid

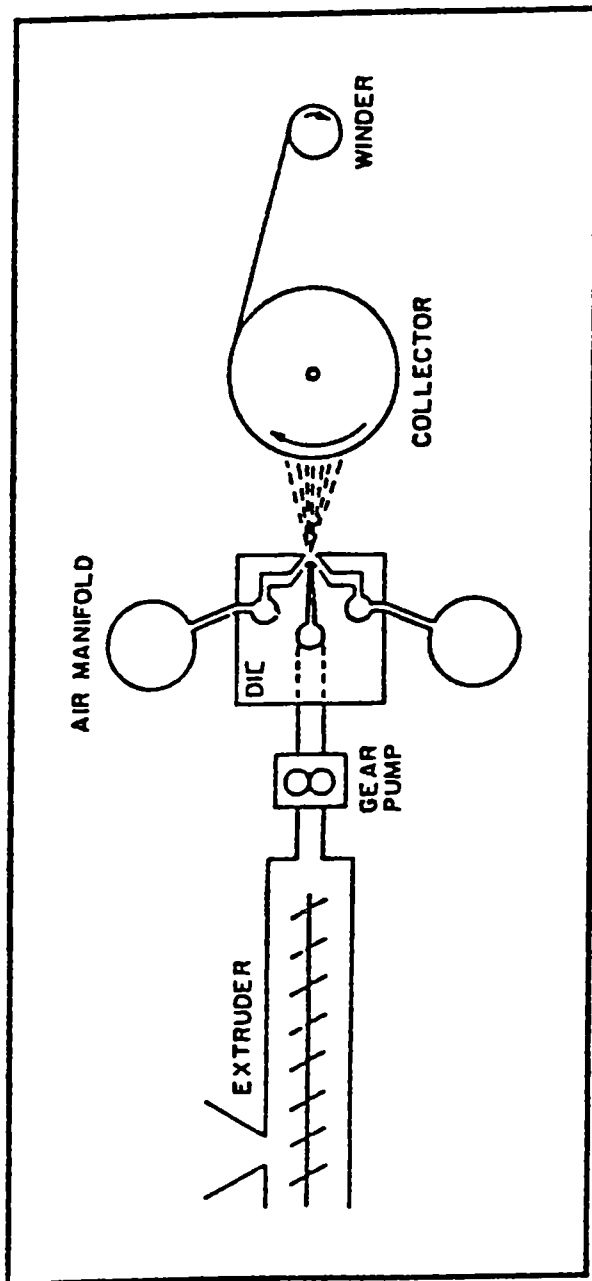


Figure 1.1 Schematic of the Melt Blowing Process.

and air filtration fabrics, lithium battery separators, clothing insulation, and feminine hygiene products [3].

These and many other applications depend on a web that is uniform with a large surface area per unit of polymer mass. The small fiber diameters result in webs with a large surface area per unit mass and, thus, meet the demands of many melt blown non-woven fabric applications. Much effort has been expended, since the original work by Wente [4] in 1956, in order to produce more uniform webs with minimum areas of non-uniformity. One of the important and undesirable defects, that produces non-uniformity in melt blown webs, is known as 'shot'. It is defined as a globule of polymer considerably larger in diameter than the fibers. **Figure 1.2** shows a typical SEM image of a shot particle.

Shot has been a continuing problem for many, if not all, production facilities. Shots impart "sandy" feel and impair the barrier properties of the web. Various mechanisms have been proposed for shot formation, but the exact mechanism of shot formation has not yet been established.

Buntin and Lohkamp [5] were researchers in the early 1970's who associated the incidence of "shot" to fiber breakage. They defined shot as a particle of polymer, considerably larger than the fibers, which is formed by the elastic "snap back" of the fiber ends upon breaking. It was their speculation that fiber breakage occurs

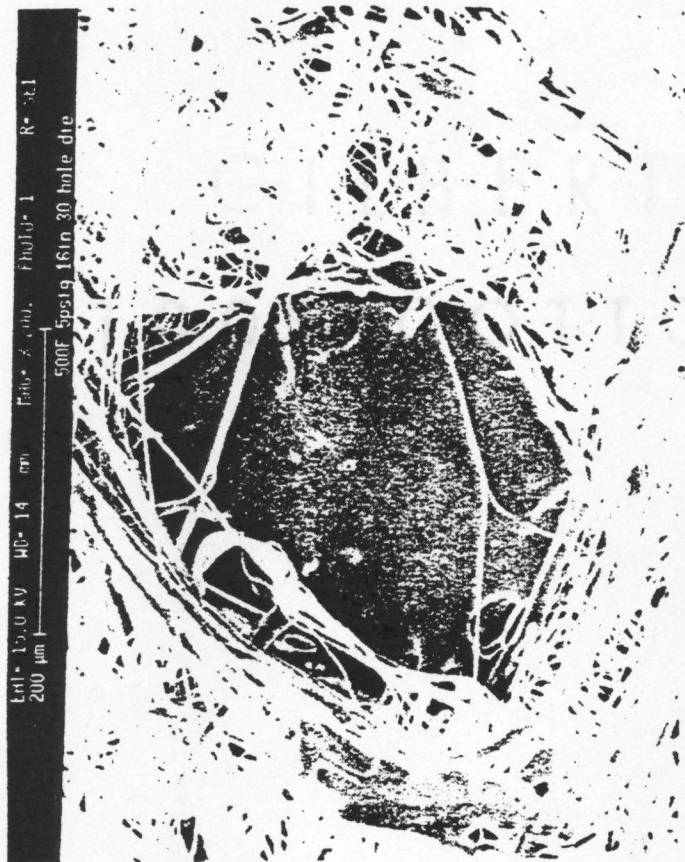


Figure 1.2 SEM Image of a Shot Particle.

continuously in a melt blowing operation and the fibers are discontinuous with a length of the order of few inches. Fiber breakage may be attributed to periodic melt fracture or melt instability, which depend on such factors as processing temperatures, shear rate, air flow rate, die configuration, and die contamination.

In early 1990's, Milligan et al. [3,6] proposed that shot is formed near the die when hot polymer streams of large diameter contact one another before they have developed the size, shape and internal morphology of the fibers. Since fused filaments will have a larger volume to surface area, they will not cool as fast as the individual fibers, and thus may be molten upon striking the collector. The probability and intensity of fusion is determined by diameter and temperature of individual polymer streams near the die.

Milligan's model of shot formation seems to be the most satisfactory model for shot formation under normal processing conditions with modern resins and dies.

In the past decade, the use of polypropylene has dominated the production of melt blown nonwovens [7]. One of the main reasons for the wide usage of PP is because it is relatively inexpensive and available throughout the world. Moreover, continuing advances make them more suitable for nonwoven applications. One of those very recent advances is the attempt to use metallocene or single-site catalyzed polypropylene in place of the conventional or Ziegler-Natta catalyzed propylene resins.

Metallocene PP manufacturers claim many advantages of the polymer such as controlled molecular structure, narrow molecular weight distribution and small amount of catalyst residue in the finished product. However, despite their numerous advantages, several technical problems need to be solved before metallocene catalyst polymers can be used widely in the industry [8,9]. In particular, the metallocene polypropylene appears to produce greater numbers of shot particles in melt blown webs.

Since "shot" in a web is very undesirable, major research was initiated here at the University of Tennessee in Knoxville in order to investigate the mechanisms by which visible "shot" is formed in webs being produced with modern dies and high MFR polypropylene resins and to investigate the possible ways of preventing shot formation.

The present research is a part of this overall effort. Specifically, this research is an effort to understand the differences in the processing of conventional Ziegler-Natta and metallocene catalyzed polypropylene.

If one prescribes to the fiber collision model, then shot is caused by molten fibers colliding and fusing together in flight. This fused mass then requires more solidification time due to its increased mass. If molten fiber collisions could be prevented then shot might possibly be prevented. If we adopt the theory of uncrystallized fibers colliding and forming shot, then increasing the crystallization kinetics would be expected to reduce shot formation. Furthermore, it is known that

metallocene based polypropylene crystallizes more slowly than Ziegler-Natta catalyzed resins, which suggests that this may contribute to greater shot formation in the metallocene resins.

One way of changing and most probably increasing the crystallization kinetics is by blending metallocene and Ziegler-Natta catalyzed polypropylene. The first part of the thesis deals with the influence of blending metallocene and Ziegler-Natta catalyzed polypropylene on the crystallization kinetics and the effect of that on shot formation.

Another way of increasing the crystallization kinetics is by the use of nucleating agents. The second part of this research investigates the effect of nucleating agents on the formation of shot. The influence of nucleating agents on the crystallization kinetics is studied, the influence of which on shot formation is investigated as well.

CHAPTER TWO

BACKGROUND AND LITERATURE REVIEW

2.1 Nonwoven Classification and Technology

Nonwoven fabric technology embodies both quite old and the very new processing techniques and materials [10]. The term “nonwoven fabrics” has been defined in many ways. In fact, the definition of nonwoven fabrics has been an area of considerable debate and discussion. Apparently, all the definitions proposed so far state in some detail what nonwovens are not, rather than what they are. The American Standard for Testing Materials (ASTM) [11] has defined the term “nonwoven fabrics” as:

“A structure produced by bonding or the interlocking of fibers, or both, accomplished by mechanical, chemical, thermal, or solvent means and the combination thereof. The term does not include paper or fabrics that are woven, knitted, tufted, or those made by wool or other felting processes

The versatile and complex nature of the nonwovens industry is depicted in **Figure 2.1**. The most significant feature of nonwoven fabrics, and the one that

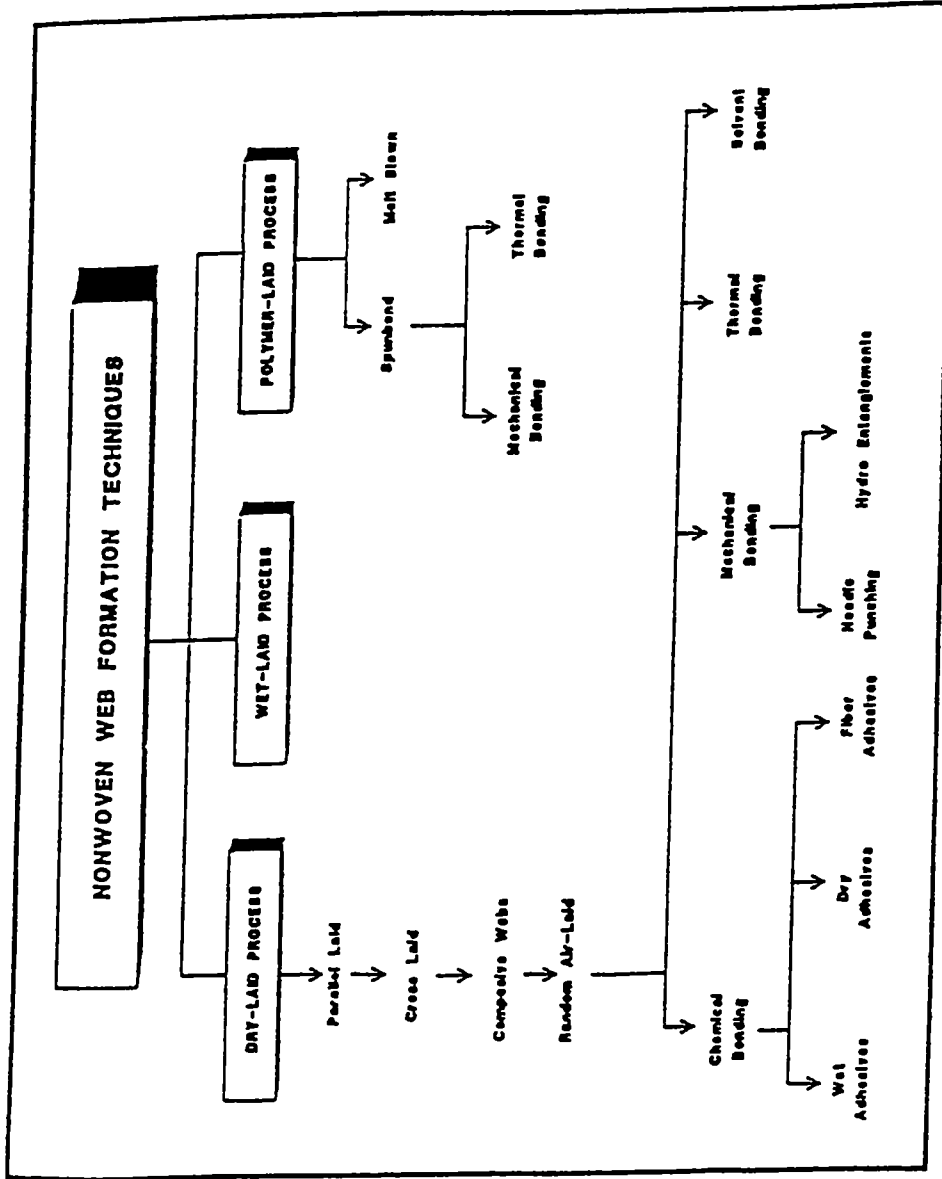


Figure 2.1 Flow Diagram of Classification of Nonwoven Fabric Formation Techniques.

Source: Nutter, W: Textile Month, No.5, 1970, pp. 94-100.

contributes most to their economic appeal, is that the fabrics are usually made directly from raw materials in a continuous production line, thus partially or completely eliminating conventional textile operations, such as carding, roving, spinning, weaving or knitting. The simplicity of fabric formation, coupled with high productivity, allows nonwovens to compete favorably with wovens and knits on a performance per cost basis in many industrial applications (as in packaging materials, for example). However, in fashion outerwear apparel fabric applications, where good drape properties, flexibility, and strength are required, nonwovens have yet to gain a significant technological advancement. On the other hand, nonwoven fabrics and composites have gained the major share of healthcare products such as surgical face masks, operating room drapes and gowns, instrument sterilization wraps, surgical towels, and personal hygiene products. Nonwovens are also used extensively for gaseous and liquid filtration applications. Nevertheless, there has been a continuous effort through innovative manufacturing processes to develop newer nonwoven products that emulate the drape and flexibility of woven or knitted structures.

Nonwoven fabrics are quite distinct and versatile in their properties and structures compared to the conventional woven and knitted fabrics. Woven and knitted fabrics manifest their properties from the arrangement of fibers in the yarn and the arrangement of yarns in the fabrics [12]. Likewise, the properties of nonwoven fabrics are largely dependent on fiber properties, fabric structural geometry, and particularly the type of fiber-to-fiber bonding. Moreover, nonwoven fabric properties can be “tailor-

made” through the use of the various web manufacturing and bonding processes, the selective use of raw materials, fibers and bonding means, and various finishing processes.

Nonwoven fabric technology is currently the most exciting segment of the textile industry and will be one of the most important in the years ahead as nonwoven fabrics penetrate many more areas now occupied predominantly by conventional textiles [13].

Nonwoven fabrics can be classified in many ways, but the most accepted classification scheme is based on web formation techniques. There are many nonwoven web formation techniques; they can be divided into the following three generic categories [12]: 1) Dry laid, 2) Wet laid; and 3) Polymer laid. Melt blowing falls into the polymer laid category.

2.2 Development and Description of the Melt Blowing Process

The nonwoven market is not static; it is growing considerably. In 1990, the world production of nonwoven fabric was twelve billion square yards and in 1994 the world production had increased to thirty eight billion square yards[14]. In financial terms, it has been estimated that the total United States dollar value of nonwoven materials and products that presently utilize nonwoven materials was about \$31 billion

in 1994. The industry as a whole is expanding at an average rate of 5% per year in the United States and greater elsewhere [14].

Nearly all nonwovens can be tailored to the filtration industry. The latest available data indicates that the filtration industry is the number one user for durable nonwovens, with annual sales in excess of one billion square yards. The melt blown portion of the nonwoven filtration business is approximately 18% with annual sales of \$230 million in 1994 [14].

2.2.1 Historical Perspective

The melt blown microfibers are generally less than about 10 microns in diameter. Such fibers are found in nature in the form of spider silk and pineapple leaf fiber [15]. Man-made microfibers are produced using a variety of materials and production techniques. The submicron glass fibers in "glass wool" are a prime example. There are basically two production techniques: **spray spinning** and **melt blowing**. These two techniques differ somewhat in details, but both involve the introduction of dissolved or molten polymers into high velocity streams of air or gas, which rapidly convert the liquid into microfibers.

The first deliberate attempt to develop a useful commercial process for making organic textile-like microfibers was made by **Carlton Francis**, an independent inventor, in 1939. **Francis** visualized that a spray gun which could produce fibers might be used

for a wide variety of applications, including the combining of adhesive or potentially adhesive sprayed fibers with other textile fibers to form microfibrinous nonwoven fabrics [16]. In the early 1950's, the **American Viscose Corporation** acquired the rights to Francis's work on sprayed fiber technology and retained **Arthur D. Little, Inc.** to research and develop the spray fiber field. No major commercial products were developed, and the company eventually discontinued the research work.

During this period of time, Dow Chemical Company also had a Research and Development program to develop microfiber products using polystyrene [17]. Dow Chemical Company did not foresee any success, so decided to abandon the project. Soon afterwards, the Army Chemical Warfare Laboratories continued Dow's work in order to produce microfibers to collect radioactive particles from the United States and Russian nuclear weapons testing. At the same time, **Van A. Wente** at the United States Naval Research Laboratory, the DuPont Company, and the Chemstrand Company (later the Monsanto Textile Company) also started an investigation on producing micro-organic fibers. During their investigation it was found that it was possible to construct a nonwoven fabric of very fine fibers for a possible use as filter media for fine aerosols [18]. This investigation eventually led the DuPont Company to market its first commercial organic microfiber known as "**Textryls**", but the product was later withdrawn from the market because of an insufficient demand [15].

In the late 1960's, the **Esso Research and Engineering Company** (now **Exxon Mobil Chemical Company**) recognized the strength and potential of microfiber technology for commercial applications. The Exxon Mobil Chemical Company started developing a low-cost method of producing blown microfibers from polypropylene. After the extensive research and development based on Wente's original work on microfiber technology [19], Exxon Mobil Chemical Company researchers patented the blown microfiber process (usually called the melt blown process). Later, Exxon Mobil Chemical Company decided to license the melt blown technology to others and concentrate primarily on producing resins to supply this novel process [20].

Based on prototype demonstration of the melt blown process, Exxon Mobil Chemical company negotiated several licenses with U S. companies. A number of companies obtained the licenses and moved quickly into commercial production. Because of the rapid commercialization of melt blown technology, Exxon Mobil Chemical Company needed a source of melt blown equipment. Exxon Mobil Chemical Company first licensed **Beloit Corporation** of Michigan, USA to manufacture complete melt blown equipment [20] and that arrangement continued for a few years. Presently, the Accurate Products Company of New Jersey, USA; Reifenhauer GmbH & Corporation of Germany; and Kasson Nozzle of Japan are licensed to manufacture melt blown production lines.

Besides Exxon Mobil Chemical Company 's patented melt blowing process, there are other companies who have their own proprietary blown microfiber production processes, such as 3M company of USA, Biax-Fiberfilm Corporation of USA, and Freudenberg Nonwovens of Germany. However, most of the melt blown production lines in operation today in the nonwoven industry were licensed through Exxon Mobil Chemical Company. Since the early 1970's, Exxon has become the industry leader and has been continuously developing and improving the melt blowing process and more recently, in conjunction with Tonen Petrochemical Company of Japan and The University of Tennessee, Knoxville.

2.2.2 Process Description:

A thermoplastic, fiber-forming resin (granule, pellets, or flakes) is fed to the extruder by a hopper. The molten polymer is metered by a gear pump to the orifices through a polymer feed distribution system. As the molten polymer jets exit the orifices, convergent streams of high velocity hot air on either side of the nose-tip attenuate them to superfine fibers. As the turbulent air stream expands, the ambient air is entrained into the flow field, which provides a convective medium of heat transfer for the polymer jets to cool. The attenuated filaments are carried by the air stream and deposited on the rotating collector. The speed of the collector can be varied to obtain the desired web basis weight [21].

Process Variables:

The melt blowing process involves many operating variables. The operating variables can be divided into two categories:

- Operational / Online variables
- Off-line variables

The online variables are those, which can be changed according to requirements during production such as polymer and air throughput, polymer/die and air temperature, die to collector distance (DCD) and quench environment. The off-line processing variables are those which can only be changed when the production line is not in operation, such as die hole size, die-tip setback, air gap, air angle, web collection type and polymer/air distribution. Most of the off-line processing variables are set constant for a particular product line.

The polymer throughput rate, air throughput rate, polymer/die temperatures, air temperature, and die-to-collector distance are the five basic on-line operational variables; they are easy to change and dictate the major fabric properties. The polymer/die and air temperature in conjunction with airflow rate affect the appearance and tactile handle of the fabric, fabric uniformity, and fabric defects during production [1].

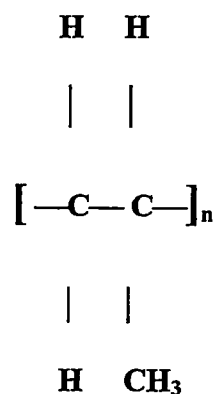
Material Variables:

The material variables include polymer type, molecular weight, molecular weight distribution, polymer additives, polymer degradation and the polymer form (such as pellets, chips, powder or granules). Melt blowing offers the advantage to process a wide variety of fiber-forming polymers and blends. Basically, any fiber-forming polymer having an acceptably low melt viscosity at a suitable processing temperature, and which can solidify before landing on the collector screen, can be melt blown into fine fibred webs [5]. A wide range of polymers have been melt blown. Polypropylene has been used predominantly in commercial production and has been thoroughly evaluated; the other successfully processed polymers are polyesters, nylons, polyethylene, polystyrene and many others.

2.3 Polypropylenes for the Melt Blowing Process

2.3.1 Basic Structure of Polypropylene

Polypropylene (PP) exhibits the following chemical structure:



PP exists in three forms: Isotactic, Syndiotactic, and Atactic. Isotactic is the principal type used in industry, due to the excellent combination of properties for numerous applications. The nature of the three types is briefly described as follows:

- Isotactic PP is a stereo-specific polymer because the propylene units are added head to tail with their methyl (CH₃) groups all located on the same side of the plane of the polymeric backbone. It crystallizes in a helical form and exhibits good mechanical properties such as stiffness and tensile strength. The isotactic homopolymer has the highest stiffness and melting point of the three types and is marketed in a wide range of melt flow rates.
- Syndiotactic PP is made by inserting monomer units so that the methyl groups alternate from one side of the polymer backbone to the other. It lacks the stiffness of the isotactic form, but can have improved impact resistance and clarity.
- Atactic PP is produced via a random arrangement of the monomer. This form lacks the crystallinity of the other two. It is mainly used in roofing tars and adhesive applications.

2.3.2 Requirements for Melt Blowing

Fiber grade PP resins are mainly isotactic homopolymer. Several important fiber technologies take advantage of the drawability of PP resins and are major consumers of PP resins. Low to moderate melt flow rate polypropylenes are used to produce

continuous filaments for ropes, textile yarns and other similar applications. The melt blowing process can accommodate resins with a wide range of melt flow rates, typically 30 to 1500 MFR.

The primary resin characteristics affecting the extrusion and spinning processes during the production of melt blown nonwovens are as follows [22]:

- **Melting Point:** Most of the conventional PP resins melt at around 160 °C by DSC. The melting point directly affects the melt temperature during processing. The higher the melting point, the greater the energy requirements and often provide desirable high melting product characteristics.
- **Melt Viscosity:** Melt viscosity is a function of molecular weight and melt temperature. The melt viscosity has to be appropriate in order to form fine filaments. One common measure of the viscosity of polypropylenes is “melt flow rate (MFR)”. MFR is a measure of polymer’s mass flow rate (grams extruded in 10 minutes) using a particular orifice under specified conditions of temperature and load. As noted above, the suitable range of MFR for the melt blowing process is 30 to 1500 at 230°C and 2.16 kg.
- **Molecular Weight Distribution (MWD):** The melt blowing process requires relatively narrow molecular weight distribution resins. The narrow MWD reduces

the melt elasticity and melt strength of the resin so that the melt stream can be drawn into fine denier filaments without excessive draw force. The presence of broad MWD increases melt elasticity and melt strength, which inhibit fiber drawing, therefore, a broad MWD resin is prone to produce fiber breaks and stiffer webs.

- **Resin Cleanliness:** Due to fine capillary diameter of spinneret in the melt blowing processes, it is important to have a resin with practically no contaminants. The contaminants plug up the spinneret holes during the processing causing inconsistency in the final product.

2.3.3 Comparison of Conventional Zeigler-Natta and Metallocene

Polypropylene

Sinn and Kaminsky's discovery of new catalytic systems based on the combination of metallocenes with alkylaluminumoxane started a new era in polyolefin technology. In comparison with conventional Ziegler-Natta systems, metallocene based catalysts offer higher versatility and flexibility, both for the synthesis and the control of the structure of polyolefins, due to their identical reactive sites as illustrated in **Figure 2.2** [8].

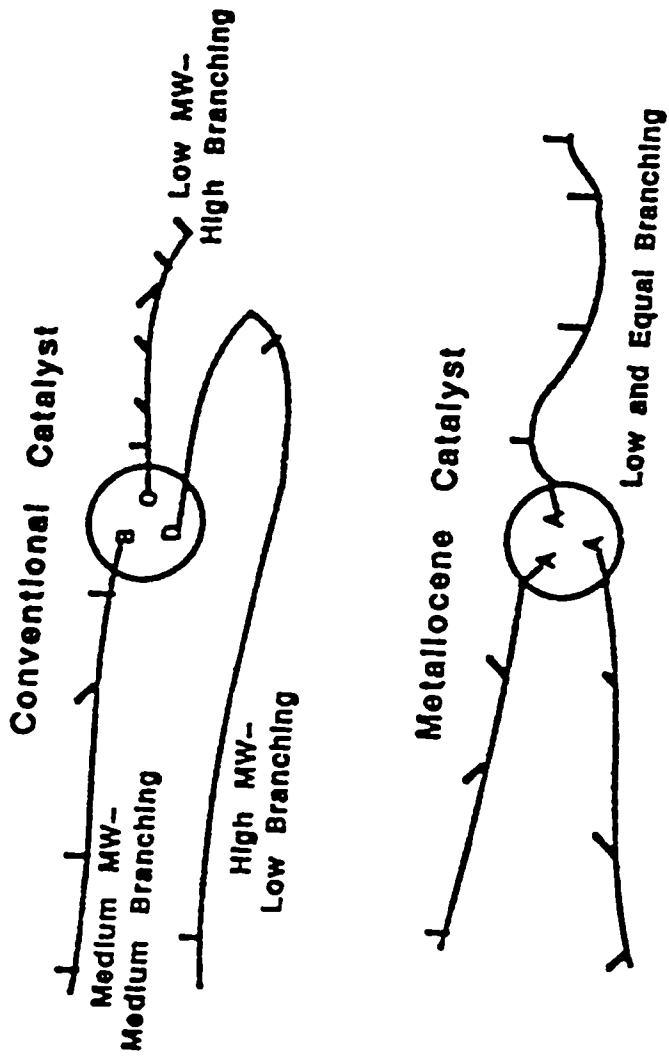


Figure 2.2 Comparison of Conventional and Metallocene Catalyst

Source: Malkan, 'Advancements in Polyolefin Resins for Polymer-laid Nonwovens,' Hi-per Fab '96 conference, Singapore, April 24-26, 1996.

Compared to conventional heterogeneous catalysts such as the well-established Ziegler-Natta system, the mechanism of metallocene-based catalysts is relatively easy to study because every catalytic site has the same molecular structure [23]. The metal center is chiral and metallocene has C₂ symmetry. Richard Jordan of Univ of Iowa and Howard Turner of Exxon Mobil Chemical Company discovered that several positively charged or 'cationic' metallocenes are active in the polymerization of ethylene and in the stereospecific polymerization of propylene. These results strongly suggest that a metal cation is the active part of the catalyst.

Before the metallocene can catalyze the polymerization it must first react with methylaluminoxane (MAO) with which it is mixed. The details of this first step are not yet understood, but somehow the chlorine atoms are removed from the metal atom, and the zirconium complex is transformed into a methylated cation. MAO acts as a balancing ion, but the structure of the cation-anion complex has yet to be discovered. It is believed that the polymerization starts in the second step, when the alkyl group moves to a propylene molecule that attaches itself at the chiral metal.

There are two possible orientations of propylene at the metal center. If one of these requires less energy to form, polymerization will be stereo-specific. The orientation, which requires more energy, is the one where propylene is attached in such a way that the methyl group comes close to the groups attached to the ring.

In the third step, propylene is inserted into the carbon metal bond. The growing polymer chain moves towards the monomer, which is still attached to the metal. Then the chain and monomer exchange positions and the whole sequence begins again to give isotactic polypropylene.

Among the key attributes found in the first generation of metallocene-based propylene polymers are narrow molecular weight distribution and composition distribution, lower melting point and lower extractables [24].

The narrow MWD mPP exhibits lower shear viscosity in the low shear rate region and higher viscosity at the higher shear rate. The reduced viscosity in the low shear region is generally correlated with low elongational viscosity. This is advantageous for post-extrusion processes where low extensional flow resistance is desirable. For example, fiber spinning processes require low elongational viscosity in order to draw to a finer fiber diameter. The low extensional viscosity is also favorable for spinning at a higher line speed.

Thermal properties of mPP are different from z-nPP due to the degree of crystallinity and type of crystalline structure. The occasional reversal of head-to-tail polymer chain growth (i.e. regio defects) hinders the crystalline growth. The melting peak temperature is therefore, lower than conventional PP by approximately 8-10 °C.

The crystallization peak temperature for mPP is generally at 100-101 °C vs. the conventional resin at 105-106 °C [22]

Since metallocene catalyst system produces a wide range of MFRs and narrow MWD product, it would seem to be an ideal catalyst system for the melt blown resin [25]. For melt blown process, the polymer needs to have narrow MWD and high MFR. The narrow MFR and MWD enable the polymer to be drawn to fine size, and presumably, might prevent formation of undrawn polymer beads (or 'shots') in the melt blown web. The high MFR (or low MW) may allow the process to operate at low temperature, and reduce energy cost, and prolongs die tip life.

Conventional catalyst (Ziegler-Natta catalyst) system produces broad MWD polymer. To increase MFR and reduce MWD, the polymer is generally extruded with peroxide coating in an extruder to thermally and chemically break down the polymer molecules (a process called "Controlled Rheology" or "CR" process) to reduce MW and narrower MWD product. In most commercial melt blown PP resins, the granules from the polymerization are blended or coated with peroxide and shipped to the end user in the coated form. The peroxide is decomposed in pressure with the polymer in the melt blown extruder and a narrower MWD and lower MW polymer is obtained at the melt blown die.

Using the metallocene catalyst system, the polymer can be used directly in a melt blown extruder without coating the granules with peroxide or undergoing the CR process. The MFR of the polymer can be tailored and polymerized in the reactor for the specific melt blown applications.

At high shear rates, the melt viscosity for the metallocene resin is higher than that of the conventional polymer of the same MFR. This is due to lower shear thinning of the narrow MWD resins. Therefore, one can expect the viscous shear heating in the plasticating extruder to be higher for the metallocene resin. The higher energy input into the polymer, through viscous shear heating, results in higher melt temperatures under similar barrel settings. The metallocene PP can be extruded at the same conditions as the conventional PP. However, because of the melt temperature being relatively lower compared to the conventional resin of the same MFR, a lower barrel temperature setting of 3 to 5 °C can be used to compensate for the higher viscous shear heating by reducing the external heat input at the melting section and increasing the cooling at the metering section of the screw [22].

The single-site metallocene catalyst produces very uniform molecular species. The molecular weight of each polymer chain is very similar (and hence the narrow MWD product). Therefore, there is a probability of reduced fractions of molecular weight species so small they can volatilize during extrusion. The emission of low molecular species during fiber spinning is much lower for mPP resin. This has a

positive long-term impact on productivity (reduced downtime and improved safety) and environmental cleanliness.

Under a given draw force, the fiber diameter of mPP resin is smaller than the conventional resin of the same MFR extruding under the same melt temperature. The difference is greater as the draw force is increased. **Figure 2.3** compares the fiber size of mPP and z-nPP in a spunbond process [7]. The relative draw force is the force caused by the air pressure dragging the fibers over DCD.

Using a metallocene based polymer can result in the following advantages:

- More consistent product by eliminating MFR variability due to CR or peroxide content variability in peroxide coated granules.
- Finer melt blown fiber due to lower elongational viscosity. Better melt quality since no chemical reaction takes place in the melt blown extruder, as when peroxide-coated granules are used.

McAlpin et al, [24] have noted that one might think that the lower melting point of the metallocene polypropylene resins would reduce their stiffness and limit their use temperature sharply. But, at room temperature the mPP resin is measurably stiffer than its conventional counterpart. Near their melting points, Crystallinity disappears and the

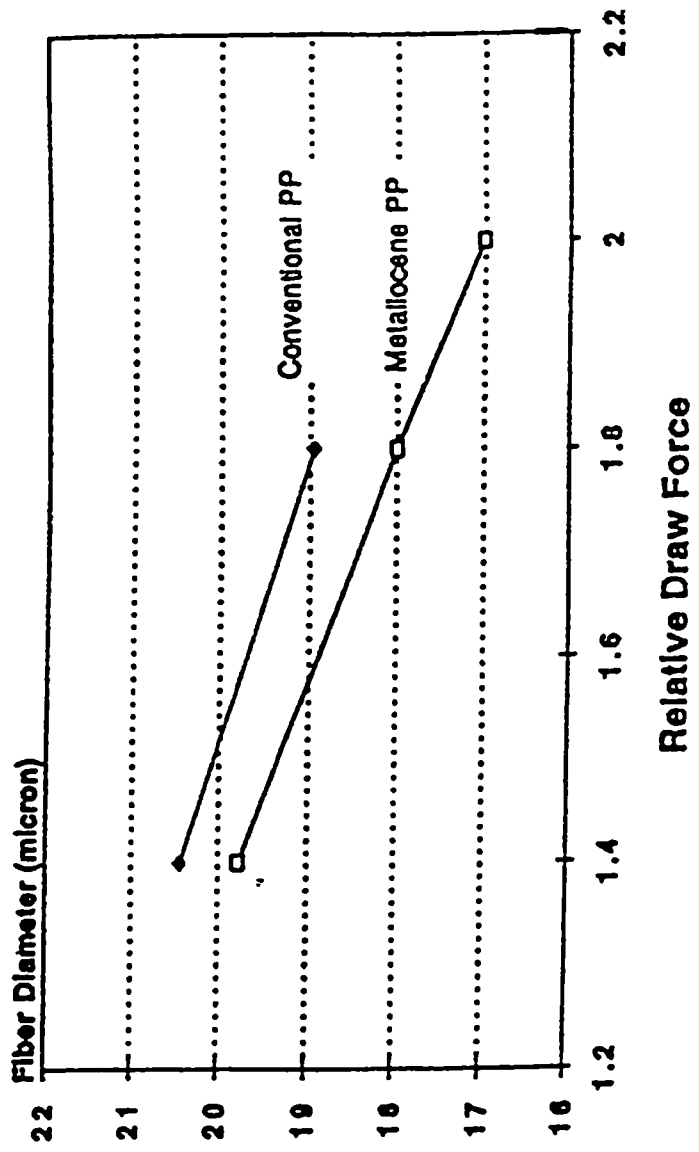


Figure 2.3 Comparison of Conventional and Metalocene Polypropylene Fibers at Different Relative Draw Force

Source: Malkan, 'Advancements in Polyolefin Resins for Polymer-laid Nonwovens, ' Hi-per Fab'96 conference, Singapore, April 24-26, 1996.

moduli drop precipitously. However, at temperatures normally thought of as the use temperature of polypropylene (<100°C or so), their moduli are almost identical. Thus in normal application, the stiffness and use temperature of first generation mPP will be equal to that of conventional polypropylene.

An important property of melt blown webs is “hydrohead”. This property is an indication of resistance to passage of fluids through the melt blown webs. It is, therefore, important in such applications as surgical gowns, oil drapes, wipes, etc. The hydrohead is defined as the pressure required to drive a drop of water through the fabric. While high hydrohead is desirable, a garment should also be comfortable to wear; hence its permeability to air is an important variable, as well. **Figure 2.4** compares the performance of melt blown webs made from metallocene propylene polymers with webs from the best available conventional materials. The data of the figure indicate two favorable aspects of the metallocene performance.

First, the extremely low melt strength of the mPP resins allows one to drive the process to extremely fine fibers and hence high hydrohead. This happens at the expense of air permeability, but the balance of hydrohead and air permeability is better for the mPP webs [24]. Another advantage of the mPP resins in the melt blown process noted by McAlpin et al [24], is that they can be processed at temperatures (melt and blowing air) 50°F or so lower than the conventional polymers. This leads to improved service factor on the line and to a significant reduction in energy costs for the process.

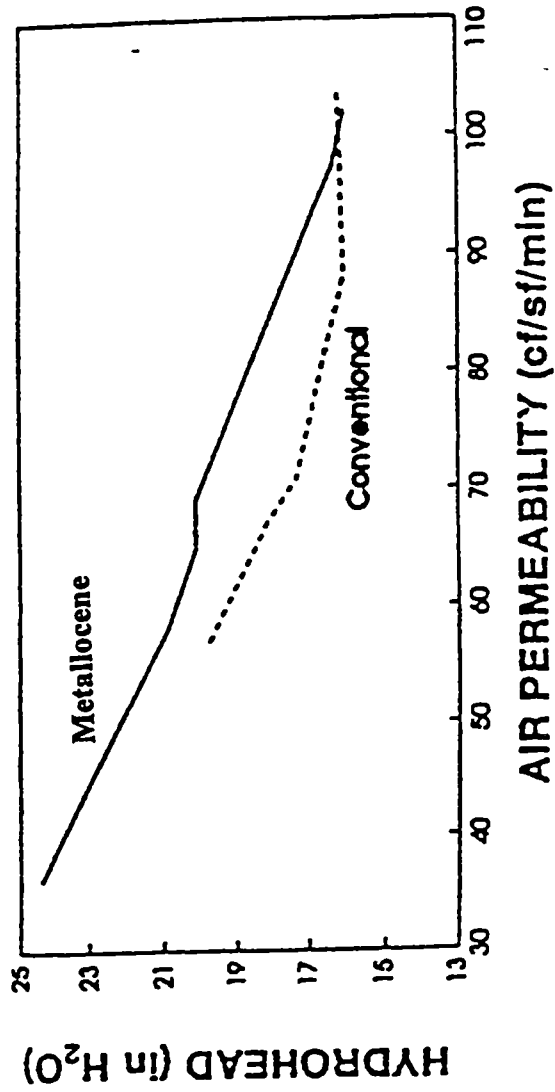


Figure 2.4 Comparison of Conventional and Metalocene Polypropylene at Different Levels of Hydrohead and Air Permeability

Source: McAlpin et al, 'Impact of Metalocene based Propylene polymers on Nonwovens, Nonwovens World, Summer 1996, p 82.

However, there are differences of opinion about this new polymer. Brookman [26] has suggested that because of the narrow molecular weight distribution, fewer higher molecular weight species, which ordinarily act as melt stiffeners, are present in metallocene polyolefins. This typically results in lower melt strength and eventually melt fracture.

Ectstat et al [27] summarized the properties of metallocenes. In addition to several advantages offered by the polymer, the following observations were also reported. The metallocene resins are stiffer than the conventional resin; metallocenes are tackier and may 'gum up' the equipment; 10 to 15% more horse power is required to move resins through equipment.

2.3.4 Polypropylene Crystalline Forms

Isotactic polypropylene is known to exhibit as many as four different crystalline forms: the α -form, which is monoclinic and generally the most predominant; the β -form, which is hexagonal; the γ -form, which is orthorhombic (earlier triclinic); and the smectic (or condis) form. X-ray diffraction patterns of the different structures of isotactic polypropylene are shown in **Figure 2.5**. The development of the various forms is dependent on the degree of isotacticity of the polymer chains, molecular weights and their distributions, presence of monomer defects (such as ethylene instead of propylene)

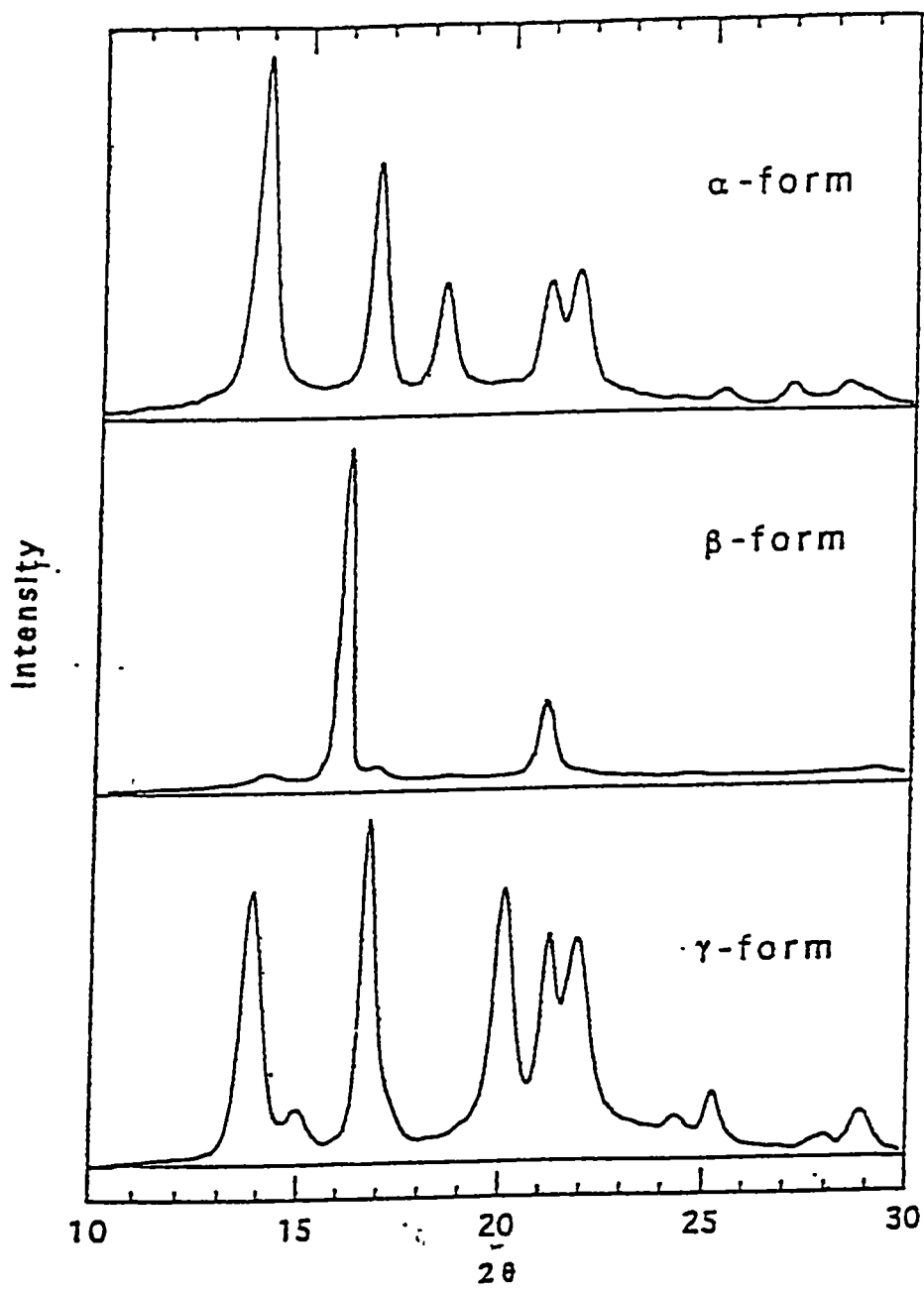


Figure 2.5 Crystal Structures of Isotactic Polypropylene.

Source: Bond E., PhD dissertation, University of Tennessee, Knoxville, 1998.

and the thermal and mechanical history of the specimen.

2.3.4.1 α - Monoclinic Form

The α -form is the crystal form commonly observed when isotactic polypropylene is crystallized from the melt [28] in the absence of nucleating agents and at atmospheric pressure. The overall geometry of the unit cell is monoclinic, with parameters: $a=0.665\text{nm}$, $b=2.096\text{nm}$, $c=0.65\text{nm}$ and $\beta=99.80^\circ$. The cell consists of 12 repeat units (four helical chains) and has a crystal density of 0.938 g/cm^3 . The space group that has been assigned is $C2/c$ and Cc for the statistically ordered arrangement of the up and down stems in the unit cell. Recent research has supported those values with only slight changes in the c -axis [29]. These values differ slightly from those proposed by Natta and Corrandini in 1960 [30].

The chain conformation is a ternary helix based on the tg^+ and g^-t conformation which minimizes the methyl-methyl steric conflicts characteristic of extended isotactic chains and lead to the left and right handed helices, respectively. The packing of the helices is such that any helix interacts mostly with helices of opposite hand. Therefore, isotactic polypropylene is based on the alternation, in the b -axis direction, of layers parallel to the ac plane and made only of left-handed, or only of right handed helices. Research [29] has shown that α -isotactic polypropylene shows various degrees of

disorder in the up and down positioning of the chains in the crystal, depending on the thermal and mechanical history of the sample.

2.3.4.2 β - Pseudo-hexagonal Form

The structure of the β -isotactic polypropylene is characterized by extensive disorder [31]. Formed under special crystallization conditions, using either a temperature gradient method, nucleating agents or at high isothermal crystallization temperatures (typically with a Ziegler-Natta catalyst using crystallization temperatures above 130°C), large amounts of this crystal structure can be formed [32]. Keith et al. [33] first identified the β phase but never fully characterized its structure, a result of this crystal structure's thermodynamic and mechanical instability.

The simplest satisfactory model for the β phase is hexagonal ($P3_121$) with $a=b=1.103\text{nm}$ and $c=0.649\text{nm}$ [31]. Three monomers form the asymmetric unit, with six chain stems in the unit cell. The crystal density is significantly lower than the other forms of isotactic polypropylene, at 0.92 g/cm^3 . The lower density, combined with the faster growth rate, indicates that high degrees of disorder exist within the β phase. Other data exists for this structure [34], but the cell is a subshell of the one indicated above. However the structure presented here is from the most recent research and consists of further investigations done by one of the original investigators who determined the initial β isotactic polypropylene structure [31].

2.3.4.3 γ - Orthorhombic Form

The nature of the γ isotactic polypropylene has drawn a considerable amount of attention and work [31]. The appearance of the γ phase is favored by molecular features such as short chain length, chain molecular defects or high pressures [35]. Previous studies have shown the formation of γ isotactic PP with the presence of molecular heterogeneity in the chain, caused by atacticity or by copolymerization [35]. Recent work has demonstrated the production of γ isotactic PP at elevated pressures from high molecular weight homopolymers with no appreciable defects, confirming an earlier finding [36].

For many years the structure was labeled as triclinic. Recent work has shown the triclinic unit cell is actually a sub-cell of a larger orthorhombic cell [29]. The triclinic cell has dimensions: $a=0.665\text{nm}$, $b=2.140\text{nm}$, $c=0.650\text{nm}$, $\alpha=97.4^\circ$, $\beta=98.8^\circ$ and $\gamma=97.4^\circ$. The cell consists of 12 repeat units having a crystal density of 0.935g/cm^3 . These parameters allow the conversion to a larger face-centered orthorhombic unit cell of higher symmetry: $a=0.854\text{nm}$, $b=0.993\text{nm}$, $c=4.241\text{nm}$ consisting of 48 repeat units with a crystal density of 0.933g/cm^3 . The overall structure is best represented by the statistical co-presence of anticlined isochiral helices at each crystallographic position. This is implied by space group $Fddd$. Local packing modes which cannot retain this feature are satisfactorily described by space groups $F2dd$ or $Fd2d$.

2.3.4.4 Conformationally Disordered or Smectic Form

The conformationally disordered (condis) or smectic form is intermediate metastable crystalline structure [37]. The smectic form is obtained by quenching thin sheets of isotactic polypropylene from the melt into ice water. The smectic structure can also be found in fibers spun with extremely high cooling rates under small stresses. The smectic structure is thought to be a disordered α -structure, with some experimental evidence to support this claim [38]. A comparison of amorphous atactic PP, the smectic structure (mesomorphic) and α -form is shown in **figure 2.6**. The density of the smectic structure is 0.88 g/m^3 . The density of atactic PP is 0.85 g/m^3 , which indicates that the smectic structure has a higher molecular order than atactic PP [30]. An annealed smectic form will gradually transform to the α -form over time or when exposed to elevated temperatures above 70°C .

Wang et al. [39] reported the structural study of irradiated polypropylene by x-ray diffraction. The study found that electron irradiation did not change the total crystallinity of polypropylene but greatly influenced its crystal structure. The amount of the β -form increased, and the α -form decreased as the irradiation dose increased. The study also suggested that the β -form may be recrystallized into the α -form at higher temperature because the melting point of the β -form is much lower than that of the α -form of the polypropylene.

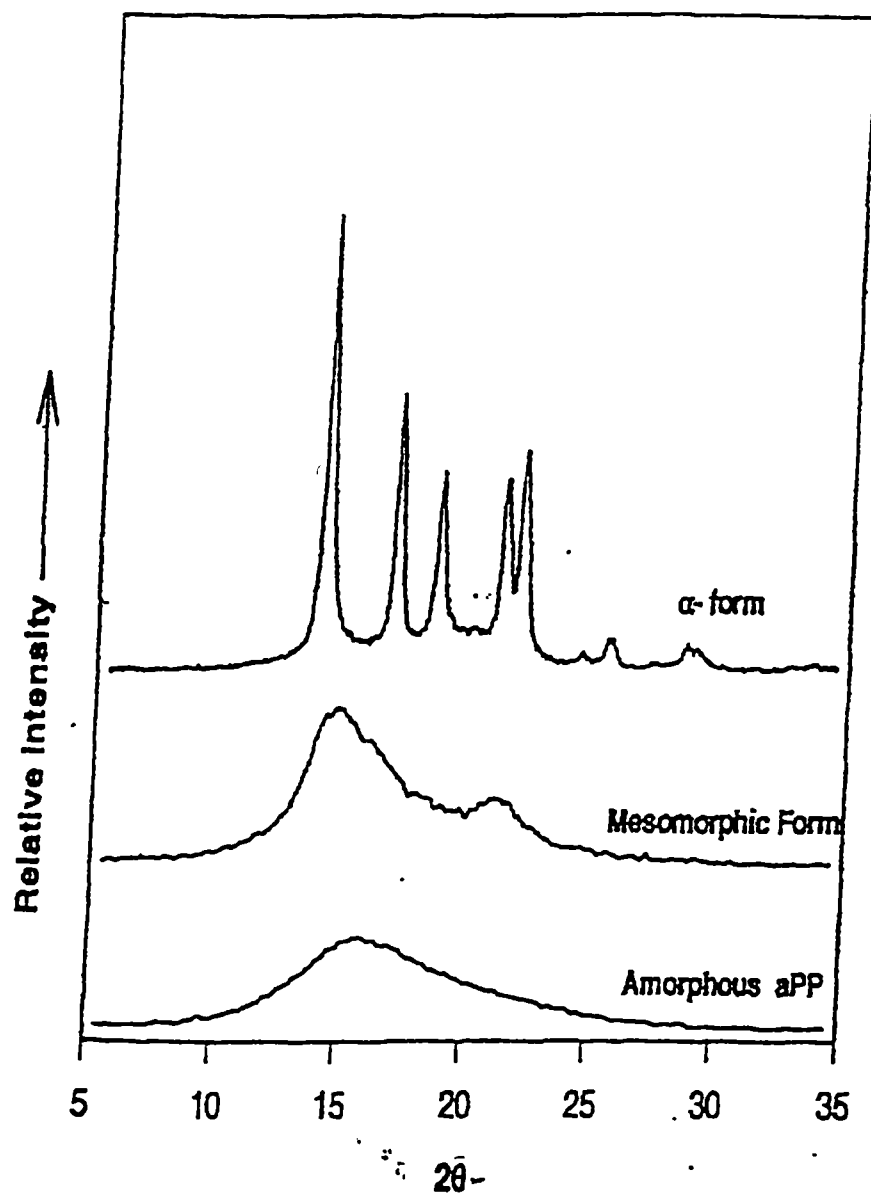


Figure 2.6 Comparison of α -iPP, aPP and the Smectic iPP Structure.

Source: Bond E., PhD dissertation, University of Tennessee, Knoxville, 1998.

Most recently, Spruiell et al. [40] conducted an experimental study on the melting behavior of Ziegler-Natta and metallocene catalyzed isotactic polypropylenes. Two metallocene (MFRs 22 and 32) and two Ziegler-Natta (MFRs 35 and 36-high tacticity) resins were used in the study. Both α and γ phases were observed in metallocene PP resins, which have been crystallized isothermally over a range of crystallization temperatures. The Ziegler-Natta resins exhibited predominantly α phase, but at high T_c 's they exhibited a weak γ -phase reflection. The combined DSC and WAXD results showed that two melting peaks were present when the γ -crystal population became significant. The relative proportion of the γ -crystal structure increased as the isothermal crystallization temperature increased.

The equilibrium melting temperatures of both α and γ crystals of the metallocene resins were measured. The α -phase equilibrium melting temperature was found to be $186\pm 2^\circ\text{C}$ for both metallocene resins and for the relatively high tacticity, conventional Ziegler-Natta resin. The latter result is consistent with literature values for the equilibrium melting temperature of high tacticity conventional Ziegler-Natta resins. The α -phase equilibrium melting temperature of the other conventional resin was found to be $178\pm 2^\circ\text{C}$. This lower value was attributed to the presence of a substantial atactic fraction (diluent) in the resin. The equilibrium melting temperature of the γ -phase in the metallocene PP resin was found to be $178\pm 4^\circ\text{C}$.

Direct measurement of the melting point by DSC gave lower values for the metallocene resins than the conventional resins. This was attributed to higher fold surface free energies of the metallocene resins compared to the Ziegler-Natta resins. It was further suggested that the higher fold surface free energies were due to segregation of the chain defects to the fold surfaces of the lamellae. Therefore, a relationship may exist between defects in the folds, higher fold surface free energy and formation of the γ crystal structure.

2.4 Properties of Melt Blown Webs

Despite the extensive research and development in the area of melt blowing, there is a paucity of published research studies mainly due to the secretive and competitive nature of the research and development work. However, there is a large body of patented literature available based on process enhancement and product development studies. An in-depth review of patents on the melt blowing process is given by Moore [41].

There are about twenty published research studies on the melt blowing process based on processing science. Also, theoretical concepts are being applied to the melt blowing process. The following is a review of literature on melt blowing. Due to the limited published studies, it was not possible to group the studies according to their specific findings. Therefore, each study is reviewed individually.

2.4.1 Factors Affecting the Physical Properties

Wente and co-workers [4,42] first established the feasibility of manufacturing submicron fibers from a variety of thermoplastic polymeric materials. The main objective of the study was to design an apparatus that would produce submicron fibers. It was thought that a nonwoven material composed entirely of submicron fibers would have great usefulness for aerosol filtration as well as for dielectric insulation. The study is thorough in its nature and describes the various aspects of the melt blown process ranging from equipment design to the single fiber properties of a web. The major findings of the study were as follows:

- Fiber diameter is a function of air temperature, die temperature, air pressure, and polymer feed rate.
- Since the molten polymer issues from the die nose tip directly into the confluence of the air stream, the greatest amount of attenuation occurs at the point of exit. Thus, the orifice size has little importance provided it is large enough to pass the melt without plugging.
- A steeper air angle gives a higher degree of fiber dispersion and random orientation. A smaller air angle yields a greater number of parallel fibers, greater attenuation and less fiber breakage.
- The ability of a polymer to attenuate to a fine fiber is dependent on its melting point, viscosity-temperature characteristics, and surface tension.

- The air resistance through a web is related to fiber diameter by the following expression:

$$\text{Resistance} = C/(\text{fiber diameter})^2$$

Where C is a constant whose value depends in part upon the porosity or density of the fiber mat.

- Below a certain melt temperature a given thermoplastic polymer forms a large granule of non-fibrous material called “shot”.
- The melt blown webs derive their strength from mechanical entanglement and frictional forces.
- The unbonded webs acquire tensile strength rapidly as fiber diameter is decreased.

Buntin and Lohkamp [5], have described the development of the melt blowing process for converting polypropylene into low-cost fine fibrous webs. Two process design concepts of using multiple dies and a circular die were also discussed. The study found that, by using multiple dies, high production rates can be achieved without increasing polymer throughput rates above the optimum. Multiple dies also produced more uniform webs with less fabric defects. The main disadvantage of the multiple dies operation was that for heavy basis weight the bonding between layers was found to be unsatisfactory. In a circular die, a die with the orifices in a circle was used. The die was operated in such a way that the conical fiber blast from the orifices was focused roughly

on a point where the fibers were formed into a continuous cylindrical roving. The technique was studied to make fine fibered cigarette filters.

Buntin and Lohkamp also made the following qualitative observations based on the processing of different thermoplastic polymers:

- Polyethylene was more difficult to melt blow into fine fibered web than polypropylene.
- Nylon 6 was easy to process and had less tendency to make shot than in the case of polypropylene.
- Most of the thermoplastics can be melt blown successfully into good finished products with few exceptions.

Jones [43], reported the effects of resin melt flow rate and polydispersity on the mechanical properties of the melt blown webs. The research was focused on the optimization of the process variables, particularly the extruder temperatures, in order to enhance the fabric properties. Several experimental resins with different melt flow rates and varying polydispersity indexes were melt blown under various conditions. In general, it was found that the strength properties peaked with the melt flow rate of 300 and decreased as the melt flow rate increased significantly above that. The fabric strength was believed to be a combination of individual fiber strength and good bonding and/or fiber entanglements.

Jones reported that the change in polydispersity of the polymers did not appreciably affect the mechanical properties. Only a slight downward trend of the fabric strength with increased degrees of polydispersity was observed. The elongation decreased with increased breadth of molecular weight distribution. The decrease in elongation was attributed to the larger diameter fibers and fewer fiber entanglements resulting from higher die swell of the broad molecular weight distribution resins.

Finally, the study showed that the effects of varying extruder temperatures and throughput rate on the strength properties were readily evident. The decreased extruder temperatures increased the tenacity and bursting strength. Increased throughput rate decreased the bursting strength.

Wadsworth and Jones [44,45] demonstrated the effects of die-to-collector distances, polymer throughput rates, and die orifice diameters on melt blown fabric properties. The study found that machine direction (MD) tenacity decreased with increased die-to-collector distance; whereas, the cross direction (CD) tenacity and bursting strength remained relatively constant. Fiber diameters increased slightly with increased DCD distance. The MD tenacity increased with increased polymer throughput rates at corresponding collecting distances. On the other hand, the CD tenacity changed little.

The study also showed that bursting strength decreased with increased throughput rates. The webs produced with a small orifice die were found to have slightly larger fiber diameters than the webs produced with standard orifice die. It was hypothesized that greater die swell could have occurred with small orifice die resulting in a net increase in filament diameter compared to the standard orifice die.

Eaton et al. [46] studied the effects of pigments on the physical properties of melt blown nonwovens. The objective of the work was to demonstrate the feasibility of processing pigmented resins into melt blown webs. Different melt flow rate pigmented polypropylene resins were melt blown under different processing conditions. The physical properties of pigmented webs were compared with the properties of the unpigmented webs. The study found that melt blown webs of uniform coloration were readily obtainable by the mass pigmentation of polypropylene resins. It was believed that the pigments acted as nucleating agents in the high melt flow rate (MFR) resins that were melt blown. The average fiber diameter decreased slightly with increased MFR for both pigmented and unpigmented webs. The apparent colors of the webs became lighter with increased resin MFR. This effect was attributed to the increased ratio of fiber surface area to the amount of pigment resulting with finer fibers produced with the higher MFR resins. The photomicrographs showed no notable differences between the pigmented and unpigmented webs in terms of fiber and web structure. The pigmented webs generally exhibited higher stiffness than the unpigmented webs.

Eaton, Wadsworth and Potnis [47] studied the suitability of melt blown fabrics for healthcare applications. The study suggested that the process parameters could be carefully controlled to produce webs with physical properties designed to meet healthcare end-use requirements. The study found that the mean fiber diameters may be largely controlled by adjusting polymer throughput and air rates. Fabric flexural rigidity provided a good indication of softness for optimized melt blown webs. In coarse, non-optimized webs, a high degree of fiber bunching was observed and there was poor agreement between tactile hand and flexural rigidity.

Wadsworth et al. [48] studied the relationships among the processing conditions, structure, and filtration efficiency of polypropylene melt blown webs. The structure of the melt blown webs was varied using different die-to-collector distances and smooth roll thermal calendering. The study found that the air permeability, and mean and maximum pore sizes increased with increased die-to-collector distance. The filtration efficiencies for water aerosols containing 0.5 and 0.8 μm latex spheres, and for bacteria (*Staphylococcus aureus*) were found to be dependent on mean pore diameter and the parameter of basis weight divided by the square of the average fiber diameter. The calendering process decreased the web thickness, maximum pore diameter, and air permeability regardless of the original values.

Spruiell et al. [49] studied the strength properties of the melt blown webs. A method to obtain the tenacity and Young's modulus of melt blown webs without direct

measurement of web thickness was proposed and tested using several series of web samples with different basis weight. The web tenacity and Young's modulus, which were, of course, normalized for weight, were found to be nearly independent of basis weight and gage length. However, these properties were greatly affected by the processing conditions. Tenacity and Young's modulus decreased with increased die temperature, air pressure at the die, and DCD distance.

Spruiell and co-workers also measured and compared the strength properties of single melt blown fibers with the strength of the web and the high speed melt spun filaments prepared from the same resins. Single fiber strength tended to be intermediate between the strength of the web and that of the high speed melt spun filaments. The low strength of the single fiber was attributed to low molecular orientation, irregular diameter profiles along the length of the fibers, and the existence of voids in the fibers.

Malkan et al. [50] reported the effects of increasing the throughput rate of polypropylene resins (300 and 1400 MFR) while maintaining constant air flow rate on the morphological and physical properties of the melt blown fibers and webs. It was found that as the throughput rate increased web elongation and bursting strength decreased. This decrease in web properties was attributed to more thermal fusing of the fibers and the presence of a greater number of larger diameter fibers.

Differential Scanning Calorimetry and X-ray diffraction studies on the web samples produced at high throughput rates in the above study indicated the presence of

more than one morphological form. It is believed that this may be a significant finding that could have an important bearing on the understanding of the melt blown process.

Malkan [50] studied the melt blowing process in a quest to assess the process-structure property relationships. He established a set of optimum melt blown processing conditions for 35, 300, 600, and 1000 melt flow rate (MFR) PP resins as a function of polymer throughput rate, air flow rate, and attenuation air temperatures. He also concluded that **Shot, Rope** (multiple fibers twisted together and deposited on the web) and **Fly** (short broken fibers formed upon breaking the polymeric streams) formation were the three limiting factors for establishing the processing temperature range for a given polymer. For this reason as the throughput rate increased, the processing window of operation (favorable conditions) became narrower, hence there was less latitude for optimizing web properties at the higher throughput rate. He also concluded that the fiber attenuation process is a function of air flow rate as well as "other mechanisms". The primary air attenuates the fiber up to a certain distance from the die, then the "other mechanisms", in conjunction with the air flow, attenuate the fibers to the final fiber diameter in the range of 2 to 8 μm .

Bodaghi [51] also reported many melt blown microfiber characterization techniques. The major finding of the study was that the water-quenched polypropylene fibers showed para-crystalline crystal structure. The air-quenched fibers showed regular monoclinic crystal structure.

Narasimhan and Shambaugh [52] attempted to model the melt blowing process. The study was based on a single die hole melt blowing process, with a circular air slot surrounding the melt blown spinnerette nozzle. Narasimhan and Shambaugh's process did not simulate the most commonly used melt blown die geometry, which consists of a row of spinnerette holes with sheets of hot air exiting from the top and bottom sides of the die. Moreover, the study lacked specific explanations of the modeling process and concepts involved.

Shambaugh continued this study [53,54] and applied macroscopic energy balance and dimensional analysis concepts to the melt blowing process. These two concepts were analyzed using different die geometries. Shambaugh proposed the existence of three regions of operation for the melt blowing process. These three regions were classified according to the extent of the air flow rate as:

Region I – is the low gas velocity region, similar to the commercial melt spinning operation insofar as the fibers are continuous.

Region II—is the unstable region, which occurs as the gas velocity is increased. In this region filaments break up into fiber segments and undesirable lumps.

Region III—occurs at a very high air velocity with excessive fiber breakage.

Shambaugh concluded that the operation of the melt blown process using predominately the low air rate (region I) was inherently more energy efficient. Further,

the author claimed that the monodisperse fiber distribution required less energy to produce than polydisperse fiber distribution. The dominant dimensionless groups in the melt blowing process were the gas Reynolds number, the polymer Reynolds number, fiber attenuation, and the ratio of the polymer viscosity to the gas viscosity.

Milligan and Haynes [55] studied the air drag on the monofilament fibers. The aim was to study the air drag by simulating the actual melt blowing conditions. The experimental set-up closely simulated the actual melt blowing operation. The two differences between the experimental arrangement and actual arrangement were: cold air was used instead of hot, and a solid monofilament was fixed on one end to a tensiometer. The air drag was studied as a function of fiber length, upstream stagnation pressure, air injection angle, and gravity orientation. Four series of experiments were conducted as follows:

1. Determination of air drag for a fiber of constant length over a range of air stagnation pressures.
2. Determination of air drag for a range of fiber length at a constant value of stagnation pressure.
3. Determination of air drag for a fiber of known length and stagnation pressure using different injection angles (15° , 30° , and 45°).

4. Determination of air drag by changing the die orientation, with respect to gravity, using a 30° air injection angle with different fiber length and stagnation pressures.

The study concluded the following:

- the drag increased with fiber length when all other parameters were constant This was due to large amplitude flapping of the fiber.
- The drag increased linearly with stagnation pressure for stagnation pressure up to 207 kPa.
- The drag increased with decreased air injection angle for any particular stagnation pressure. This finding was in basic agreement with the fundamental momentum consideration.
- Orientation of the die with respect to gravity using an injection angle of 30° showed no measurable difference in drag. It was concluded that the viscous and pressure forces on the filament far exceed the gravitational force for the flow conditions investigated.

Milligan [56] has analyzed several design concepts to minimize the energy cost in the melt blowing process. The study found that the pressure losses associated with air piping and the air heater were two of the principal energy cost areas.

The design rules are summarized as follows:

1. the piping between the air compressor and die assembly should be as short in length and as large in diameter as feasible.
2. The air heater should be as close as possible to the die assembly.
3. The number of pipe fittings should be minimized, and all piping should be well insulated.

The study also described the importance of the correct sizing of a compressor intended to serve a melt blown pilot line. The author derived equations to estimate the energy cost for a required air flow rate and discharge pressure. It was stated that, if a compressor operated at less than its designed or rated capacity, the energy cost per unit of air compressed would be increased. This increased cost was due to the fact that when the compressor was unloaded it still required a significant fraction of the rated power. Therefore, the required air flow rate and discharge pressure should be carefully established before preparing specifications for the air compressor.

Milligan M. [57] investigated the energy requirements for the melt blowing of different polymers. The studied polymers were: polypropylene, linear low-density polyethylene, nylon and polyester. The energy requirements were reported in kW-HR per kg of polymer. It was apparent from the reported data that the energy cost per unit mass of the product greatly depended on the air flow rate, air temperature, polymer throughput rate, and polymer molecular weight. The results also showed that a large fraction (greater than 85% for all the materials investigated) of the energy required was

associated with the hot air streams. The study also found that the difference in total energy consumed and the actual energy required at the die can be attributed to improper compressor size, compressor cooling, and heat losses from the die and piping. The study suggested that substantially lower energy consumption is possible if a melt blowing line is carefully designed and operated with an objective of minimizing energy consumption.

Milligan [58] concluded that a range of fiber diameter exists regardless of the operating conditions. This phenomenon is the result of the transient behavior of the drag force caused by the dynamic nature of the fiber flapping. At one instant in time, the shape of the fiber in a profile is such that the overall drag is not as great as the drag at some other instant in time, resulting in a diameter change.

Increasing the air velocity or flow rate decreased the average fiber diameter for a fixed geometry and polymer throughput. The study also concluded that the variation in diameter was nonlinear with velocity. An increase in the processing temperature reduced the average fiber diameter. This is due primarily to a decreased polymer viscosity and a reduction in the die swell. An increase in the initial air jet temperature resulted in a longer section of molten fiber polymer material since the jet temperature would be above the polymer melt temperature over a longer span.

Wadsworth and Muschelewicz [59] reported the result of a study designed to produce extremely fine melt blown fibers using 35, 300 and 700 MFR resins. The study

reported that increased airflow rates decreased mean fiber diameters. In another study, Straeffer et al [60] reported the effects of resin melt flow rate and polydispersity index on the properties of melt blown webs. The study concluded that the fiber diameter distribution appeared to be narrower as the air velocity was increased.

Warner et al [61] concluded that a) Melt blowing is a heterogeneous process that produces highly non-uniform fibers and b) properties of the fibers are a strong function of the fiber diameter.

2.4.2 Factors Affecting Shot Formation

Milligan and Utsman [3] conducted an investigation to study shot formation. Based on this investigation, it was concluded that the random type of shot formation mechanisms for well designed dies using modern, high MFR polypropylene resins involve one of the modes described below or a combination of the two:

- Molten polymer which consists of fused fibers arrives at the collector and results in an area of polymer or film spot which shows signs of melting the adjacent fibers. The occurrence in the webs is random with no detectable pattern.

- Fused filaments which are solidified but not significantly drawn arrive at the collector and show no evidence of melting on the web. The occurrence in the web is random with no detectable pattern.

Both of these modes are consistent with filaments touching and fusing close to the die. Since fused filaments will have a larger volume to surface area they will not cool as fast as the non-fused individual fibers and thus they may be molten upon striking the collector, whereas all of the surrounding fibers are solidified before reaching the collector. Not only were these mechanisms consistent with the photographs but they were also consistent with all of the observed techniques of reducing shot. The list below of actions, which will reduce shot, was developed:

- a- *Increase primary air velocity*, which increases heat transfer by increasing the heat transfer coefficient and by increasing the filament drawing.
- b- *Reduce the primary air temperature*, which will give a lower jet temperature and thus more cooling before the collector.
- c- *Reduce the polymer temperature*, which reduces the amount of cooling required to solidify the filaments. Will also result in larger average fiber diameter.
Limited by chugging or fracture of the filaments.
- d- *Decrease throughput*, which results in less die swell and smaller filaments, which cool quicker and are farther apart near the die.
- e- *Use a higher MFR resin*, which results in smaller diameters and the same changes as a decreased throughput.

- f- *Use a more uniform resin* including a narrower molecular weight distribution.
Any time the resin has a non-uniformity there are variations in the discharge from the orifice which results in lateral movement and thus a greater probability of two filaments touching near the die.
- g- *Use fewer holes per inch in the die*, which moves the filaments further apart.
- h- *Improve orifice alignment*, which reduces the probability of two filaments touching near the die.
- i- *Use water spray or reduced temperature ambient air*, both of which increase cooling and thus allow filaments to touch and not fuse.
- j- *Use cool crossflow air* to give lower jet temperatures and behavior similar to item (i) above.
- k- *Increase the distance between the die and collector*, which results in more filament cooling before the collector (limited by non-uniformity in the form of roping).

Since any one of these actions will change web characteristics in addition to shot, it will require a combination of techniques to eliminate shot and at the same time obtain the desired web characteristics such as average fiber diameter. In addition, it is concluded that in general fused filaments result not only in producing "shot", but also in producing larger average fiber diameters and less uniform fiber diameters. The result is less uniform webs with degraded performance for most applications.

Wallen [62] conducted an experimental investigation using light scattering experiments on the melt blowing process, he was able to quantitatively develop a method to measure shot. He measured the shot intensity which is a measure of the number of shot particles in a one inch square web per weight of the sample in milligrams per area of the sample in centimeters squared. He concluded that there was a strong correlation between initial fiber motion and the amount of shot found in the melt blown webs. The amount of shot formed varied inversely with the rate of the loss of linear collimated fiber orientation. The results from the fiber orientation and shot formation studies, the fiber motion studies, and the video images indicated that the mechanism responsible for shot formation is the touching and thermal fusion of molten fibers near the die.

Bresee [63] studied the shot development in melt blown webs, he obtained several shot observations from melt blown webs by using simple techniques that cannot be disputed easily. Some of these measurements produced unexpected and interesting results, which indicate that shot development is more complicated than was previously thought. He reported the following experimental observations related to shot in melt blown webs:

- Shot is common in melt blown webs and uncommon in other webs.
- Most (or all) features describing shot (size, shape, etc.) vary substantially.
- No definite structural distinction between fibers and shot exists.

- Some webs contain a large number of very small shot particles.
- The vast majority of shot particles that are visible to the human eye have diameters in the range of 0.1-0.3 mm.
- The over-all shape of most shot particles that are visible to the human eye is approximately circular; most visible shot particles on the collector side of webs are disk-shaped, being approximately circular and flat.
- The volume of an individual shot particle that is visible to the human eye is roughly estimated to be 0.007 mm^3 .
- The amount of web area containing shot is quite small, typically being less than 0.1%.
- Shot particles that are visible to the human eye are mostly well crystallized and contain large spherulites.
- Perimeters of shot particles often contain fiber-like structures; most shot particles are connected to numerous neighboring fibers in the web
- Medium and large sized shot particles often cause substantial melting of nearby fibers in the web.
- The number of shot particles per unit basis weight decreases with increasing basis weight when basis weight is varied only by changing collector speed.
- The number of shot particles per unit web area decreases with increasing die-to-collector distance.

- More shot particles are located on the collector side of lower basis weight webs, but more shot particles are located on the other side of heavier basis weight webs, when basis weight is varied by changing only the collector speed.

Bresee also proposed three models for shot development. The most difficult challenge of these models, he reported, was the ability of these models to explain how the location and speed of the web collector significantly influence shot availability in webs.

A) Direct-shot-formation Model In this model, fibers and shot are both formed initially, so shot particles are produced directly without undergoing a fiber-to-shot transformation. The number of shot particles present in a web would be expected to depend on the rate of shot formation and the rate of shot destruction. Since the size, shape, and internal morphology of shot differ significantly from those of fibers, different resin structures or processing experiences must exist for shot and fiber.

B) Shot-precursor Model This model involves forming fibers and other objects that subsequently undergo a transformation to shot particles. These objects are called shot precursors, and they may include a variety of structures, including large-diameter resin streams that touch one another near the die, thick fibers, fragmented polymer melt, and almost any resin structure without fiber shape. Most precursors are small compared with shot particles that are visible to the human eye.

C) Fiber-transformation Model This model involves first forming fibers and then subsequently transforming them into shot particles. The number of shot particles present in a web would be expected to depend on the rate of the transformation. The development of very small shot particles is plausible by this model because a complex transformation is not required to change small fibers into small shot.

Jana [22] conducted a study on a set of melt blowing resins in an effort to understand the complex process of melt blowing metallocene polypropylene by comparing it with conventional Ziegler-Natta propylene polymers. Two sets of metallocene and conventional resins were melt blown. The first set of resins had an MFR >1000 and the second <900. The webs were then characterized for their structural and mechanical properties. A detailed statistical analysis was carried out on the results to understand and optimize the process conditions for melt blowing of different melt flow rate conventional and metallocene polypropylenes. The study concluded that smooth processing equivalent to that of conventional polypropylene could be carried out on the metallocene resins of medium and high MFR ranges using the conventional melt blowing equipment. Both conventional and metallocene resins of <900 MFR, process well at different processing temperatures and conditions. The advantage of metallocene polypropylene is that, it can be processed at lower processing temperatures compared to conventional polypropylene to achieve comparable structure and properties such as fiber diameter, filtration efficiency, hydrohead, etc.

The >1000 MFR polymers are very susceptible to the change in processing conditions and perform even better than <900 MFR resins but only at specific processing conditions. The metallocene polypropylene resins performed best at 218°C with DCD of 12 inches, maximum air flow and air temperature close to the melt temperature while conventional PP performed well at 246°C with similar processing parameters as in the case of metallocene PP. The results of the study show that the processing window for the metallocene PP at lower processing temperature is wider compared to conventional PP as the variations in properties were less, with change in the process parameters. The conclusions were drawn from the observed fiber diameter and other performance properties.

The study also reported that <900 MFR resin requires slightly higher processing temperature typically 232°C for metallocene PP and 260°C for conventional PP. A fact that can lead to savings in energy in processing polypropylene melt-blown webs with better properties. **Tables 2.1 and 2.2** show the summary of the statistical analysis regarding shot production for the different resins in the study:

**Table 2.1: Effect of Processing Conditions on Shot Production for the
>1000 MFR Resins in the above Study [22]**

Processing Condition	Conventional PP	Metallocene PP
Melt Temperature	Significant	Significant
	Low@204°C	Low@204°C
	High@260°C	High@260°C
Air Temperature	Not significant	Significant
		Low@ lower temperatures
		High@ higher temperatures
DCD	Significant	Significant
	Low@ 30 cm	Low@ 30 cm
	High@ 20 cm	High@ 20 cm
Air Flow	Not significant	Significant
		Low@ Medium
		Moderate @ Max& Low

Table 2.2: Effect of Processing Conditions on Shot Production for the <900

MFR Resin in the above Study [22].

Processing Condition	Conventional PP	Metallocene PP
Melt Temperature	Significant	Significant
	Low@ lower temperatures	Low@ lower temperatures
	High@ higher temperatures	Very high@ higher temperatures
Air Temperature	Not significant	Not significant
	Low@ equal melt	Low@ lower temperature
	High@ higher temperatures	High@ higher temperatures
Air Flow	Not significant	Not significant
	Almost equal results	Almost equal results
OVERALL BETTER RESULTS OF CONVENTIONAL PP		

CHAPTER THREE

EXPERIMENTAL APPARATUS AND PROCEDURES

This chapter describes the experimental apparatus used to produce the melt blown fabrics and the procedures used to characterize these fabrics. This research effort is a part of a continuing investigation here at the University of Tennessee that is supported by Exxon Mobil Chemical Company.

3.1 Materials

The polypropylenes used in this study were supplied by Exxon Mobil Chemical Company. An early generation commercial metallocene resin and a conventional Ziegler-Natta resin were used as base resins. A description of the resins is listed in the following sections. Melt flow rate of the resins and gel permeation chromatography measurements of the collected webs were conducted by Exxon Mobil at its Baytown Polymers Center. Two sets of resins were used in this research and are described in sections 3.1.1 and 3.1.2.

3.1.1 First Part: Blends of Metallocene Based PP and conventional Ziegler-Natta Polypropylene.

The first group of resins were blends of different percentages of metallocene and conventional Ziegler-Natta resins. Table 3.1 shows the blend ratios of the different

Table 3.1: Blend Ratios of the Different Blend Resins

Resin	Metallocene %	Zeigler-Natta %
B1	100	0
B2	80	20
B3	60	40
B4	40	60
B5	20	80
B6	0	100

resins. The conventional Ziegler-Natta PP (B6) resin is a 600 MFR. The metallocene PP resin (B1) is a 700-800 MFR resin.

3.1.2 Second Part: Nucleated Resins

All of the resins studied were supplied by Exxon Mobil Chemical Company. The purpose of adding a nucleating agent is to accelerate the crystallization (solidification) process of the fibers during the attenuation process. If the nucleating

agent were to successfully accelerate the crystallization process then the probability of filaments fusing would be presumably reduced. The resins differed by the parts per million (ppm) content of the nucleating agent and the agent type itself, but the base resin (BR) was always the same metallocene 700-800 MFR resin. **Table 3.2** lists the content of the first kind of nucleating agent (nucleating agent 1). **Table 3.3** shows the content of the second kind of nucleating agent (nucleating agent 2).

Table 3.2: First Kind of Nucleated Resins (Sodium Benzoate Nucleating Agent)

Resin	Content of Nucleating Agent (ppm)
BR	0
NR1	500
NR2	1000
NR3	1500
NR4	10,000

Table 3.3: Second Kind of Nucleated Resins (Millad Nucleating Agent)

Resin	Content of Nucleating Agent (ppm)
NR5	500
NR6	1000

3.2 Fabric Processing

The melt blowing experiments were conducted on a melt blowing pilot line (Figure 3.1) equipped with a single hole die or a die containing thirty holes in a one inch length. The extruder used for these experiments was a Killion Extruder, KLB series, with a one inch diameter screw, a L/D ratio of 28, and a Maddox mixing head. The air pressure for the experiments was supplied by the house air compressor. The pressure difference was adjusted by means of a valve that controlled the amount of compressed air let into the system. The air velocity was calculated from the pressure difference between the compressed air and the atmosphere, and the temperature of the air. The melt pressure was monitored at the die entrance by two probes calibrated in psig. The temperature of the polymer was monitored at several positions in the extruder and at the die exit. The temperatures of the polymer and air at the die exit were monitored by means of Omega Type K (Chromel-Alumel) thermocouples, accurate within one degree Celsius. Also, the pressure of the air near the exit was monitored by a probe calibrated in psig.

The die configuration did not include a gear pump or a feed distribution system. The polymer melt was fed directly into the die. Two wire mesh screens filtered the melt, the first being a very fine mesh and the second being a very coarse mesh. The L/D ratio for both of the dies was 8.5 with holes approximately 0.016 inches in diameter. The multihole die had holes spaced approximately every 0.02 inches. The angle of the air

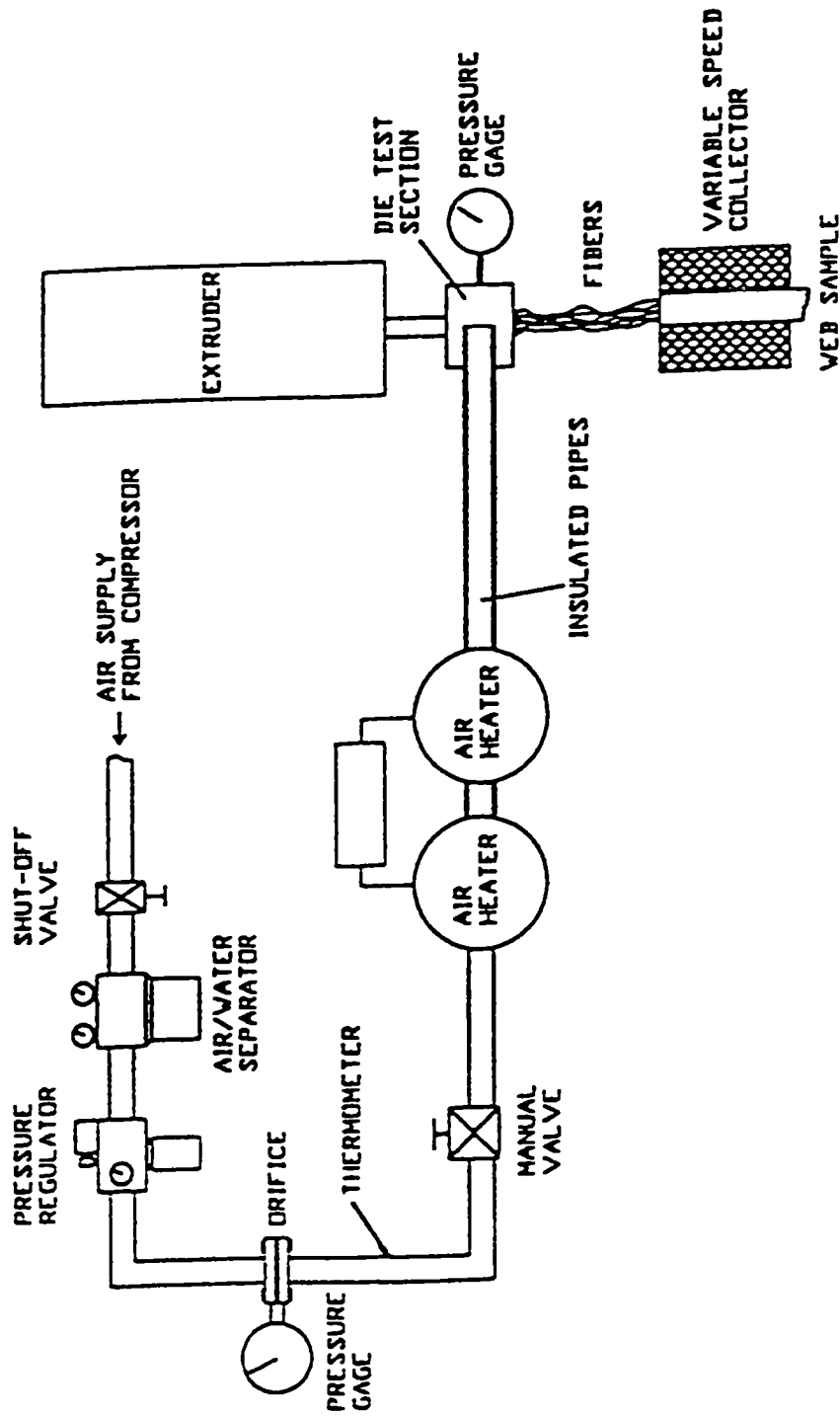


Figure 3.1 Schematic of the Melt Blowing Facility at the University of Tennessee, Knoxville.

Source: Utsman, F.M., Master's Thesis, University of Tennessee, Knoxville, 1995.

flow in the nose piece was sixty degrees and a setback gap of 0.079 inches was used for all experiments. The die configuration can be seen in **Figure 3.2**

The webs were collected on a rotating drum collector, equipped with a variable rheostat to control the collection speed. The drum consisted of a cylindrical piece of sheet metal and did not have adjustments for height. The webs were produced at a basis weight of 1.5 oz/yd². The collection speed was calibrated daily by means of collecting web samples from the collector, weighing the samples, and adjusting the drum speed accordingly.

3.3 Processing Conditions

The resins were processed on the line described above under the following conditions:

Extrusion Temperature: 420°F, 450°F, 475°F, 500°F

Die (Air) Pressure: 3 psig, 5 psig, 7psig

Die to collector distance (DCD): 12, 14 and 16 inches.

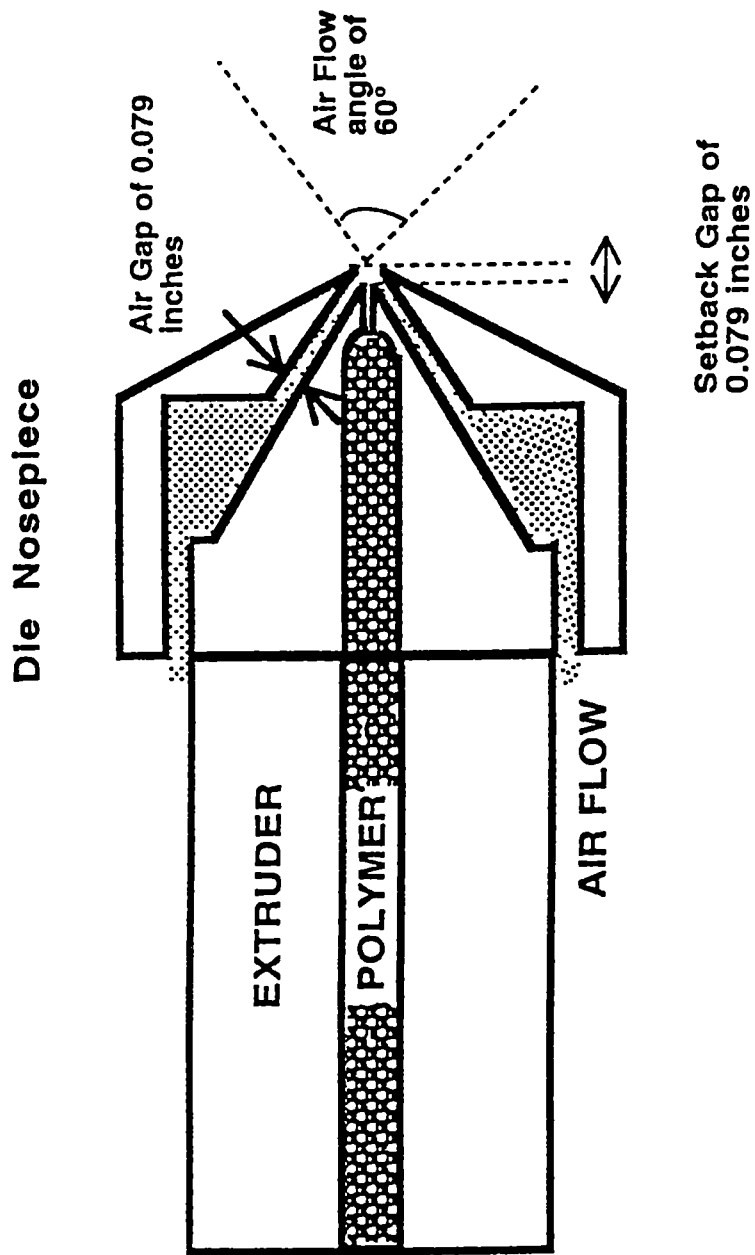


Figure 3.2 Experimental Melt Blowing Die Nosepiece Configuration.

3.4 Melt-Blown Web Creation

In order to create a melt blown web sample, the first operation that must be performed is the determination of the process conditions and the resins. This involves choosing the following: resin/polymer itself, polymer throughput, polymer temperature, test section die geometry, air temperature, air flow rate/die pressure, die to collector distance (DCD) and basis weight of the melt blown web. Once the desired experimental parameters are determined, the actual production of the web samples can proceed. First a steady state operating condition must be obtained. This was done by opening the shut off valve and opening the manual valve until the pressure gage read two inches of water. The air heaters and five zone heaters along the extruder were set to the specified process temperature (Figure 3.3). Once the five zone heaters had reached the temperature set point, the cartridge heater was activated to heat the die tip. When the cartridge heater had reached its desired set point, the extruder motor is engaged. The screw motor speed is varied to provide the desired polymer throughput. This throughput is verified by collecting a sample of the web over a specific time and measuring its mass using a digital balance. With the throughput set and melt pressure noted, the air velocity is increased by increasing the die pressure to its specified value and the air heater set point is increased or decreased in order to obtain the proper air temperature at the specified die air pressure. The basis weight of the web is controlled by the collector drum RPM. The RPM of the collector drum was controlled by the ten turn potentiometer which varied the rotational speed of the ¼ horsepower electric motor.

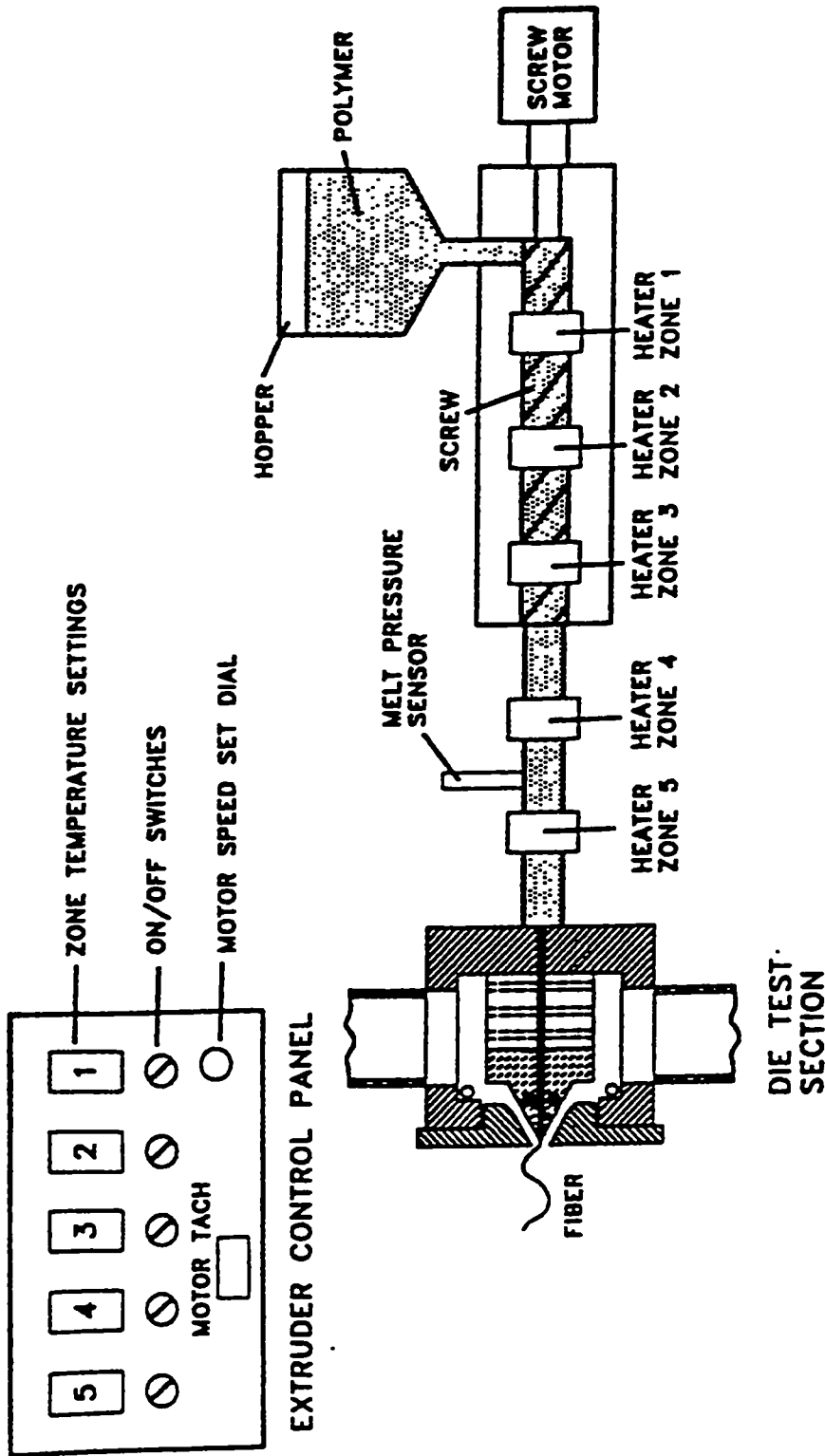


Figure 3.3 Cross-sectional View of the Single Screw Extruder and the Die Test Section

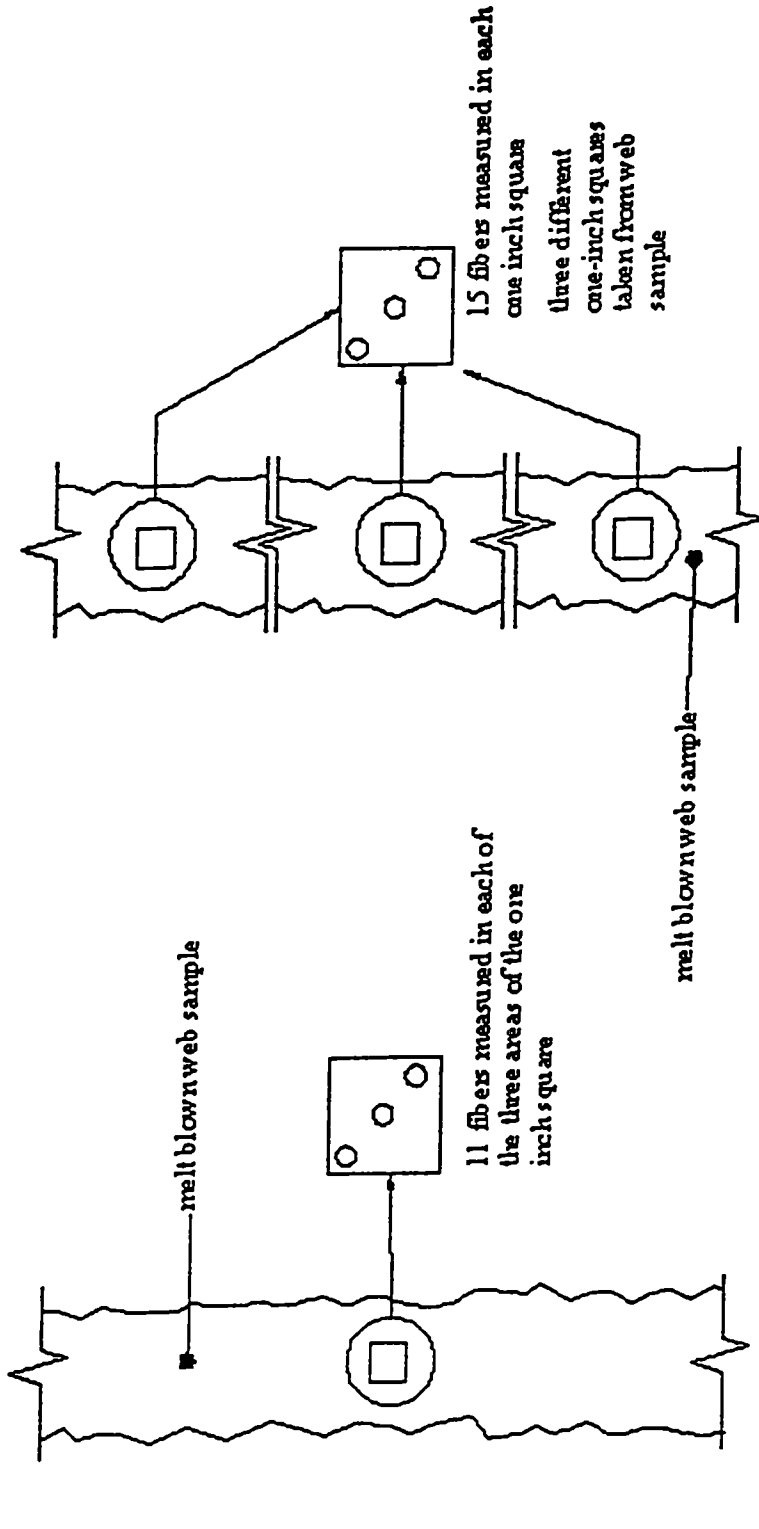
Source: Utsman, F.M., Master's Thesis, University of Tennessee, Knoxville, 1995.

3.5 Analysis of Web Samples

The melt-blown webs were analyzed in order to determine average fiber diameter, the number of shot per unit area and the size and shape of the shot particles.

3.5.1 Average Fiber Diameter Determination

The average fiber diameter was determined using one of two methods. These methods are optical microscopy and scanning electron microscopy. The optical microscopy method is performed using an optical microscope with a scaled eye piece and a total magnification of 400. Previous experimenters [64,65] have all determined the average fiber diameter of the web by cutting a one-inch square sample, **Figure 3.4**, and placing the sample under the microscope. Three locations in the sample were then selected and the diameters of at least eleven individual fibers were measured using the scaled eyepiece for a total of at least thirty-three fibers. The sizes of these thirty-three fibers, based on the divisions of the scaled eyepiece, were entered into a BASIC program and using the known magnification of the microscope, the average fiber diameter, standard deviation, coefficient of variation, fiber dispersity and diameter histogram were determined. The methodology used to determine the average fiber diameter for this investigation was similar to that of previous experimenters [64,65]. The only variation was that this research did not remove just one inch sample from the melt-blown sample for all diameter measurements. In this study, three one-inch square



Previous Research
Diameter Analysis

Current Research
Diameter Analysis

Figure 3.4 Methodology Used to Determine the Average Fiber Diameter for Previous and Current Investigation.

samples, **Figure 3.4**, were removed from three locations in the web sample and fifteen diameter measurements were taken from each of the three samples using the same scaled eyepiece, for a total of forty-five diameter measurements. The purpose of the change was to take diameter measurements from different locations in the web sample itself not just three locations in same one-inch square sample. The only other deviation from the methods used previously was the use of a spreadsheet to calculate the parameters previously calculated by the BASIC program. The use of an optical microscope is susceptible to human influences. In order to reduce this influence, the same person performed all diameter measurements used throughout this research. Once the location in the web sample was selected for diameter measurements, the microscope was focused into the web sample and any fiber that could be brought into focus and crossed the scale in the eyepiece was measured. **Figure 3.5** illustrates this process. In this figure the three white lines are fibers and the scale is shown in the center of the microscope view. In this figure the two smaller diameter fibers actually cross the scale where the larger fiber in the lower left does not. Therefore the two smaller fibers are measured and the larger, more easily measured, fiber is not. This process helps reduce any human influences.

The other method used for the determination of average fiber diameter is scanning electron microscopy (SEM). This method allows the researcher to make the SEM image and measure the diameters of the fibers from the image. The SEM image of the web sample is captured and recorded on a 4 inch by 5 inch photograph. This

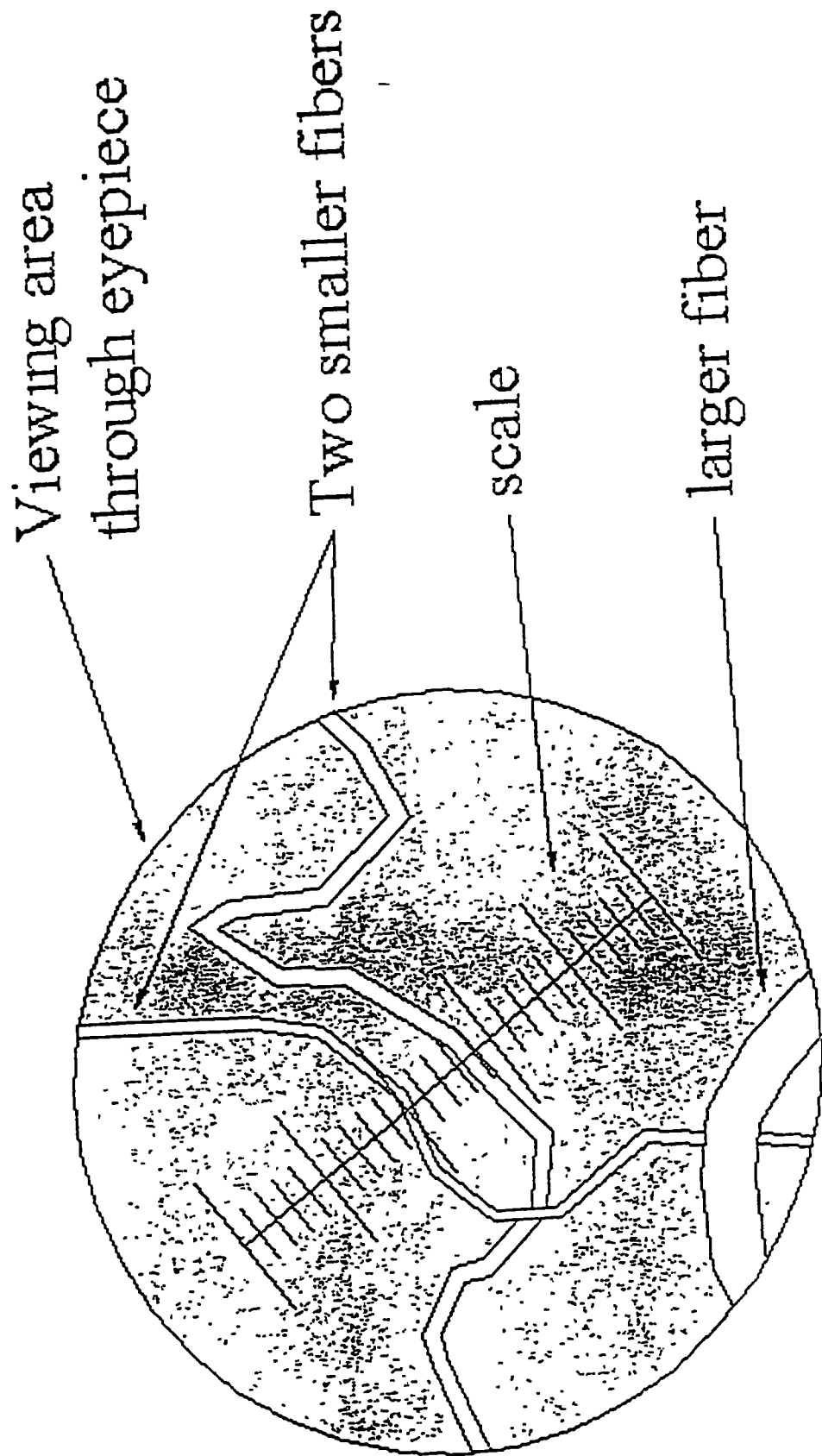


Figure 3.5 Drawing of View Through the Microscope During Diameter Analysis.

photograph is then scanned using a flatbed scanner and a personal computer. The scanned image is then imported into an imaging program, and the diameters of any selected fiber are recorded by knowing the magnification of the SEM image. The researcher can measure diameter of as many fibers as he or she wishes. Usually, a line is drawn across the image and any fiber crossing the line is measured. Again, this is done to remove any human influence in the choices of which fibers to measure. The SEM diameter trends agree with the optical microscopy tests performed by this research group. **Figure 3.6** shows the technique used to chose the fibers under measurement. In order to have representative and accurate average diameters, two diagonal lines were drawn across each photomicrograph. The diameters of all the fibers at the points where the lines crossed were measured. A minimum of 30 fiber diameters were measured for each photomicrograph

Scanning electron microscopy was used in combination with a thin gold coating to produce high resolution images. A Cambridge Instruments Stereoscan 360 scanning electron microscope with a tungsten filament and a resolution capability of 2.5 nm (under ideal conditions) was used. The gold plating was done on a Technics Hummer I gold plater under a 100 millitorr vaccum. A current of 10mA was set for a time of 2 minutes for all samples. The photomicrographs were taken at 15kv accelerating voltage in order to minimize the charging effects and the thermal degradation of the specimens.

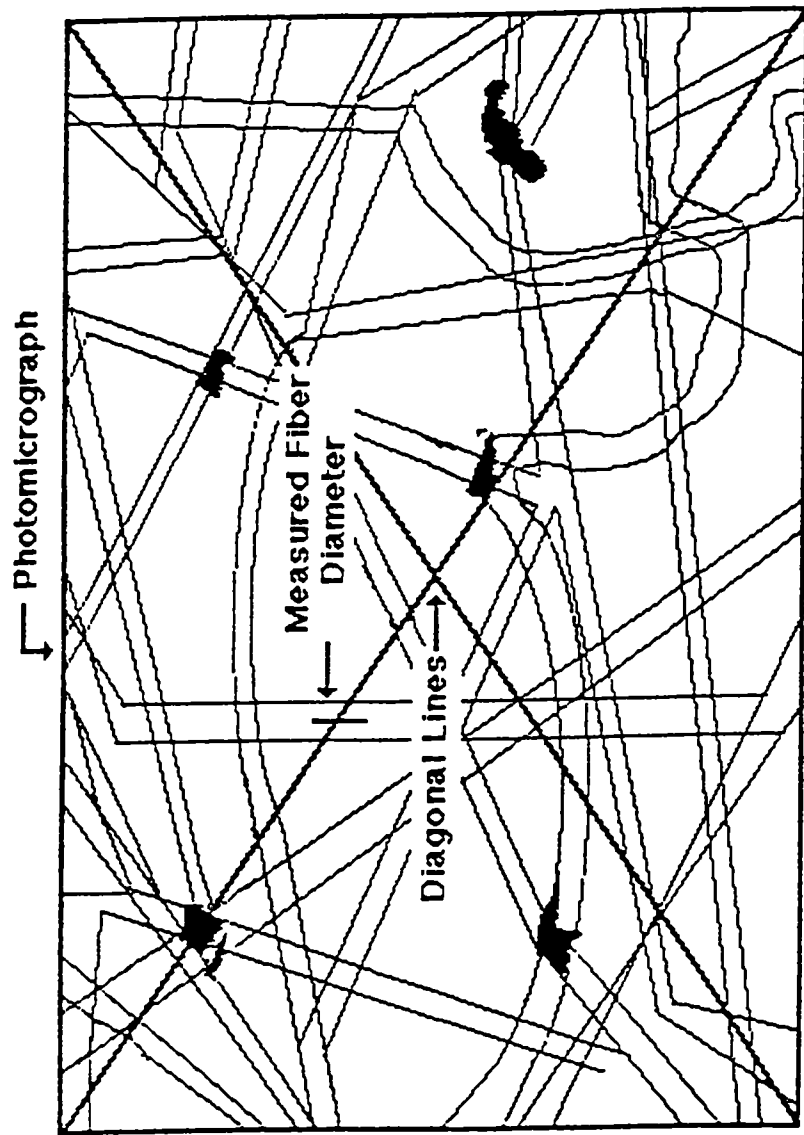


Figure 3.6 Schematic Showing Fiber Diameter Measurement.

3.5.2 Number of Shot per Area Determination

Since shot has already been defined as a globule of polymer that has a diameter much greater than that of the average diameter of the surrounding fibers, it is important to determine a method to count shot properly. Previous experimenters [62,64] used a shot rating and/or shot intensity system. The shot rating system is a system developed at TANDEC to evaluate the shot quantity in a web sample by assigning each sample a rating from one to five. These numbers correspond to a baseline group of webs that have previously been assigned one of these values. The sample to be rated must have the same basis weight as that of the baseline group. The sample to be rated is then placed on a light table where the shot particles become more visible. This is due to the fact that the light passes through the shot easily, but light can not easily pass through the fibers. With this knowledge, the shot particles appear as bright spots in a diffuse background due to the surrounding fibers. This method has been used in the past but it is limited by the basis weight aspect of the rating system and the fact that a true quantitative shot value is not produced. For this reason, Utsman [64] developed the shot intensity method. This method involves counting the number of shot greater than 100 μ m in a one-inch square sample and dividing that value by the mass of the sample. The number of shot is counted using an optical microscope. Shot is detected in the same manner as the shot rating method and a scaled eyepiece is used to determine the size of the detected shot. The method is quantitative in that an actual number is produced as an output but it is extremely tedious and time consuming.

The shot determination chosen for this research effort is the computer operated WebPro method. The WebPro shot determination method is similar to the previous methods in that it also uses the contrast in light level between the fibrous web area and shot itself. A complete description of the WebPro system is provided in a paper by Bresee and Yan [63] but a brief description is included here for convenience. A schematic of the WebPro system is shown in **Figure 3.7** [63]. This system includes a diffuse light source, a motorized table with x-y motion capability, a video camera, and a computer to capture the video images and run the WebPro software program. The web sample is placed between two pieces of glass in order to flatten the sample. The sample's orientation between the glass plates is determined by the size of the motorized table. Control of the WebPro shot detection analysis is maintained through operator controlled parameters. These parameters are comprised of light source intensity as detected by the video camera, light contrast level, and threshold value or detection sensitivity. The program assigns a light level to each pixel the video camera views. The program then scans the pixel light level and when it discovers a bright pixel next to a darker pixel, it marks the pixel boundary. Once the computer completes its scan it has marked a boundary between the dark and light pixels. An example image of the process is provided in **Figure 3.8** and **Figure 3.9**.

The WebPro system is advantageous in that it is automated and more than one square inch of the web sample is examined for shot. The amount of web area that can be

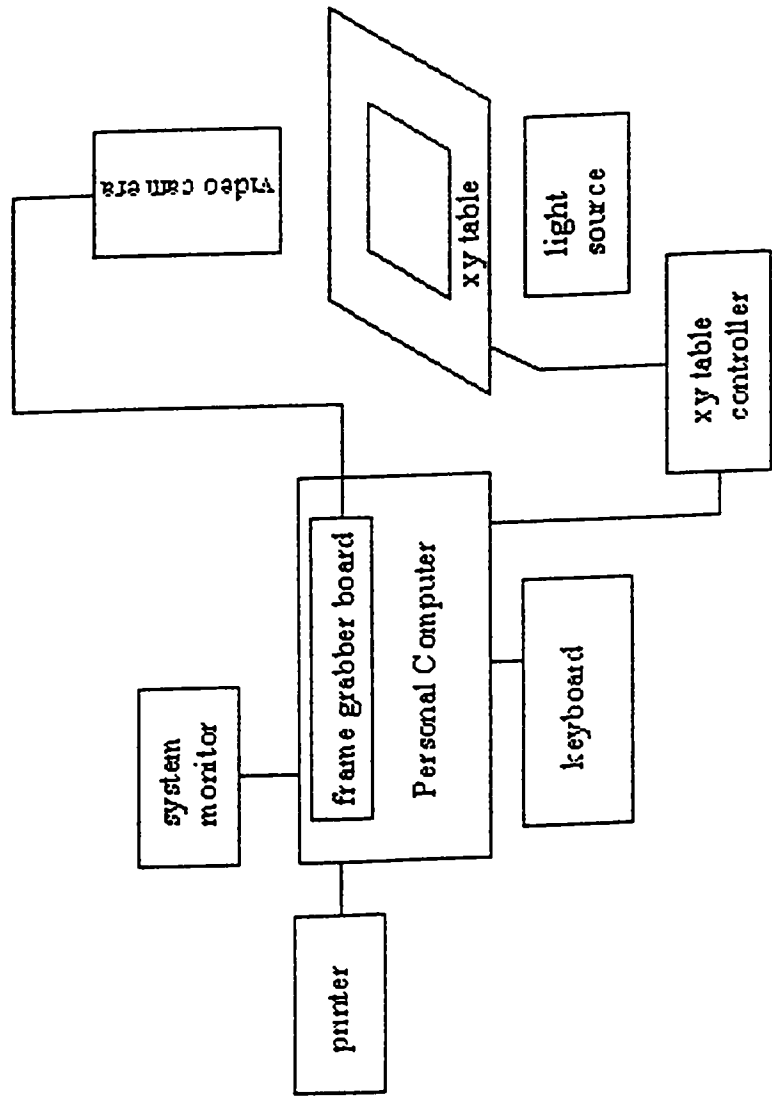


Figure 3.7 Hardware Configuration for Shot Analysis.

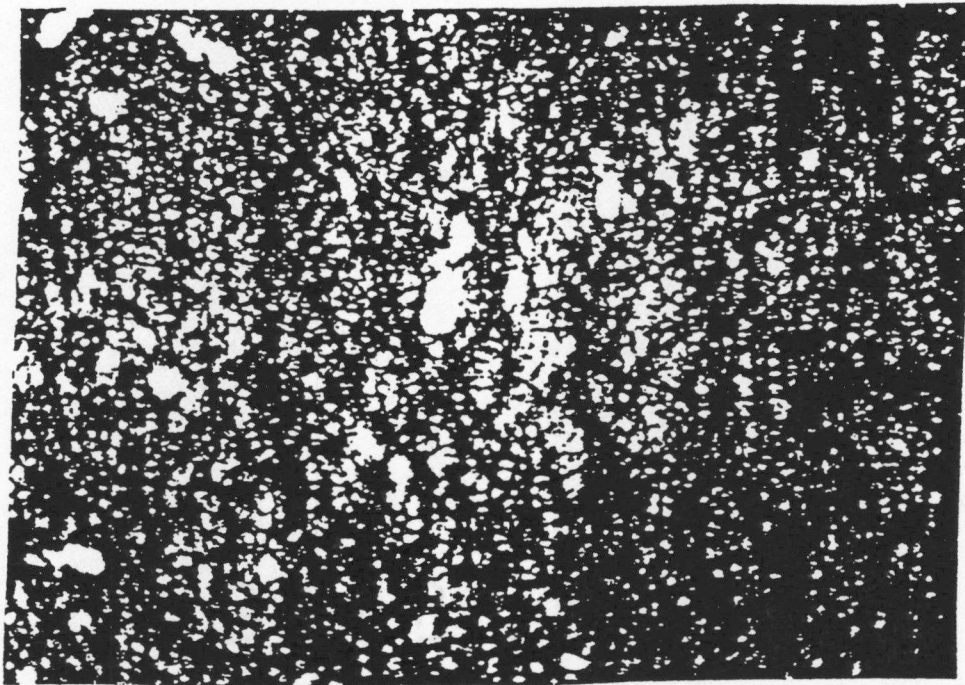


Figure 3.8 WebPro Image Before Scanning Process (Bright Spots are Shot)

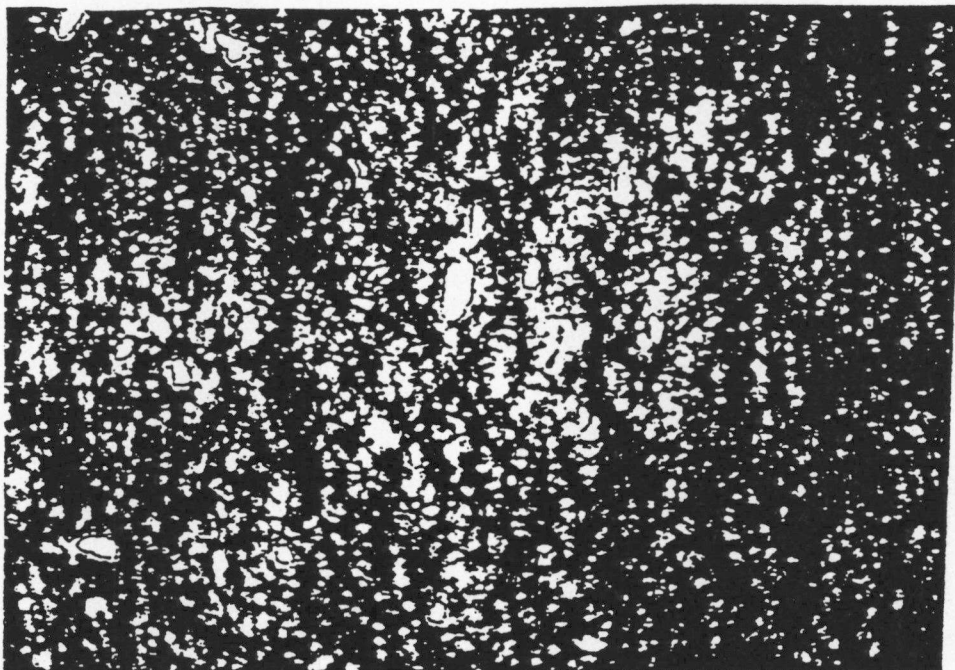
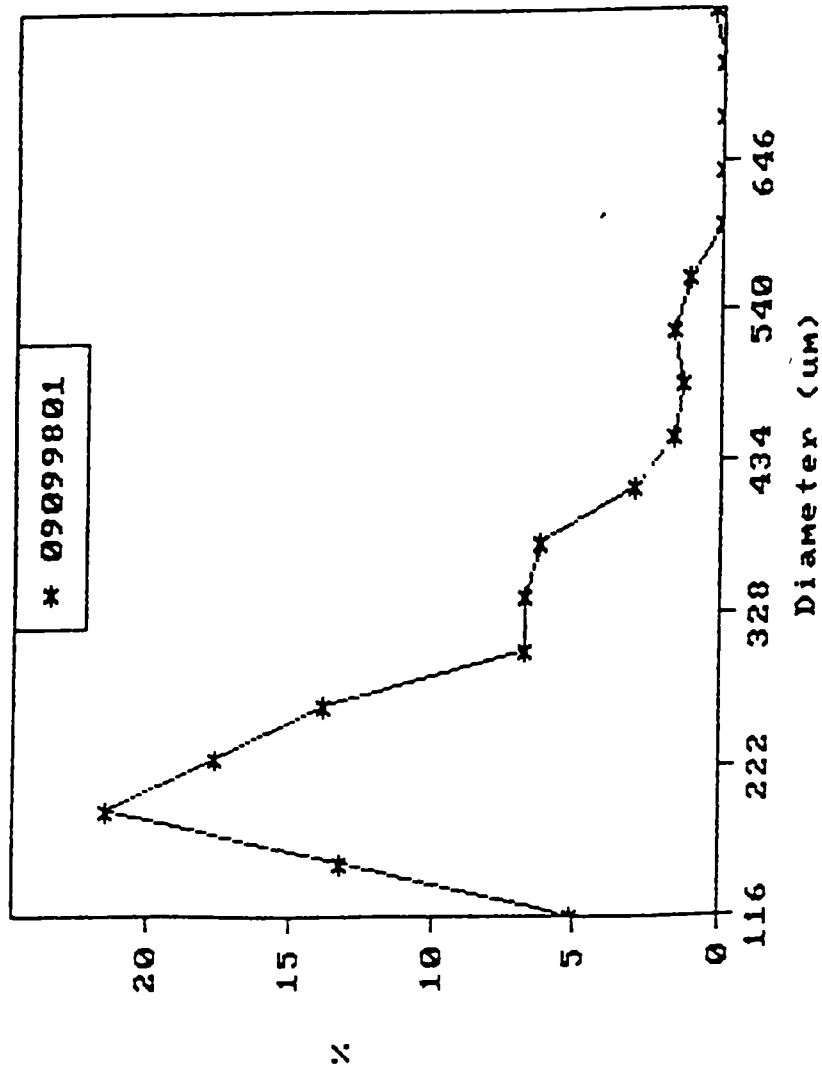


Figure 3.9 WebPro Image After Scanning Process (Notice Line Around Bright Spot)

scanned by WebPro's video camera is determined by the size of the motorized table and the physical characteristics of the web sample itself. The physical characteristic of the web that is more important is uniformity. The edges of a web sample are "ragged" or non-uniform and therefore the web area inside the sample edges is scanned by WebPro. The samples created on the melt blowing line in Dougherty Engineering building are approximately three inches in width. Once the ragged edges are ignored, there is approximately a ¼ inch to one inch strip down the center of the produced sample. The WebPro setup used for this research allowed the analysis of thirty three web samples that were 0.63 in. by 0.47 in. This sampling amount is almost ten times the area of the optical shot intensity method, and therefore is more representative of the shot in the entire sample. WebPro returns the following values from its analysis: number of shot [Shot (N)], shot per cm² [N/cm²], mean shot size [Mean], maximum shot size [Max], minimum shot size [Min] and percentage shot cover area [Cover (%)] of the measured sample. The program also produces a graph displaying the shot size distribution in the analyzed sample. **Figures 3.10 through 3.12** are examples of a typical WebPro analysis output

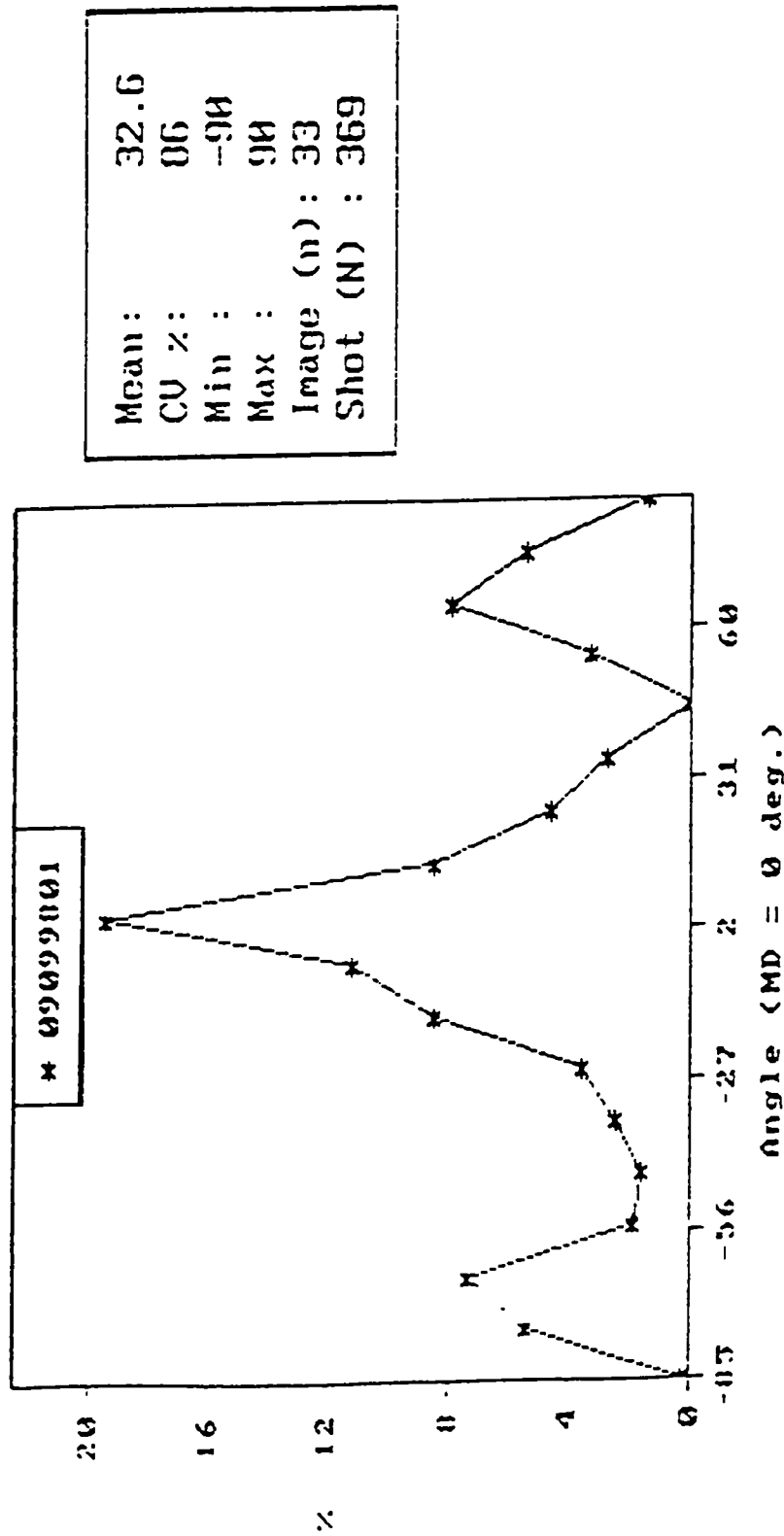
Figure 3.10 provides the shot diameter distribution in the web sample. This figure also provides important statistical data for the detected shot. The most useful information provided in this figure is the shot per cm² and the shot cover percentage. Even though Figure 3.10 contains most of the information that was utilized in this research, WebPro provided information about the shot orientation distribution and shot



Mean:	254
CV %:	39.4
Min :	97.7
Max :	770.5
Image (n):	33
Shot (N) :	369
N / cm ² :	5.8
Cover (%):	0.4

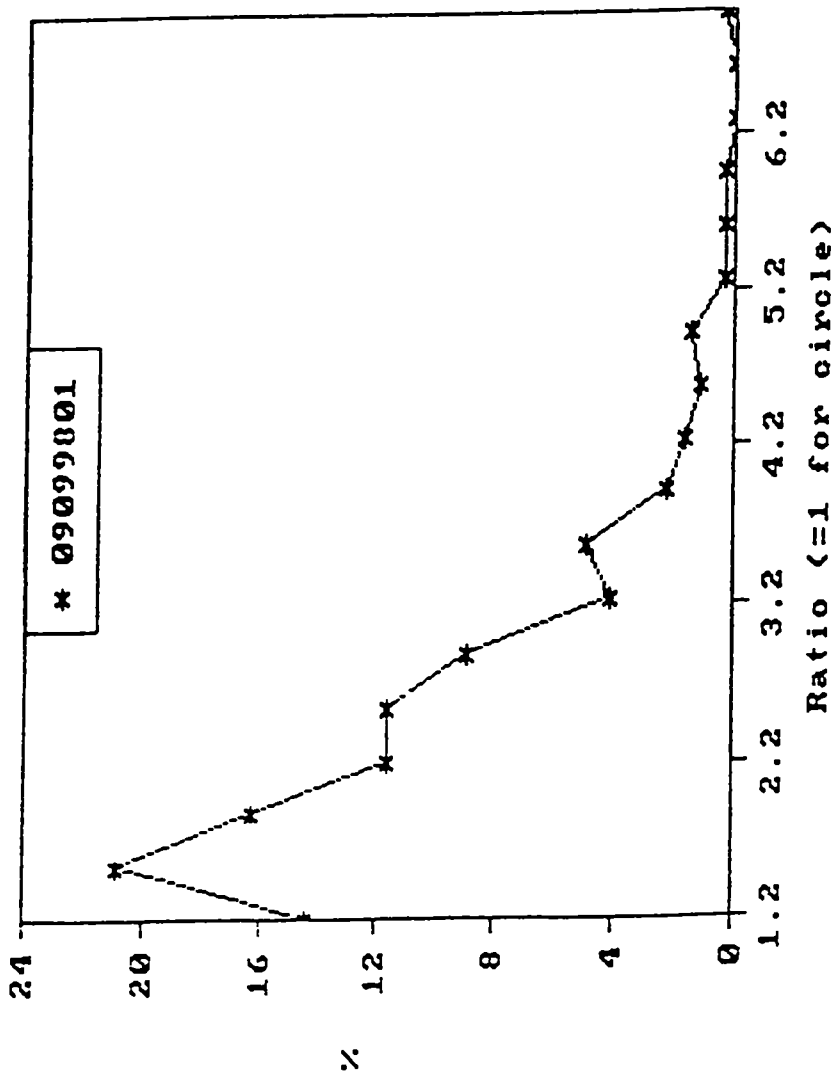
Shot diameter distribution.

Figure 3.10 WebPro Shot Analysis Output- Shot Diameter Distribution



Shot orientation distribution.

Figure 3.11 WebPro Shot Analysis Output-Shot Orientation Distribution



Mean:	2.23
CV %:	42.19
Min :	1.01
Max :	7.12
Image (n):	33
Shot (N) :	369

Shot aspect ratio distribution.

Figure 3.12 WebPro Shot Analysis Output-Shot Aspect Ratio Distribution

aspect ratio distribution in the web samples as well. This information is shown in Figures 3.11 and 3.12.

3.5.3 Effect of Processing Parameters on WebPro Shot Detection

During the shot data reduction process, a few WebPro anomalies were encountered. The most important of these anomalies is the effect of process temperature and die air pressure on the effectiveness of the WebPro shot detection process. As previously shown by other experimenters [65,66], and shown later in the following chapter, the average fiber diameter decreases inversely with process temperature and die air pressure. With the production of small fibers comes a finer, denser web sample. This type of web is more optically opaque and a shot particle will transmit light more easily than the average web and thus a distinct bright spot in the web is produced. As the process temperature and die air pressure is decreased the web fibers are larger and the light transmittance of the web sample is drastically increased. The light transmittance of the larger fiber web samples is due to the larger open spaces between fibers and WebPro evaluates this light transmittance as shot particles. Therefore at the lower process temperatures and die air pressures the web sample is visually inspected and if no shot is seen the sample is graded as having zero shot. If numerous shot particles are viewed during this inspection then the sample is carefully analyzed using WebPro. With this type of web the shot threshold value in WebPro must be increased to a value where this light transmittance is not detected as shot. Even with this increased

shot threshold value, any light transmittance that is still detected as shot and is not shot can be manually removed from the shot output file. This process allows the experimenter to exercise more control over the WebPro analysis in order to obtain shot data at the lower process conditions.

3.6 Thermal Analysis

DSC is the most common experimental method used in studying and characterizing polymeric materials, and for good reason. DSC is relatively fast and simple method for determining a material's thermal properties.

A DSC typically consists of a sample and reference arrangement with the chambers made of a Pt/Rb alloy. Each chamber is a separate calorimeter and has a resistance heater and sensor for temperature measurement and control. Instead of relying on a heat reference from a single sample, governed by the temperature difference, reference and sample are heated separately as required by their temperature and temperature difference. The losses from the two calorimeters are equalized as much as possible, and residual differences between the two calorimeters are eliminated through calibration. In reality, this type of calorimeter operates by a difference potential generated by the presence of a sample. The temperature difference is proportional to the differential power applied and gives information on the difference in heat input per

second into each calorimeter. The heat input difference is then displayed and used for any sample characterization (i.e. glass transition, heat of fusion, etc.).

DSC scans were run at 20° C/min unless otherwise indicated on a Perkin-Elmer series 7 differential scanning calorimeter using Indium with a melting point of 156.50°C as a calibration standard.

The samples were prepared via an O-punch from the fabrics. The samples were then placed into Aluminum DSC pans. The sample weight was between 3 to 4 mg. All reported values are the average of a 3 sample population. Estimates of the crystallinity were obtained using the heat of fusion. The percent crystallinity was calculated from the heat of fusion data by using the following equation:

$$X_c = (\Delta H_f / \Delta H_f^*) \times 100\%$$

Where

ΔH_f is the heat of fusion of the sample.

ΔH_f^* is the heat of fusion of a 100% crystalline material.

ΔH_f^* is taken to be equal to 167 J/g for the α -monoclinic crystal structure[40].

3.7 Orientation

Birefringence is commonly used to quantify the degree of orientation of a system. It can be divided into three components: orientation birefringence ($\Delta n_{\text{orientation}}$), form birefringence (Δn_{form}), and deformation birefringence ($\Delta n_{\text{deformation}}$). The relationship between birefringence and its components is as follows:

$$\Delta n = \Delta n_{\text{orientation}} + \Delta n_{\text{form}} + \Delta n_{\text{deformation}}$$

The orientation birefringence results from physical ordering of anisotropic elements (e.g. chemical bond) in a preferential direction. The form birefringence arises from the distortion of a light wave's electric field at phase boundaries. It is usually small and is thus often neglected. Deformation birefringence results from changes in bond angles and/or bond lengths or from changes in packing (lattice spacing) due to an external deformation. This type may occur in optically isotropic materials or in anisotropic systems [67].

The orientation in semicrystalline polymer systems is described by both an amorphous component and a crystalline component. The equation for birefringence can be rewritten assuming zero form and deformation birefringence as:

$$\Delta n = X_c \Delta^{\circ}_c f_c + (1-X_c) \Delta^{\circ}_a f_a$$

where:

Δ_n is the optically measured birefringence

X_c is the crystallinity

Δ_c° is the intrinsic birefringence of the crystalline phase

f_c is the crystalline orientation function

Δ_a° is the intrinsic birefringence of the amorphous phase

f_a is the amorphous orientation function

Birefringence measurements of fibers extracted from the webs were performed on a Olympus optical microscope with a Leitz four order Berek compensator. Tables in the Leitz compensator manual were used for determination of the retardation. The fiber diameter was determined with a fillar eyepiece equipped with an adjustable dial. Distances on the fillar scale were calibrated before each batch of measurements with an Olympus graduated slide which was delineated in 0.01 mm increments. A 40X objective and a 10X eyepiece were used in all cases. The optical birefringence was determined from the retardation and fiber diameter with the following relationship:

$$\Delta_{\text{tot}} = \Gamma/d$$

where.

Δ_{tot} is the total birefringence of the fiber

Γ is the retardation

d is the fiber diameter

3.8 Wide Angle X-ray Scattering (WAXS)

X-ray diffraction (or X-ray scattering) is a technique used to determine structural information about materials. Wide angle x-ray diffraction WAXD is used for analysis of three dimensionally, regularly repeating arrangements of atoms or groups of atoms (crystals).

WAXD was used to obtain flat plate film patterns and diffraction scans. Flat plate patterns were used as a qualitative determination of crystalline orientation and crystal structure of the melt blown fibers. Diffraction scans were used to determine the crystal structure present in the melt-blown fibers and webs.

A special method was used to obtain the melt blown fibers to be analyzed by flat plate WAXD. A rectangular plate made of Aluminum was quenched in liquid nitrogen while the melt blowing process is running. The Aluminum plate was then passed very fast through the fibers in flight to stop the fiber crystallization in order to study the crystal structure of the fibers at that instance before reaching the collector. This was done at different die to collector distances. The samples were collected and analyzed by flat plate WAXD.

The samples for the diffraction patterns of the webs were taken directly from the webs. One inch by one inch samples were used to study the crystal structure of the webs. Some of the fibers obtained using the quenched rectangular Aluminum plate had a semi-web structure. Those samples with the semi-web structure were used in the diffractometer to observe the crystalline structure of the melt blown fibers. Both flat plate and diffractometer patterns resulted in the same output in the nature of crystalline structure of those melt-blown fibers.

X-rays for wide angle x-ray analysis used in this work was produced using a copper target and monochromatic nickel filtered CuK_α radiation with a wavelength of 1.5416 \AA [68].

Diffraction scans were performed on the Rigaku X-ray Diffractometer (D/MAX-IA), which is controlled by a microprocessor. Diffractometer patterns were run in reflection mode.

3.9 Melt Flow Rate

The MFR of the different resins was verified using a Dynisco-Kayeness polymer test systems, series 4000 Melt indexer, Model 4003.

CHAPTER FOUR

RESULTS AND DISCUSSION

Most of the earlier research of the melt blowing process has been focused on optimizing the processing conditions to get good properties of the webs and the least amount of defects and non-uniformity in the final product. The majority of the melt blowing research has been focused on the influence of processing conditions on the structure, properties, and shot formation in the webs. Little research has been done on the polymer properties and the effect the polymer itself plays in the production of shot. The main goal of this research was to study the production of shot and possible ways of reducing shot.

As previously stated, the theory that shot was caused by melt fracture during attenuation has been mostly discarded since 1991 when Milligan and Haynes used photographic methods to prove that fibers in melt blown webs were actually continuous filaments. This revelation has given rise to the theory that molten filament collisions during attenuation cause more massive filaments, which produce shot upon impact with the collector.

If one adopts the filament collision model, shot is caused by molten filaments colliding and fusing in flight. This fused mass then requires more solidification time due

to its increased mass to surface area ratio. If more solidification time is not supplied then a semi-molten fused mass will impact the collector surface and create a shot particle in the web sample. Therefore, if molten filament collisions that possibly cause these more massive filaments could be reduced then shot could possibly be reduced. If one wants to reduce the number of molten filament collisions then one must do one of the two following items:

- Create a situation in which fibers do not collide during the attenuation process. This is an aerodynamic problem. This is almost impossible to achieve in the highly dynamic environment the melt blown fibers experience.
- Create a situation in which fibers are not molten upon collision. This is a material property problem if the rate at which heat is transferred from the filaments remains constant.

A possible way to create such a situation is to make the crystallization kinetics faster, so the fibers are not molten upon collision. To make the crystallization kinetics faster and supposedly reduce shot, two investigations were conducted in this study. First, the effect of blending metallocene and conventional Ziegler-Natta resins at different ratios on shot production is studied. The effect of using nucleating agents on shot production is examined in the second part of this thesis.

4.1 Investigation of the Effect of Blending Metallocene and Zeigler-Natta Catalyzed Resins on Shot Production

The results of the melt blowing behavior of the different resins B1 (100% Metallocene), B2 (80% Metallocene & 20% ZN), B3 (60% Metallocene & 40% ZN), B4 (40% Metallocene & 60% ZN), B5 (20% Metallocene & 80% ZN), B6 (100% ZN) resins are presented. The percentages of the components of the blends, as can be seen, were changed in steps of 20%. Exxon provided the resins; each resin was melt blown under the following processing conditions on the experimental line described in chapter three. The processing conditions were:

Process temperature (Air and Polymer)	-	500°F, 475°F, 450°F, 420°F
Die pressure	-	7 psig, 5 psig, 3 psig
Nosepiece	-	30 hole die
Polymer throughput	-	0.8 grams/minute/hole
Die setback and Die Gap	-	0.079 inches
Die to collector distance	-	16, 14, 12 inches

The processed resins or fabrics were then analyzed for shot production using the WebPro system discussed in chapter three of this thesis. **Figure 4.1** is the number of shot

Number Of Shot/cm² versus processing Conditions

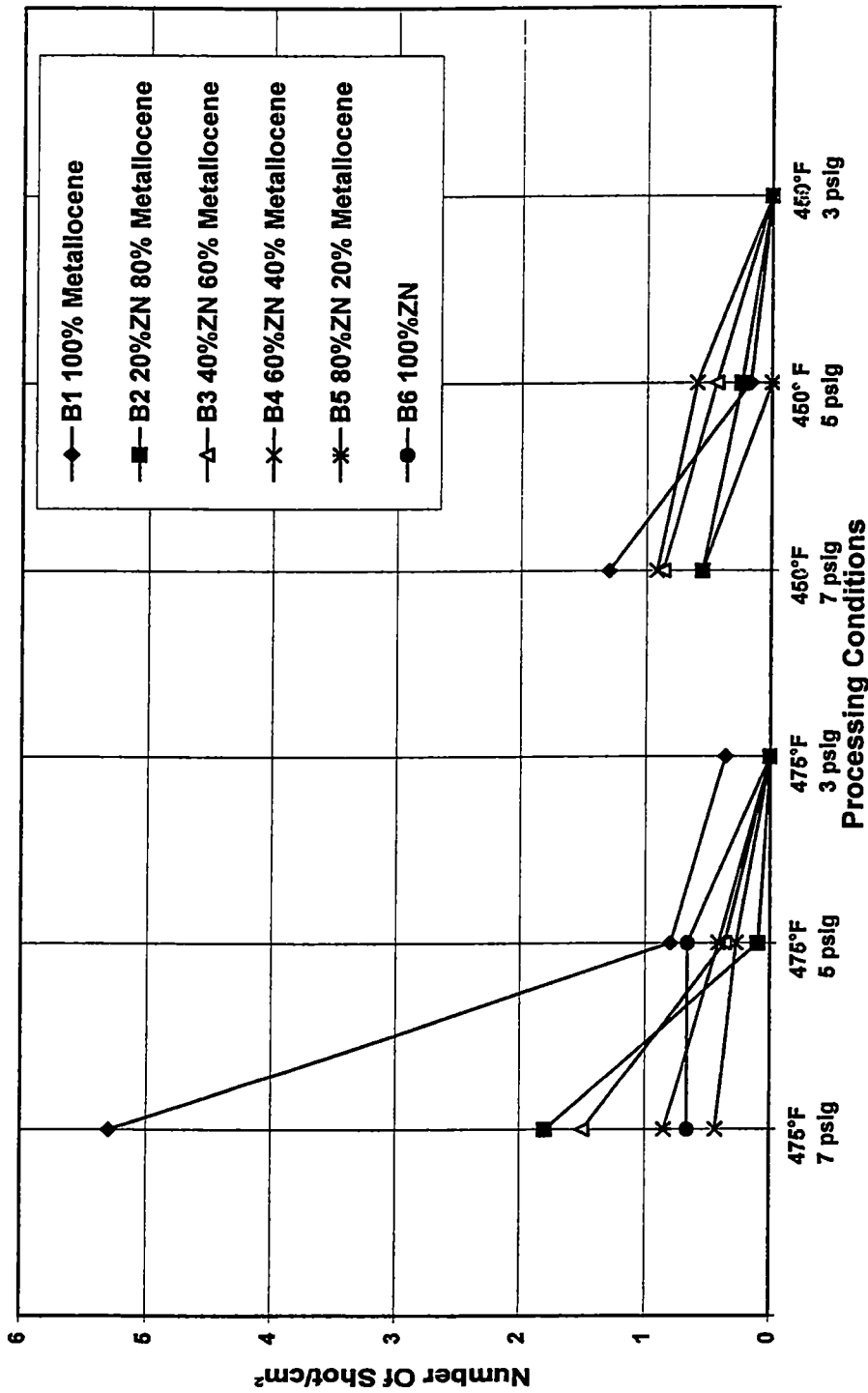


Figure 4.1 Number Of Shot/cm² versus Processing Conditions
 (30 hole die, 0.8 grams/min /hole, 16" DCD)

per cm^2 versus the processing conditions of the six different webs. The figure shows the B1 resin (100% metallocene) has the highest number of shot. The number of shot decreases as the air pressure and extrusion temperature decreases. The air pressure causes the fibers to attenuate and flap. As the air pressure increases, the flapping increases and the fiber diameter gets smaller. As the extrusion temperature decreases the fibers take less time to crystallize, not giving time for fibers to join together and form shot.

Figure 4.2 shows the number of shot/ cm^2 of the different webs versus DCD (Die to Collector Distance) at 500°F. The data shows that the number of shot decreases as the DCD increases.

Figure 4.3 shows the number of shot/ cm^2 of the six blend resins versus DCD at 475°F. The same trends of **Figure 4.2** are observed here as well. **Figure 4.4** shows the number of shot/ cm^2 of the different resins versus DCD at 450°F.

An important fact that can be seen in these figures is that the number of shot generally increases with decreasing die to collector distance (DCD). This has been observed with all the resins. A reasonable explanation for this observation may be the fact that as the DCD decreases the polymer is still viscous and hot when it arrives at the collector. Thus, when hitting the collector, it splashes and forms a shot that can be observed with the naked eye or with the image analysis system used in this experiment.

Number Of Shot/cm² versus DCD
500°F, 5 psig

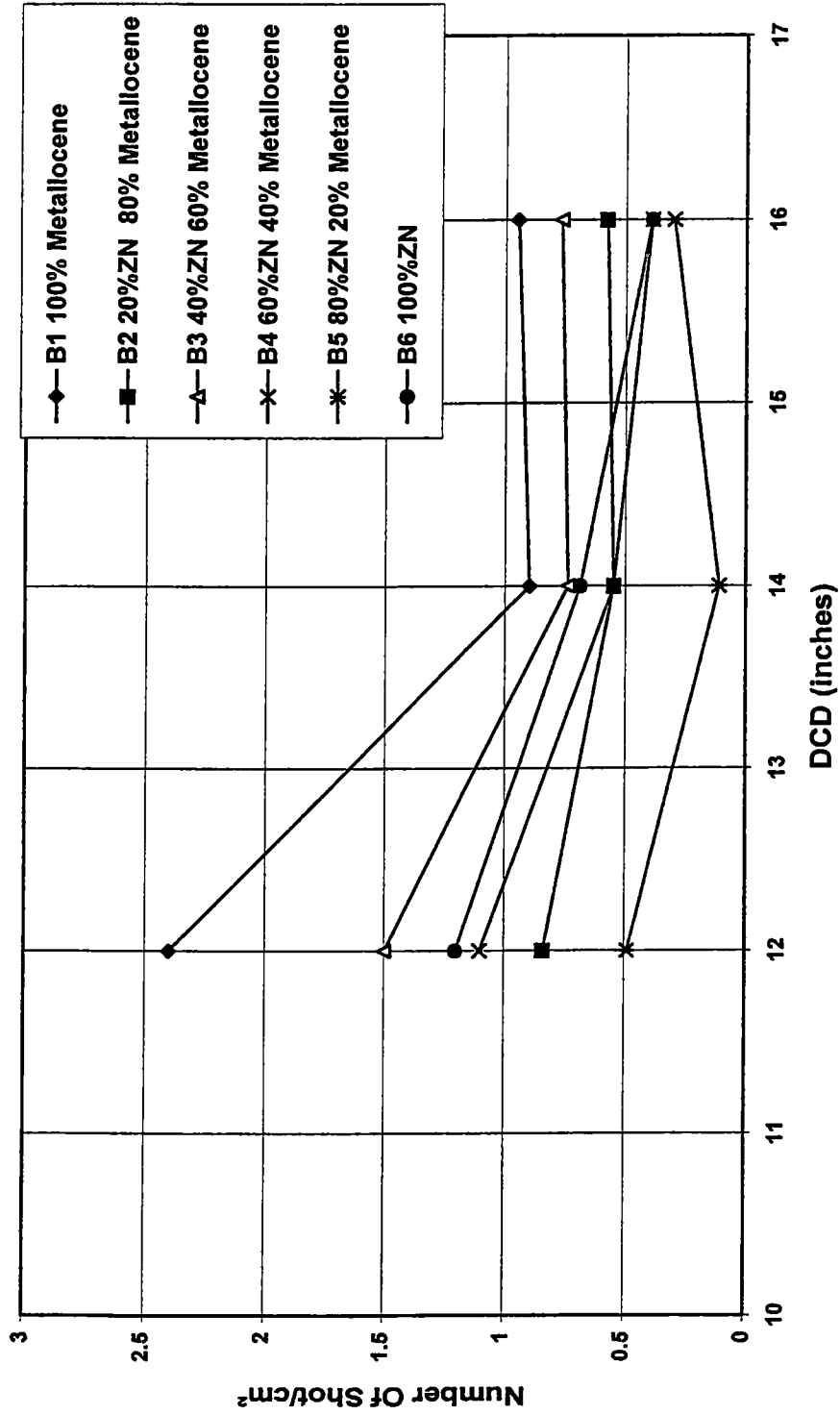


Figure 4.2 Number Of Shot/cm² versus DCD

(30 hole die, 0.8 grams/min./hole, 500°F, 5 psig)

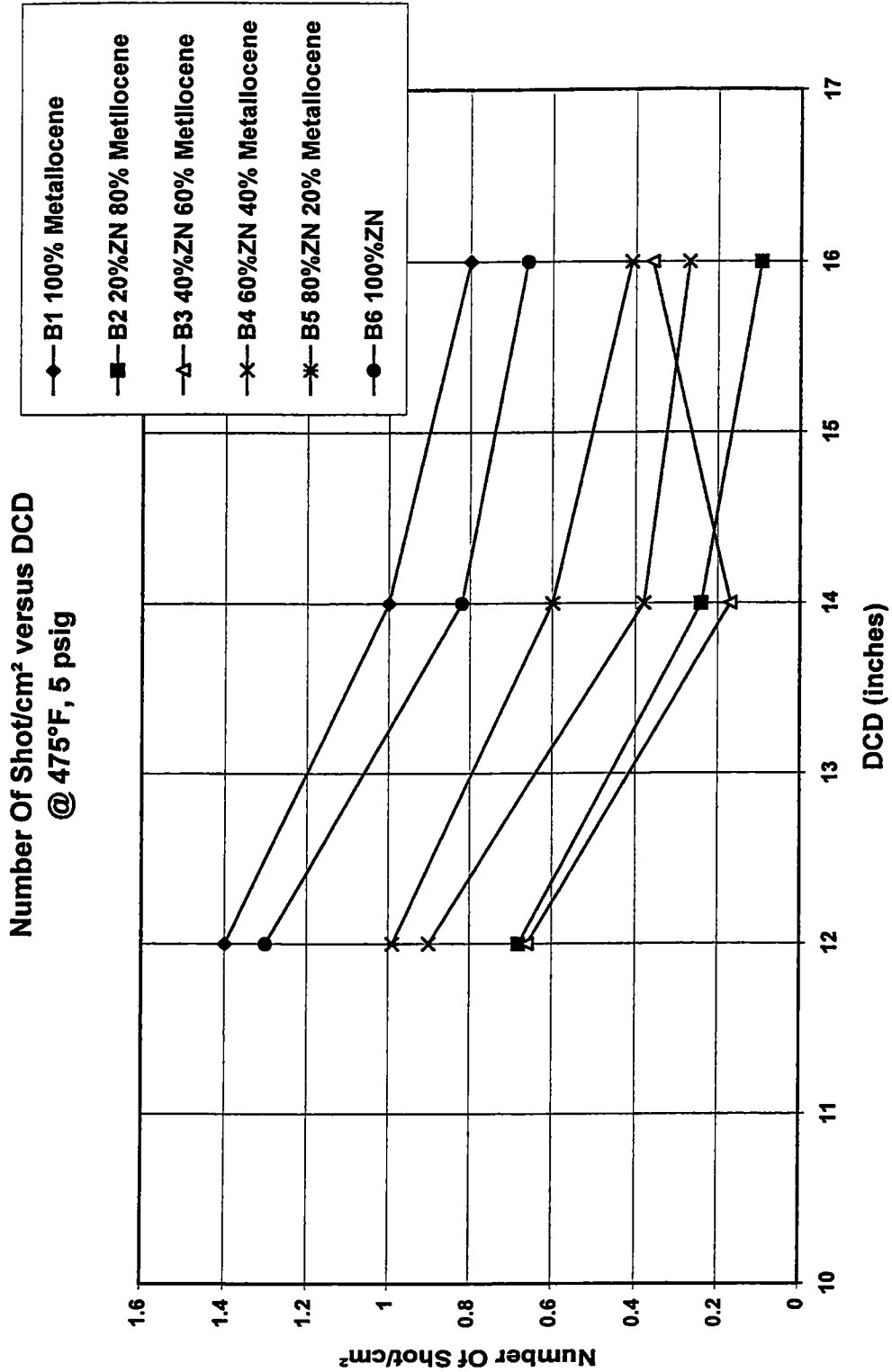


Figure 4.3 Number Of Shot/cm² versus DCD
(30 hole die, 0.8 grams/min./hole, 475°F, 5 psig)

**Number Of Shot/cm² versus DCD
@ 450°F, 5 Psig**

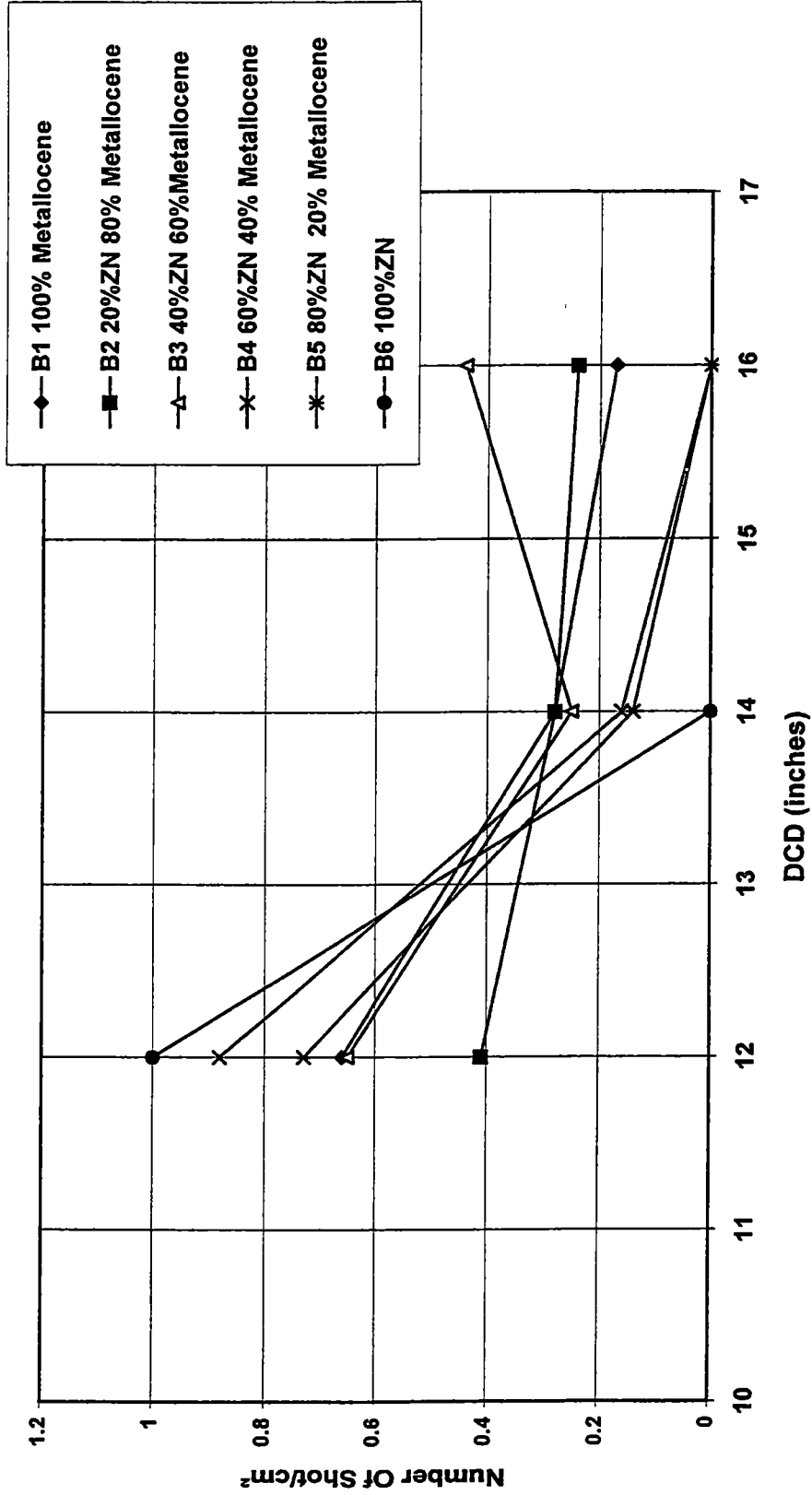


Figure 4.4 Number Of Shot/cm² versus DCD
(30 hole die, 0.8 grams/min./hole, 450°F, 5 psig)

further, as the DCD decreases, the fibers hit the collector more powerfully.

Although the data shows significant scatter, the number of shot appears to decrease, generally, as the Ziegler-Natta content increased in the blends, so the question that comes up here is: does the crystallization kinetics of the blends change upon changing the ratio of the blend contents and whether this is correlated to shot production. With that in mind, it was decided that the next step was to study the crystallization kinetics of the different resins under quiescent conditions using Differential scanning calorimetry (DSC).

Table 4.1 lists the peak crystallization temperatures and heat of fusion of the several blend resins using the DSC technique. Obviously in this table, the crystallization temperature increased as the Zeigler-Natta content increased, indicating that as the Zeigler-Natta polypropylene percentage in the blend increased, the crystallization kinetics became faster indicating that the Zeigler-Natta content is nucleating the metallocene base resin. The heat of fusion also increased as the ZN content increased, indicating higher crystallinity. **Figure 4.5** (a), (b), (c), (d), (e), (f) shows differential scanning calorimetry scans of the different resins B1 to B6. The cooling exotherms show one crystallization peak for all the resins as can be seen in **Figure 4.5**, however, upon heating, the scans start showing double peaks that are sensitive to the ratio of the metallocene and Ziegler-Natta polypropylene in the blend. This is likely attributed to having different lamellar thicknesses in the different catalyst systems resins. The

Table 4.1 : Non-isothermal Thermal Characterization of the Metallocene-ZN

Different Blends.

Resin	Metallocene%	ZN%	Peak Crystallization Temperature (°C)	Heat of Fusion (J/g)
B1	100	0	102.989	93 707
B2	80	20	104.639	96 031
B3	60	40	105.821	98 512
B4	40	60	106.585	103 937
B5	20	80	107.508	106.722
B6	0	100	108.207	109 007

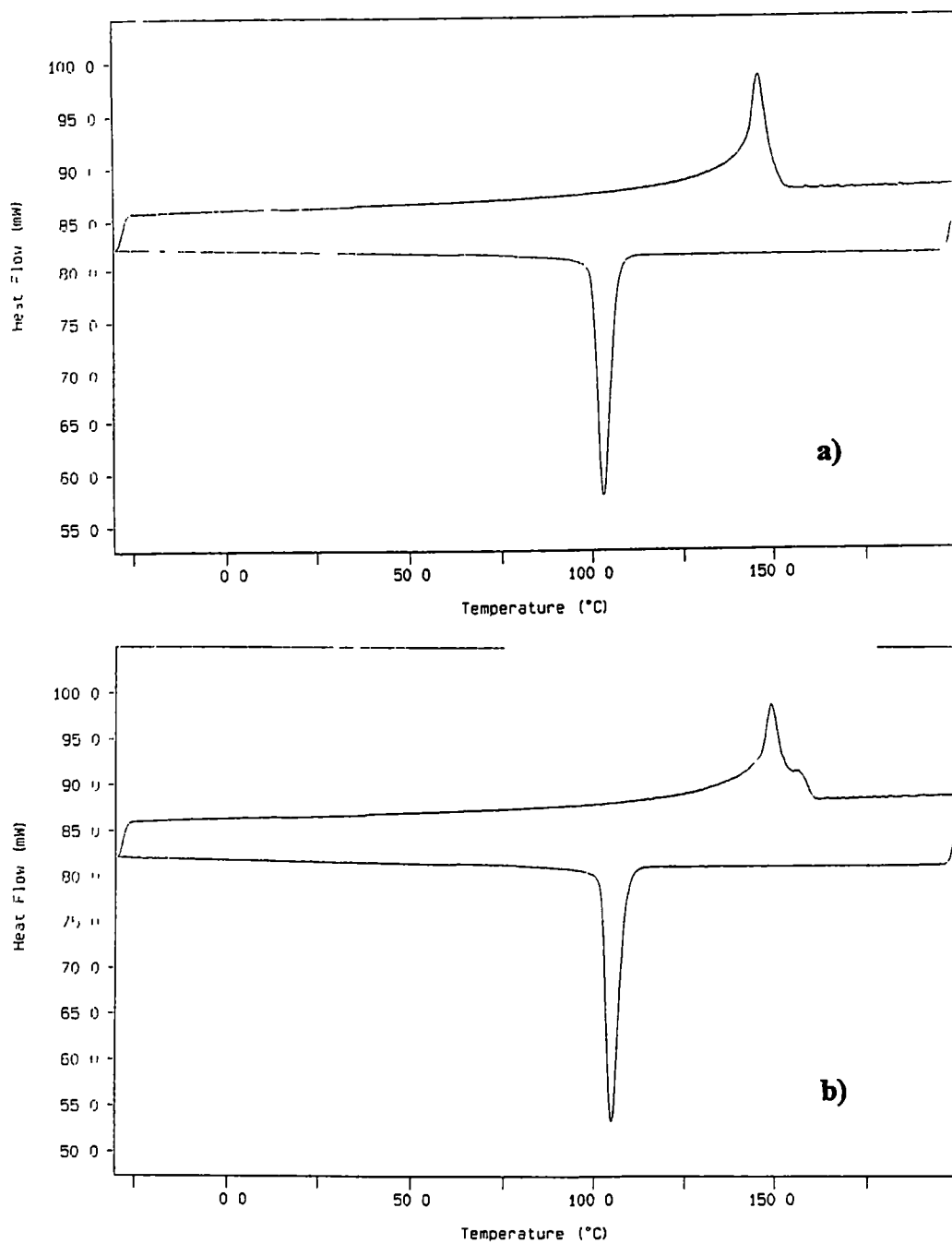


Figure 4.5 DSC Heating and Cooling Curves of the a) B1 and b) B2

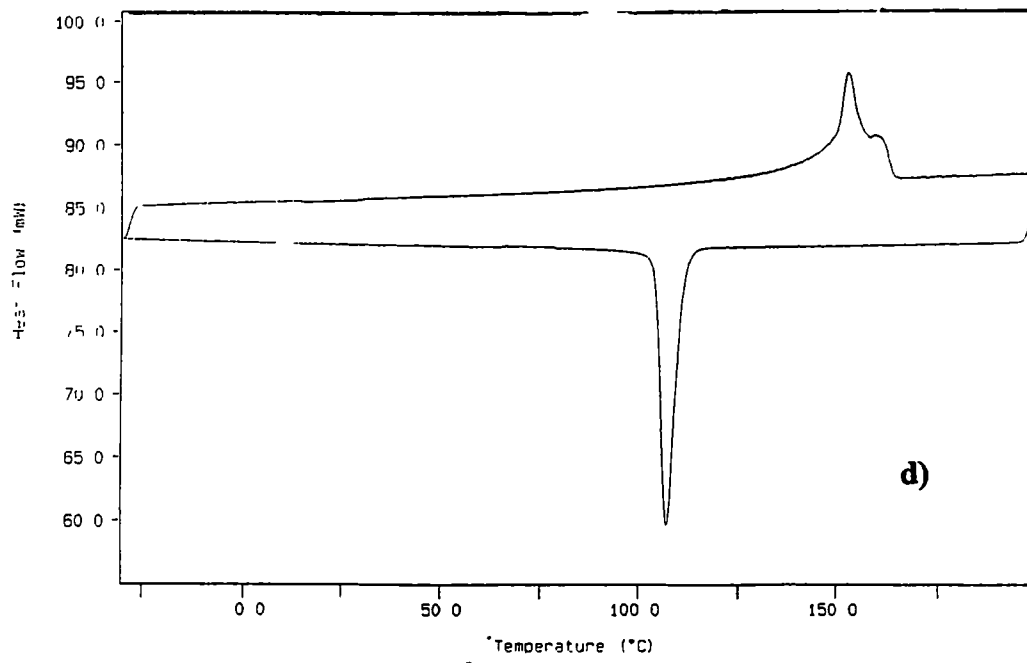
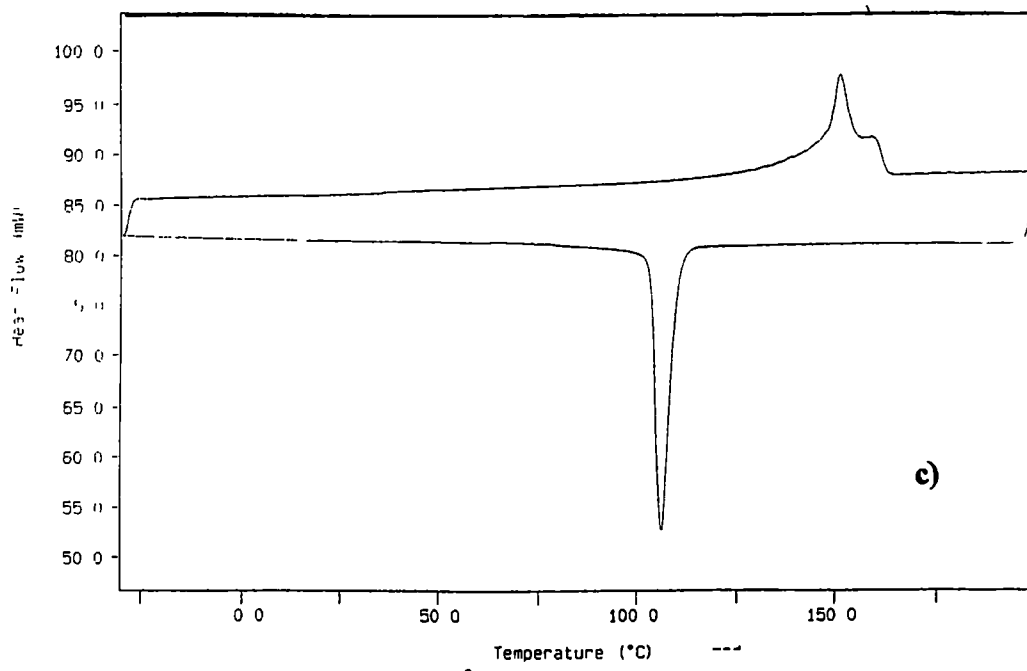


Figure 4.5 DSC Heating and Cooling Curves of the c) B3 and d) B4

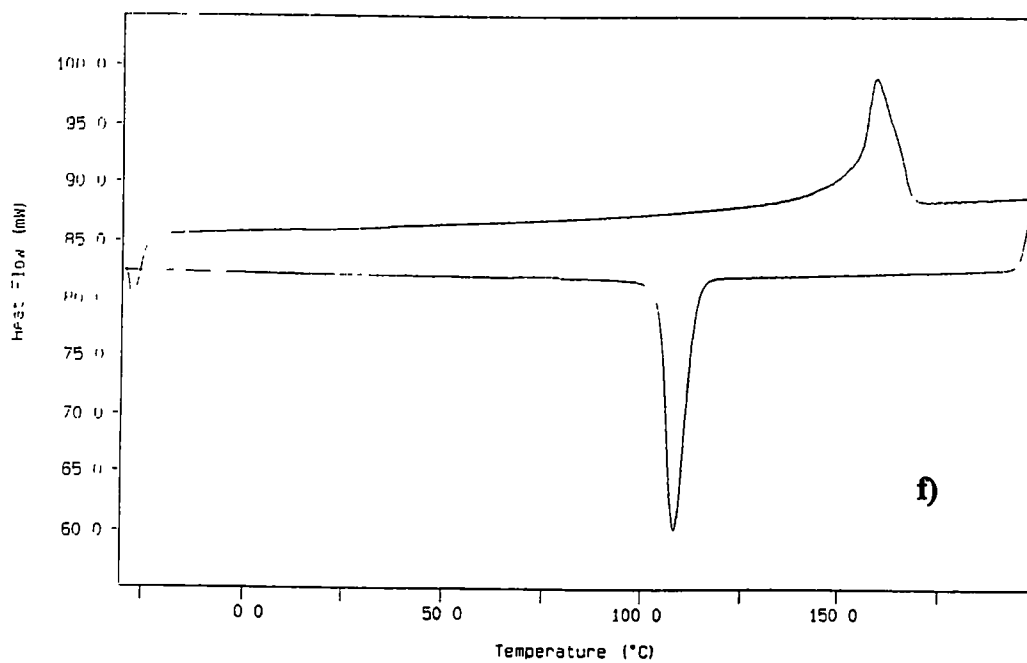
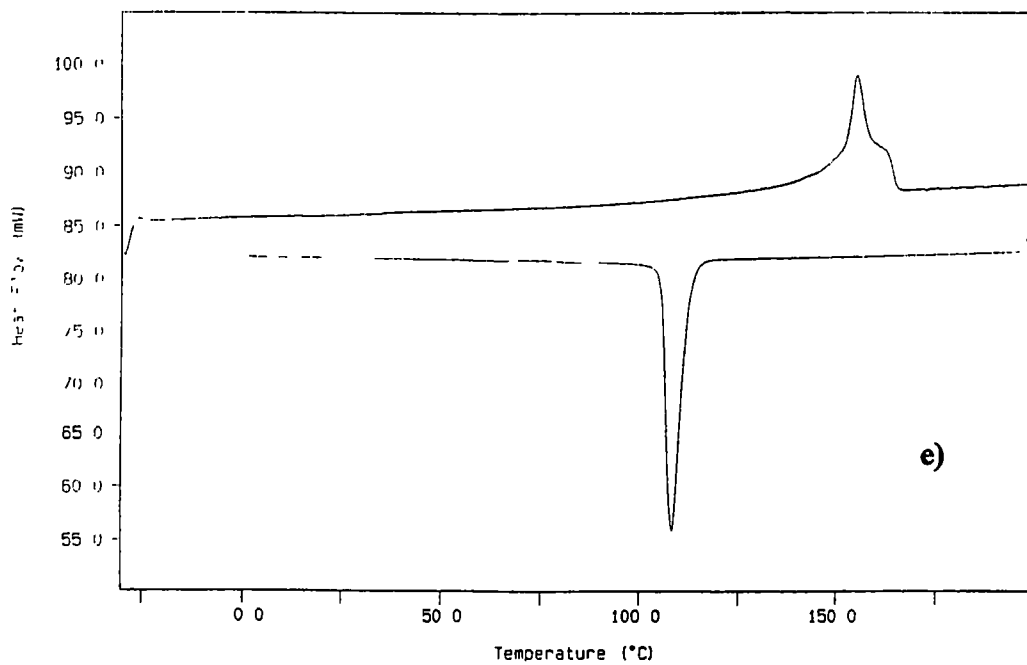


Figure 4.5 DSC Heating and Cooling Curves of the e) B5 and f) B6

metallocene polypropylene has different lamellar thickness than that of the Ziegler-Natta catalyzed polypropylene portion of the blend. However, it is surprising that the template provided by first crystals to form is not maintained throughout. Certainly, there are many questions left to be answered about the crystallization and melting behavior of the blends. For the current research we are mainly concerned with differences in crystallization rate and crystallization temperature. Thus, the crystallization morphology and other details were not pursued here

Figure 4.6 shows the bulk isothermal half-times of crystallization of the six blend resins versus the crystallization temperature. The B1 resin (100% Metallocene) has the longest crystallization half-times (slowest crystallization kinetics). The half-times start becoming shorter as the Zeigler-Natta percentage increases, and, as can be seen, the B6 resin has the shortest half-times. This is apparently related to the difference in the number and distribution of stereodefects in the polypropylenes prepared by different catalysts. The metallocene resins have a uniform defect distribution and enough defects to suppress the crystallization rate. The Zeigler-Natta resins tend to have a non-uniform distribution of defects with some molecules with high molecular weight being relatively defect free. These molecules tend to control the nucleation of the crystallization. In this case it appears that the Zeigler-Natta percentage is nucleating the metallocene percentage of the blends, and as the percentage of Zeigler-Natta increases, the nucleation increases and crystallization kinetics is enhanced.

Isothermal Crystallization Half-times of the Different Blend Resins

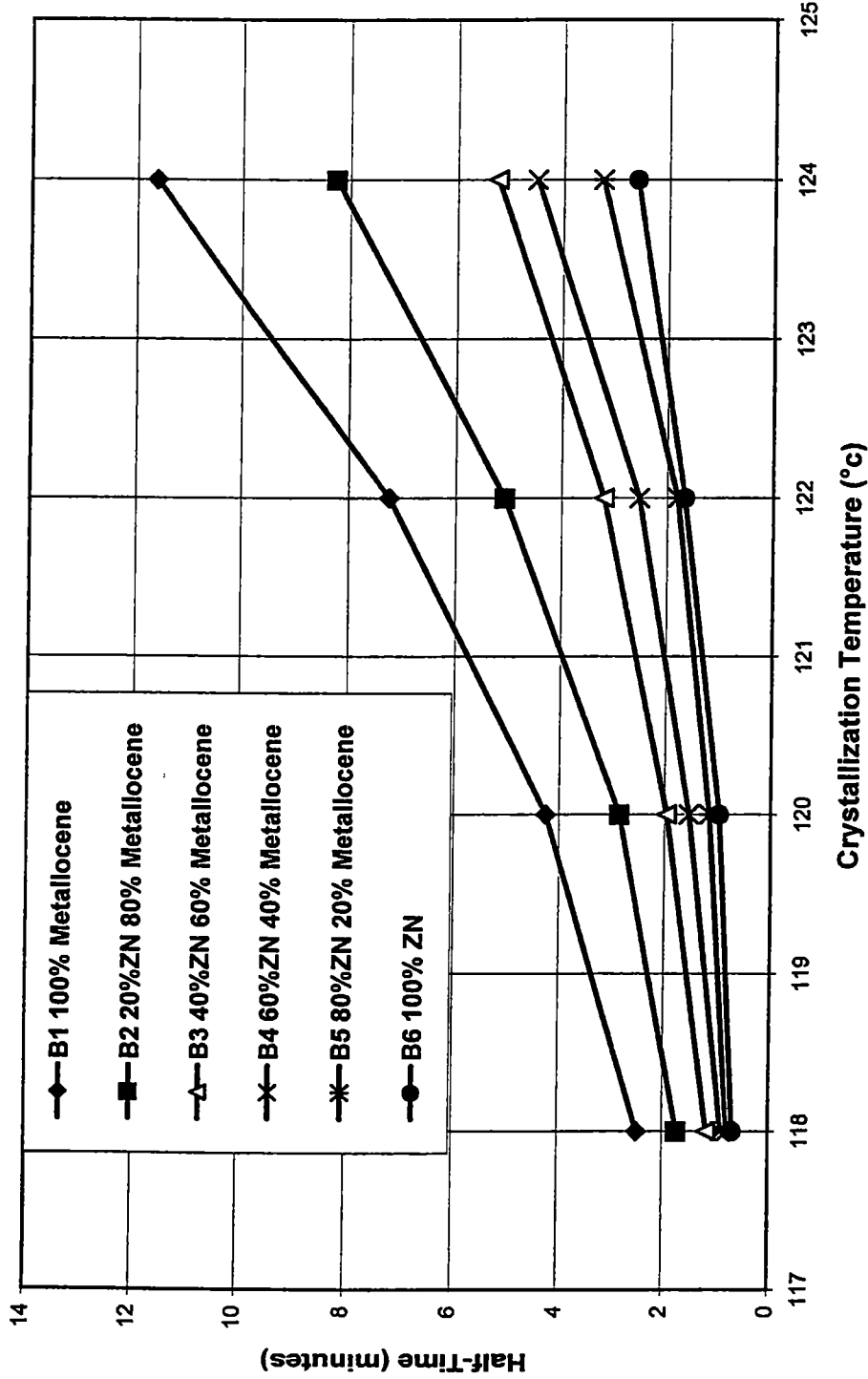


Figure 4.6 Half-time Of Crystallization versus Crystallization Temperature
 (30 hole die, 0.8 grams/min./hole, 475°F Processing Temperature, 5psi Air Pressure, 16" DCD")

An interesting piece of information about the crystalline structure in the different webs is that all the final webs consisted of an α -phase after processing. The α -phase is the most common form observed in isotactic polypropylene when crystallized from the melt in the absence of nucleating agents and at atmospheric pressure. **Figure 4.7** shows an X-ray diffraction pattern that was done on a Rigaku diffractometer in our labs of the 100% metallocene resin, which is the same as the base resin used in the second study of this thesis. This pattern shows an α monoclinic structure. The α -phase was observed in all the different webs.

One of the obstacles in studying the melt blown fibers is that there is no straightforward way of getting the as-blown fibers before they hit the collector and form a web. In order to get an idea about the crystalline structure in the melt-blown fibers prior to deposition on the collector, a metal Aluminum plate was quenched in liquid nitrogen and passed through the stream of fibers at different distances from the die. The collected fibers were then analyzed for crystalline structure using the Rigaku diffractometer in our lab. The X-ray results, **Figure 4.8** showed a smectic phase in those fibers. The smectic phase was observed at different distances from the die and at the collector. The smectic phase, which is a conformationally disordered form of isotactic polypropylene, is intermediate metastable mesophase. The smectic or condis form is usually obtained by quenching thin sheets of isotactic polypropylene from the melt into ice water. It also can be found in fibers spun with extremely high cooling rates under small stresses. An annealed smectic phase will gradually transform to the α -phase over time or when

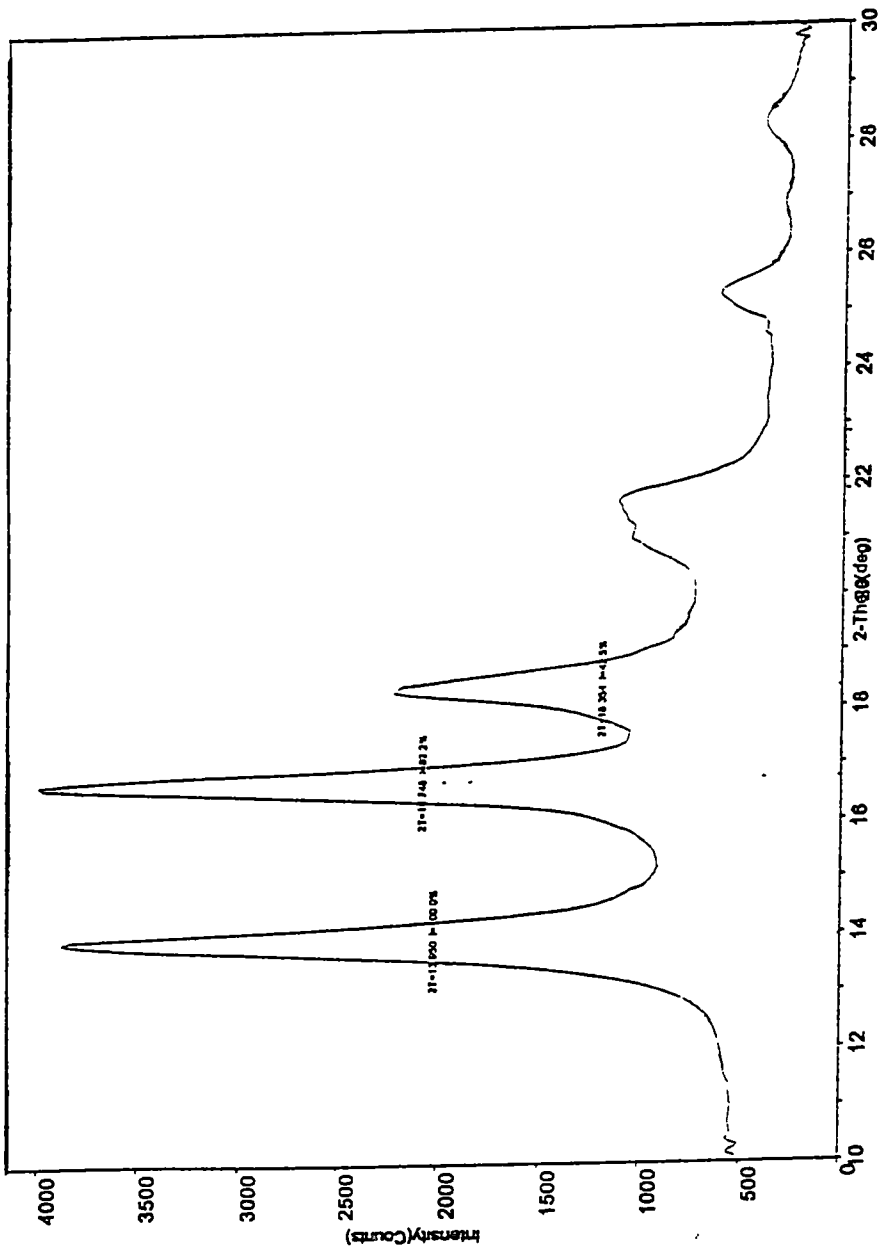


Figure 4.7 X-ray Diffraction Pattern of the Melt Blown Webs.

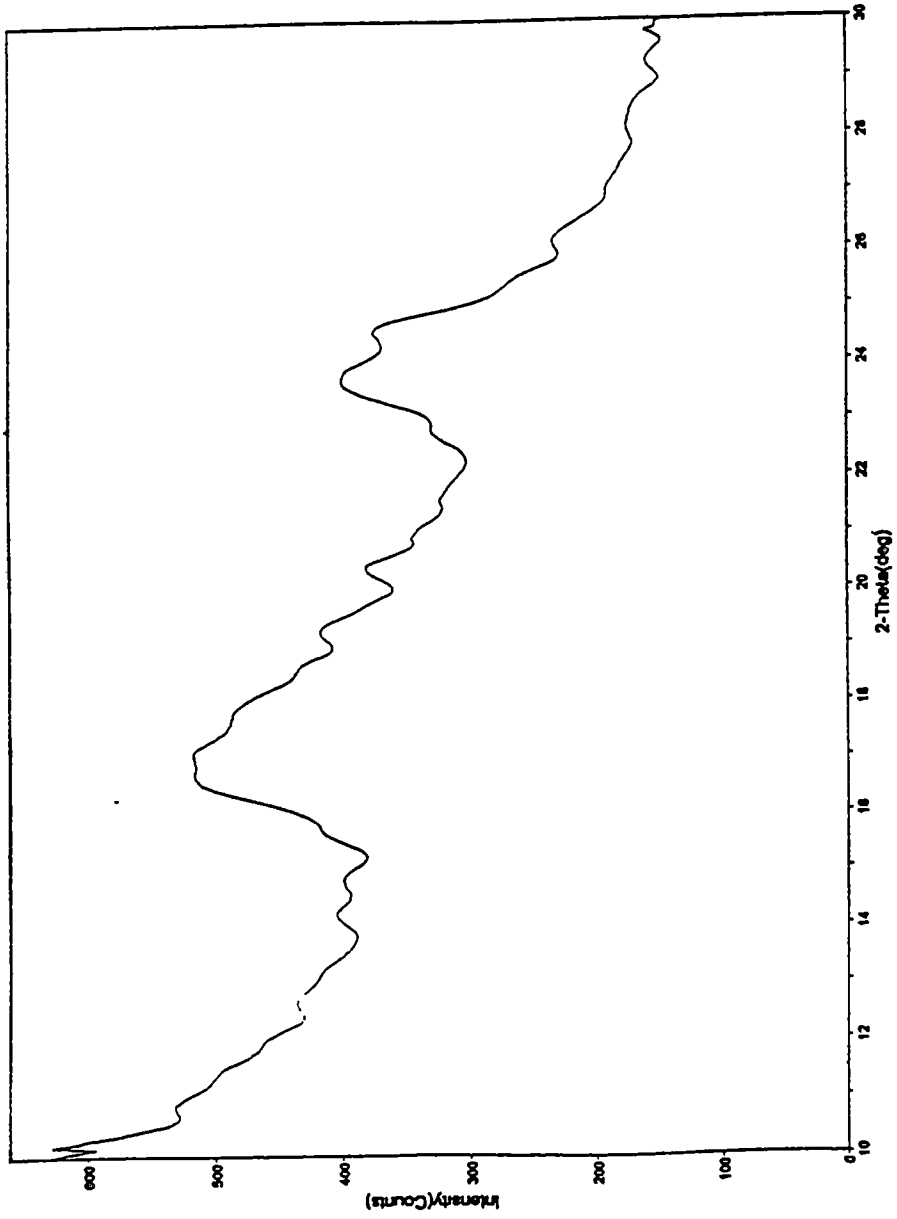


Figure 4.8 X-ray Diffraction Pattern of the As-Blown Fibers.

exposed to elevated temperatures above 70°C [69]. The temperature at the collector is usually higher than 70°C during processing.

Taking the above results into consideration, it is apparent that shot production was influenced by the blending of the Ziegler-Natta and metallocene catalyzed resins, and there was a tendency toward a decrease in the number of shot as the Ziegler-Natta content increased. Furthermore, it is obvious that the crystallization kinetics changed gradually as the Ziegler-Natta content increased in the blends. The question that needs to be answered is whether shot production is really correlated to the crystallization kinetics because of the observed parallel gradual changes in both. To answer this question, it was decided to further pursue the crystallization kinetics study and investigate its effect on shot production. In order to do this, nucleating agents were used to change the crystallization kinetics and consequently study their effect on shot production.

4.2 Investigation of the Effect of Nucleating Agents on Shot Production

Exxon provided the investigator with two sets of resins that each contained a nucleating agent. The purpose of the nucleating agent additive is to accelerate the

crystallization process (solidification) during the attenuation process. If the nucleating agent were to successfully accelerate the crystallization process then the probability of filaments fusing would be reduced. The resins differed by the parts per million (ppm) content of nucleating agent and the agent type itself, but the base resin was always the same BR metallocene resin. These resins were melt blown at the following process conditions:

Process temperatures (Air and Polymer) -	475°F, 450°F, 420°F
Die pressure	- 7 psig, 5 psig, 3 psig
Nosepiece	- 30 hole die
Polymer throughput	- 0.8 grams/minute/hole
Die Setback and Die Gap	- 0.079 inches
Die to collector distance	- 16, 14, 12 inches

The web samples were then analyzed to determine the average fiber diameter and shot production. Since the nucleating agents should reduce the time a filament is molten then the nucleated resins may have a slightly larger average fiber diameter than that of the base resin, BR. As seen above a multi-hole (30 hole) die was used since this die would have more filament to filament collisions than that of a single hole die.

The first set of resins tested contained sodium benzoate nucleating agent at two different concentrations. These resins are designated as NR1 and NR2 with NR2 having

twice the level of the sodium benzoate nucleating agent. Again, these nucleated resins are all based on the metallocene resin BR. **Figure 4.9 and 4.10** provide the results for the shot production tests and fiber diameter test of these resin's web samples. The base resin's web samples were tested also and the results are included in the figures for comparative purposes. **Figure 4.9** indicates that the shot production of the nucleated resins was not reduced below that of the BR base resin. This figure seems to indicate that the addition of the nucleating agent was not successful in reducing shot production. **Figure 4.10** indicates the base resin has the smallest average fiber diameter as expected. The average fiber diameter decreased as the die pressure increased, this is expected because as the die pressure increases, the attenuation of the fibers is stronger, hence producing thinner fibers. As the extrusion temperature increased, the average fiber diameter decreased, this can be explained by the fact that at lower processing temperature, the fiber takes less time to crystallize or solidify, causing the fiber not to attenuate further, producing larger fiber diameters. An increase in the processing temperature reduces the average fiber diameter. This is primarily due to a decreased polymer viscosity, which is a function of temperature, and a reduction in die swell.

With the previous results in hand, it was decided that maybe the amount of nucleating agent was insufficient to affect the highly dynamic system of the melt blowing air jet. Exxon provided four more nucleated resins with more nucleating agent content or a different nucleating agent altogether. Two of these resins (NR3 and NR4) utilized the same nucleating agent (sodium benzoate) as the previous investigation.

Sodium Benzoate Nucleating Agent

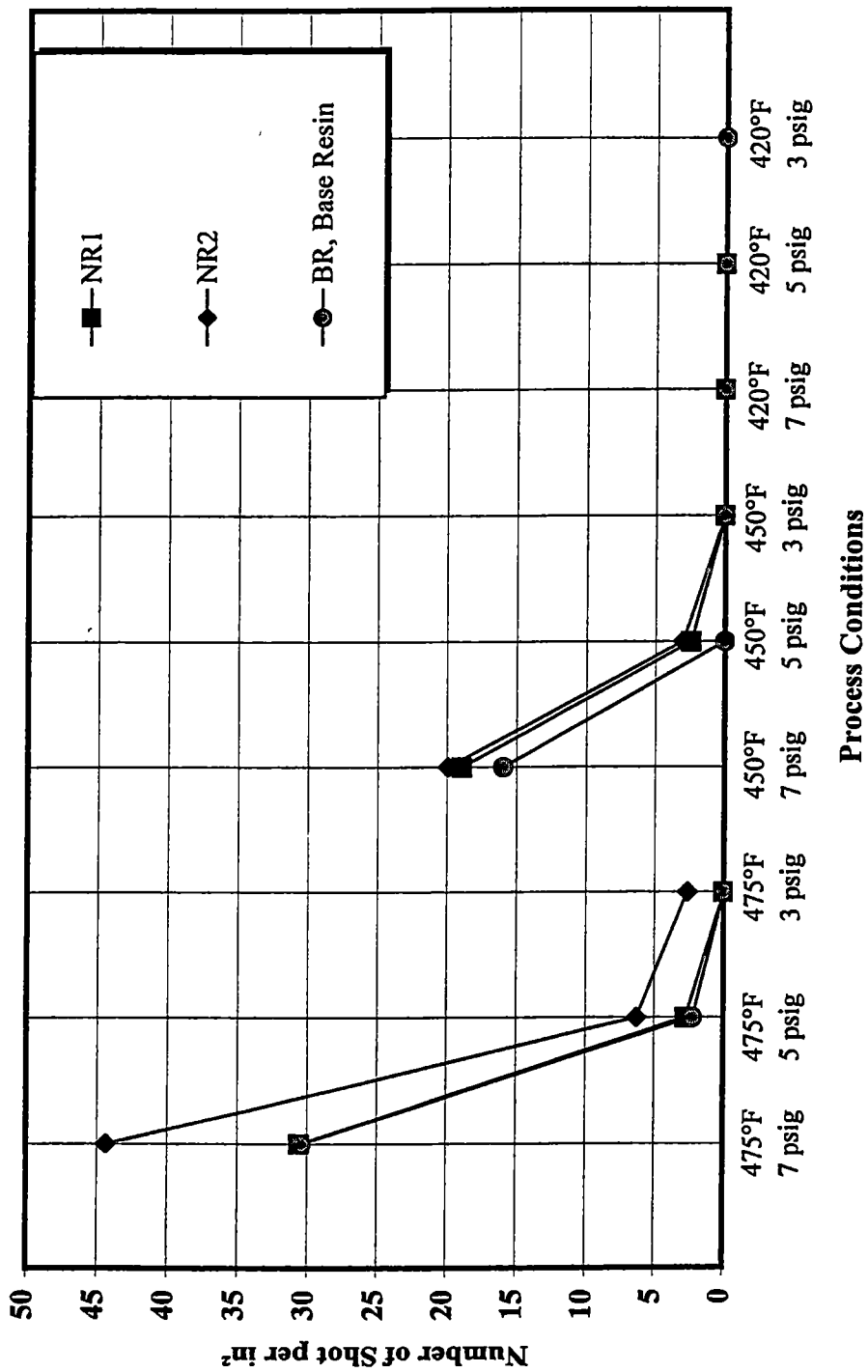


Figure 4.9 Number of Shot per in² vs. Process Conditions
 (30 hole die, 0.8 grams/min./hole, 16" DCD)

Sodium Benzoate Nucleating Agent

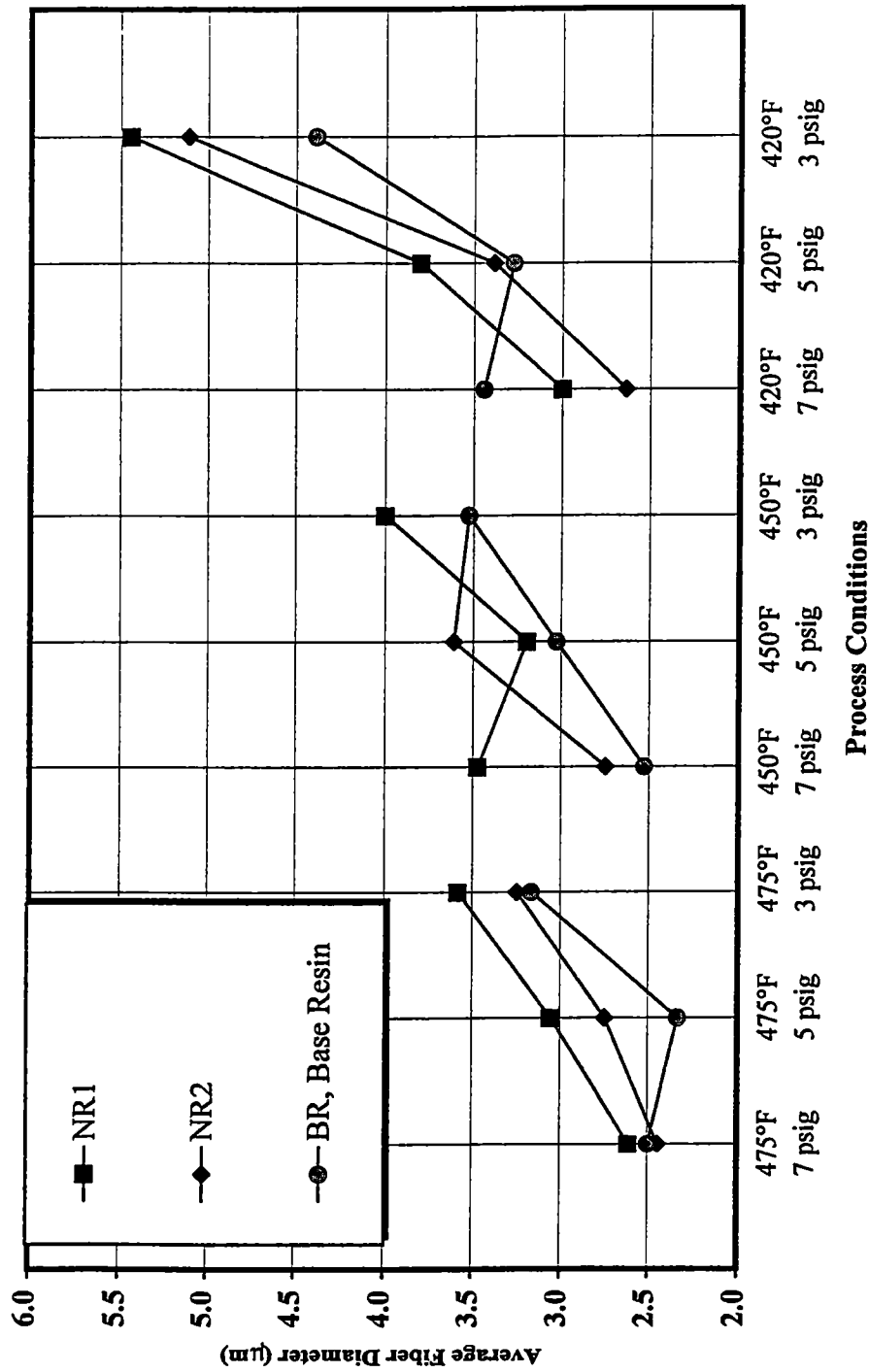


Figure 4.10 Average Fiber Diameter vs. Process Conditions
(30 hole die, 0.8 grams/min./hole, 16" DCD)

NR3 has three times the nucleating agent of the NR1 resin and NR4 has twenty times the nucleating agent of the NR1 resin. The other two provided resins (NR5 and NR6) utilize a different nucleating agent. These resins use a nucleating agent (Millad) at levels equal to the level of sodium benzoate in the NR1 and NR2.

Figure 4.11 is a plot of shot production versus process temperature for all the sodium benzoate nucleated resins. Again, this figure indicates the further addition of nucleating agent to the base resin made little difference in the shot production. **Figure 4.12** is similar to Figure 4.10 in that the smallest fibers are usually created with the base resin but any changes in diameter due to nucleating level appear to be within the diameter measurement's uncertainty. **Figure 4.13** indicates that the addition of the Millad nucleating agent to the base resin BR does not reduce the shot production. **Figure 4.14** indicates that the smaller fibers are created with the BR base resin. However, as with the previous resin, any changes in fiber diameter are within the experimental uncertainty of the diameter measurements.

Since **Figure 4.11** and **4.13** indicate that the shot production is not reduced by the addition of the nucleating agent one might question whether the nucleating agent had any effect on the resin at all. In order to test this, the produced web samples were subjected to tests to determine if the crystallization kinetics of the nucleated resins were different than that of the base resin. This was accomplished by performing differential scanning calorimetry (DSC) tests on a portion of a melt blown web sample created with

Sodium Benzoate Nucleating Agent

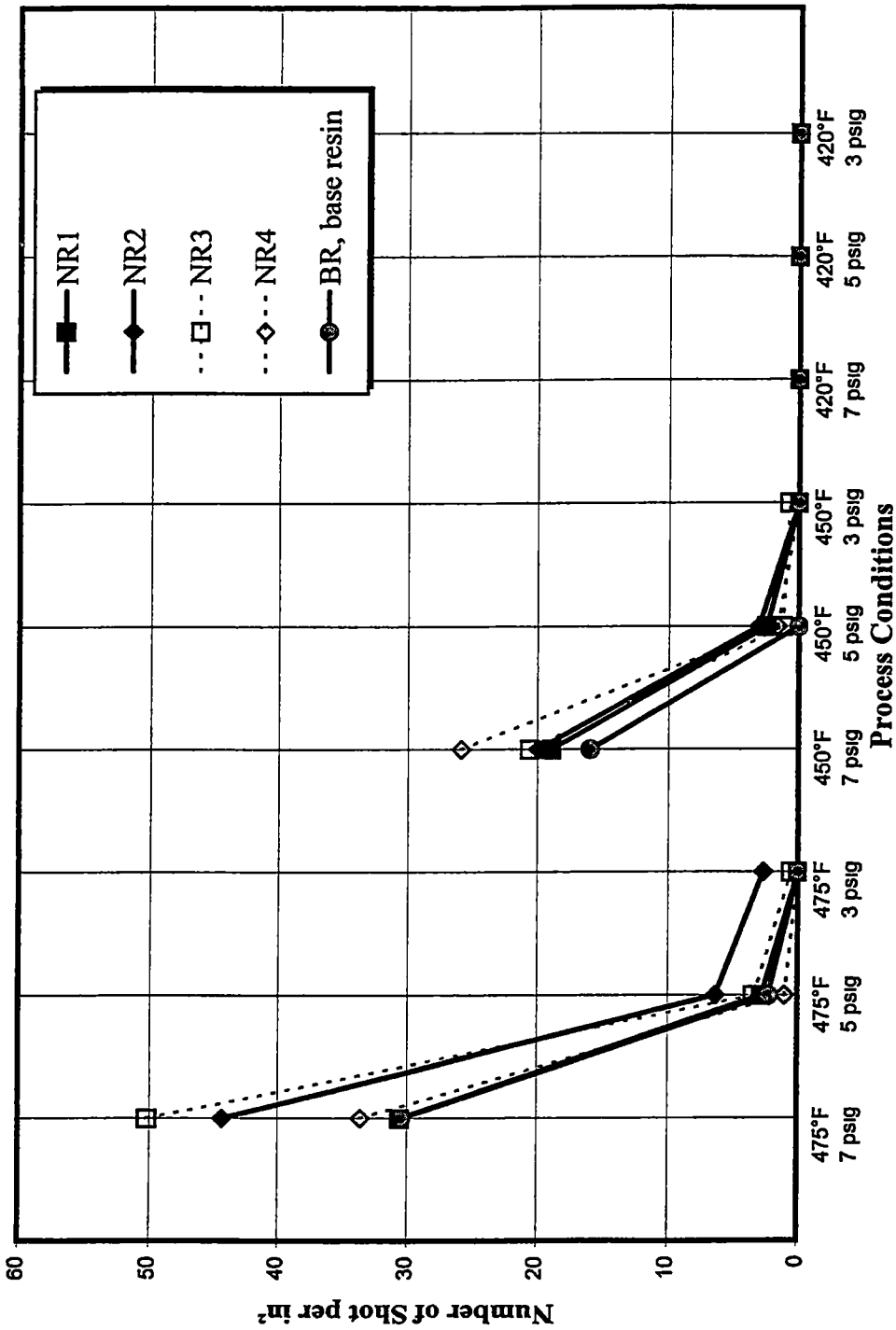


Figure 4.11 Number of Shot per in² vs. Process Conditions
 (30 hole die, 0.8 grams/min./hole, 16" DCD)

Sodium Benzoate Nucleating Agent

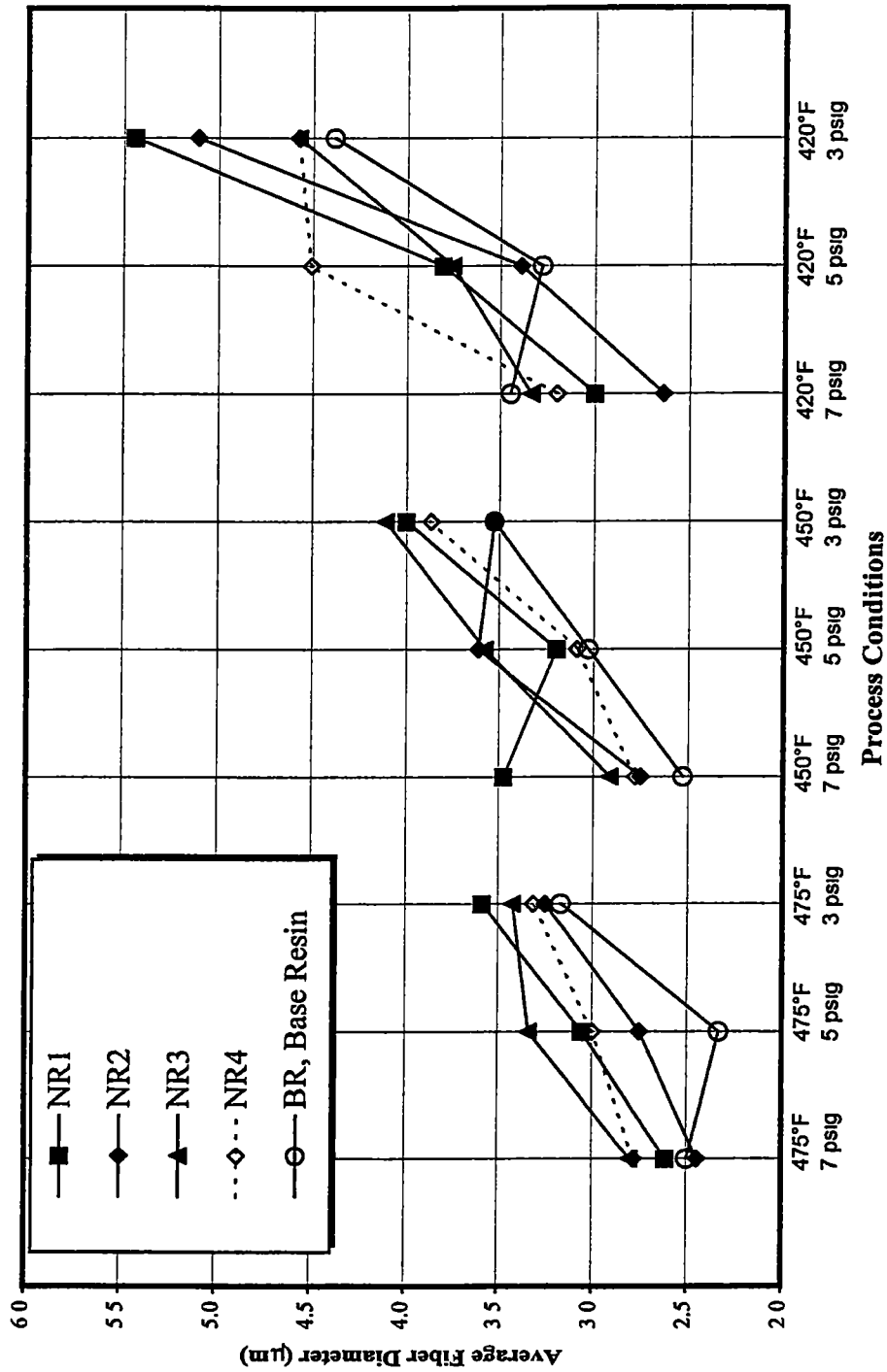


Figure 4.12 Average Fiber Diameter vs. Process Conditions
 (30 hole die, 0.8 grams/min./hole, 16" DCD)

Millad Nucleating Agent

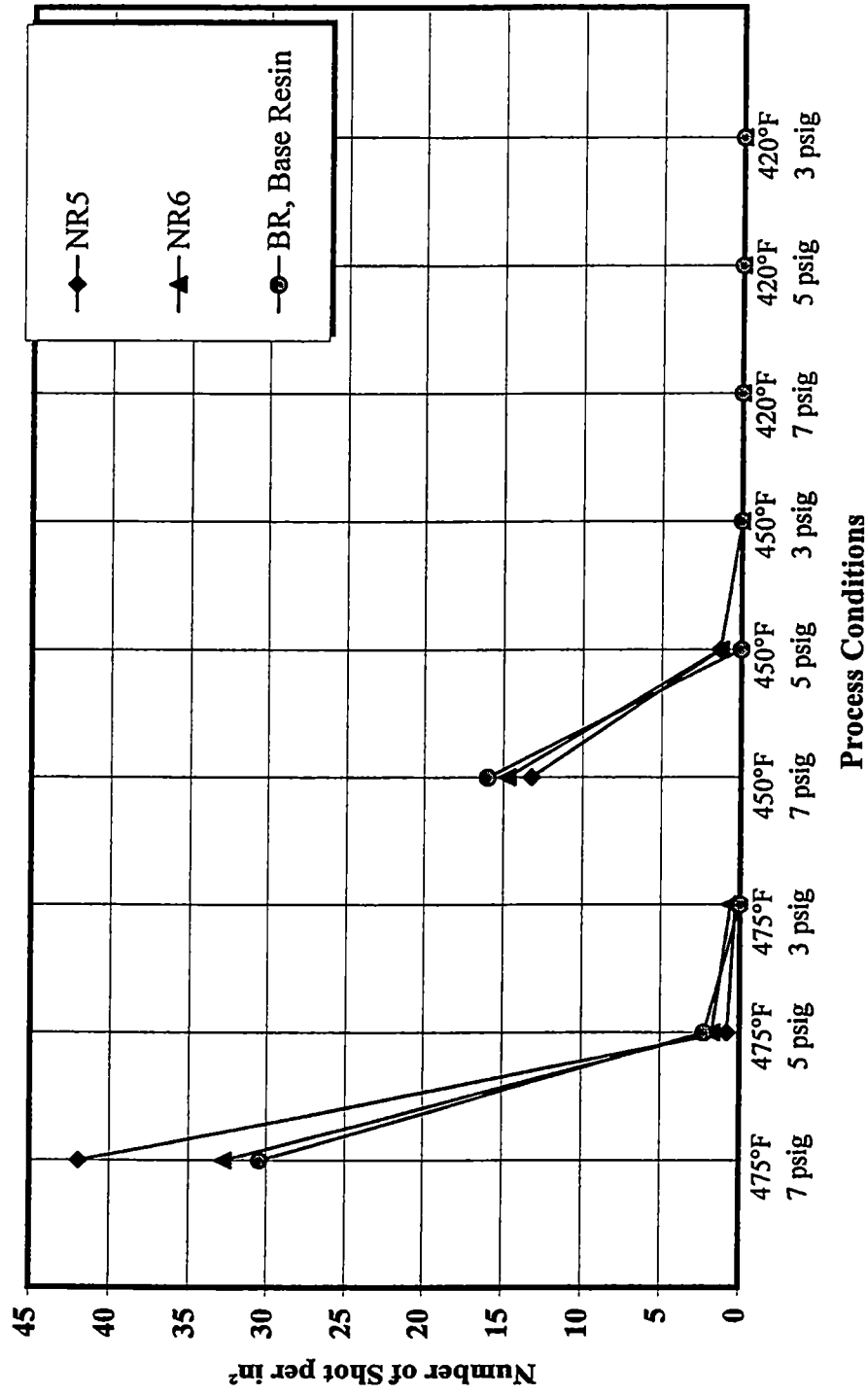


Figure 4.13 Number of Shot per in² vs. Process Conditions
 (30 hole die, 0.8 grams/min./hole, 16"DCD)

Millad Nucleating Agent

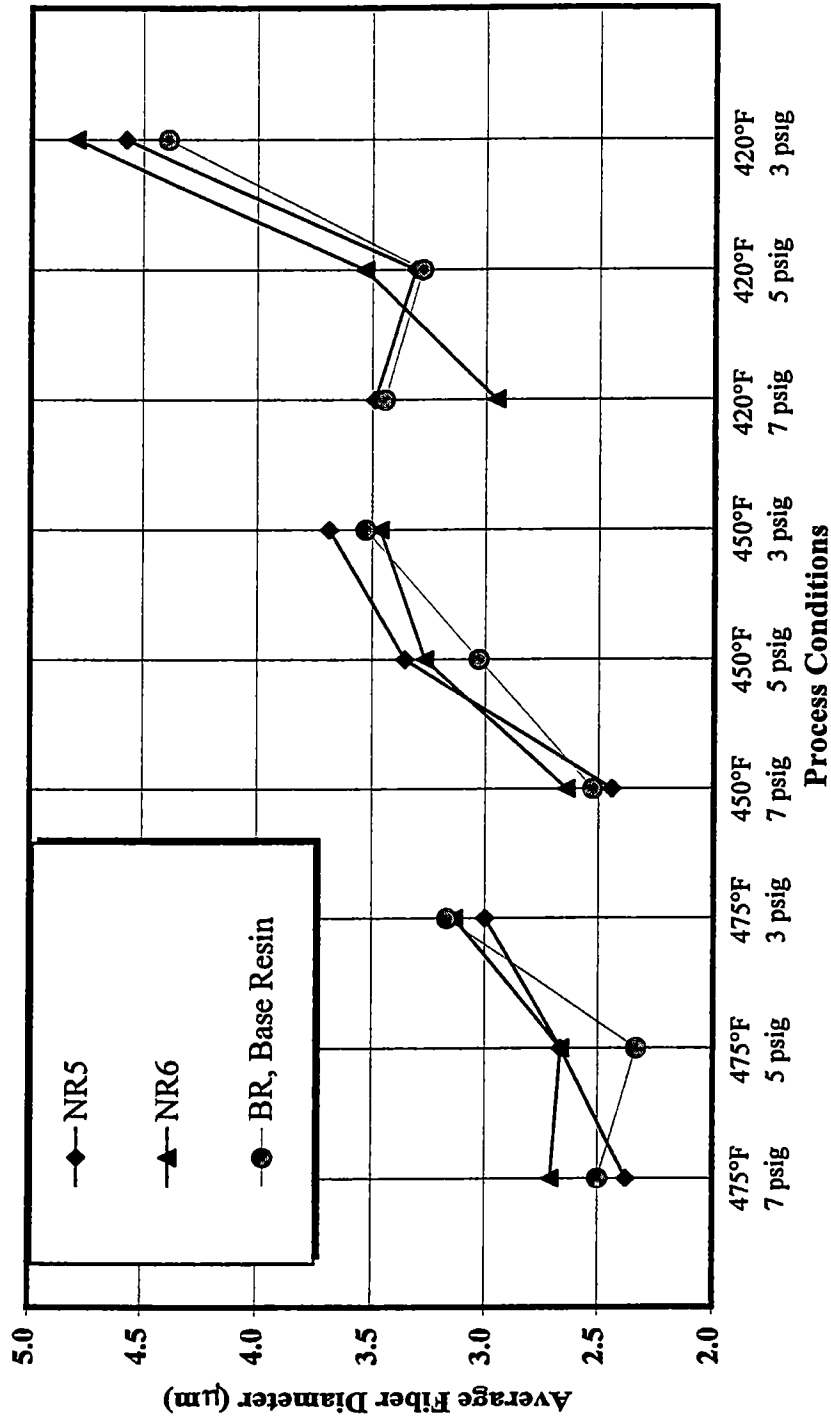


Figure 4.14 Average Fiber Diameter vs. Process Conditions
(30 hole die, 0.8 grams/min./hole, 16" DCD)

each of the nucleated resins and the base resin. The DSC measures the time required for crystallization in a quiescent cooling environment. **Figure 4.15** indicates that the addition of the nucleated agent in various percentages did indeed change the quiescent crystallization kinetics. **Figure 4.15** is a plot of crystallization half-time versus environmental temperature at which crystallization occurs for an isothermal quiescent process. This figure indicates that the nucleated resins, for the most part, have a shorter crystallization time than that of the base resin. Also, **Figure 4.15** indicates that the half-times for a constant environmental temperature decrease as the percentage of nucleating agent is increased. Recall that the resins NR1, NR2, NR3 and NR4 utilize the sodium benzoate nucleating agent in increasing percentages. The NR4 resin has the highest percentage of sodium benzoate at levels twenty times that of the NR1 resin. Therefore it is understandable why the NR4 half-time curve in **Figure 4.15** is so displaced from that of the other resins. This figure also indicates that the Millad nucleating agent used in the NR5 and NR6 resins was not nearly as effective as its sodium benzoate counterpart.

Table 4.2 shows the non-isothermal thermal characteristics of the different resins, the peak crystallization temperature and the heat of fusion of the different resins. As the percentage of the nucleating agent increases, the peak crystallization temperature increases. The peak crystallization temperatures and the heats of fusion of the different metallocene resins are lower than those of the conventional resins as can be seen from this table (except for NR3 and NR4). The lower crystallization temperatures of the metallocene resins is attributed to the higher fold surface free energies compared to that

Isothermal Crystallization Kinetics of the Different Resins

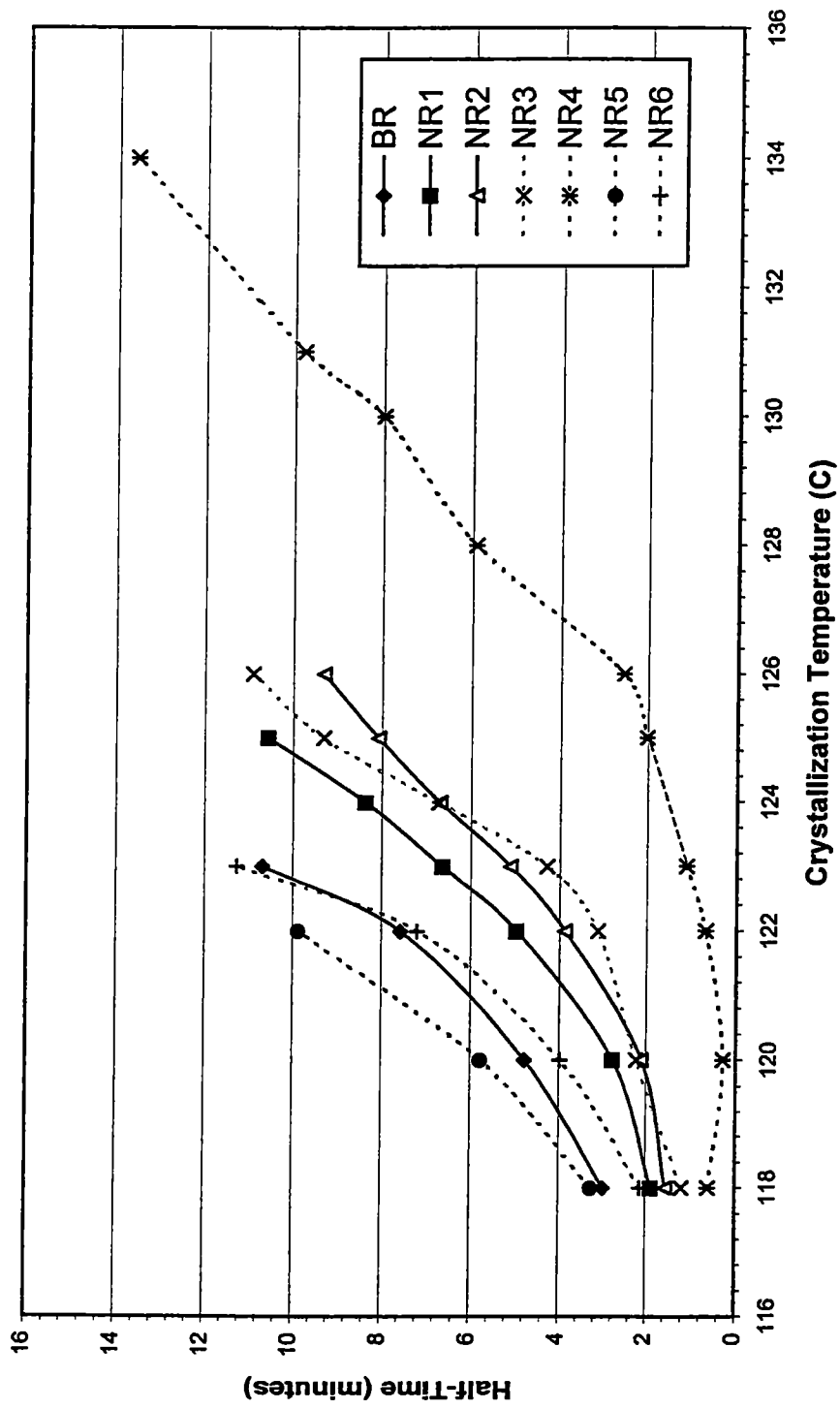


Figure 4.15 Half-Time vs Crystallization Temperature Of The Different Resins

Table 4.2: Non-isothermal Thermal Characterization of the Different Nucleated Agent Resins

Code	Resin	MFR	Crystallization Temperature (°c)	Heat of Fusion (J/g)
BR	Metallocene Base Resin	700-800	102.9	93.4
NR1	500 ppm Na Benzoate	653	105.9	91.2
NR2	1000 ppm Na Benzoate	653	106.9	96.4
NR3	1500 ppm Na Benzoate		108.6	94.9
NR4	10000 ppm Na Benzoate		112.8	94.8
NR5	500 ppm Millad		103.1	94.0
NR6	1000 ppm Millad		104.3	93.5
ZN1200	Ziegler-Natta catalyst	1200	108.0	104.4
ZN1500	Ziegler-Natta catalyst	1500-1600	108.7	106.8
ZN700	Ziegler-Natta catalyst	700-800	108.1	104.5

of Ziegler-Natta resins. The higher fold surface free energies are suggested to be due to segregation of the chain defects to the fold surfaces of the lamellae [40].

The shot data indicates that the addition of a nucleating agent in the provided concentrations does very little to affect the shot production of the BR metallocene base resin. The conclusions drawn from this nucleating agent investigation are as follows:

- The addition of nucleating agent does affect the crystallization kinetics of the base resin in a quiescent environment in the desired manner for the sodium benzoate nucleating agent. The Millad agent demonstrated relatively little effect (compared to sodium benzoate) on the base resin crystallization kinetics in the same quiescent conditions.
- The nucleating agents have little effect on shot production during the highly dynamic fiber attenuation period.

With both investigations in mind, it is apparent that shot production is more complicated than what it was thought. It is apparent that other factors are affecting shot production in the highly dynamic environment of the melt blowing process. One of those other factors that emanates from the first investigation of the thesis, the blends of the metallocene and Ziegler-Natta polypropylenes, is the effect of the molecular weight

distribution and its possible correlation with shot production. Ziegler-Natta or conventional resins have broader molecular distributions than their metallocene counterparts. The high tail of the molecular weight distribution of the conventional resins could be correlated to the reduced shot production of these resins. Furthermore, broader molecular weight distributions are more susceptible to stress-induced crystallization as a result of the high molecular weight tails in the distribution providing a source of 'row nuclei' which seed the stress-induced crystallization [70].

The following section is a test done on different fabrics to compare the differences in molecular weights and molecular weight distributions in these different webs fabricated from different resins. The molecular weights and molecular weight distributions of the different fabrics were measured using the gel permeation chromatography technique (GPC) performed at Exxon Baytown Polymer Center.

4.3 Molecular Weights and Polydispersity Results

Figure 4.16 shows the number average molecular weight of the different webs versus the processing temperature, which is the most important factor influencing the different molecular weights and molecular weight distributions. It can be seen that the number average molecular weight of the webs fabricated from the conventional (Ziegler-Natta) resins have lower number average molecular weights than those of their metallocene counterparts. Between the conventional resins, the resins with the highest

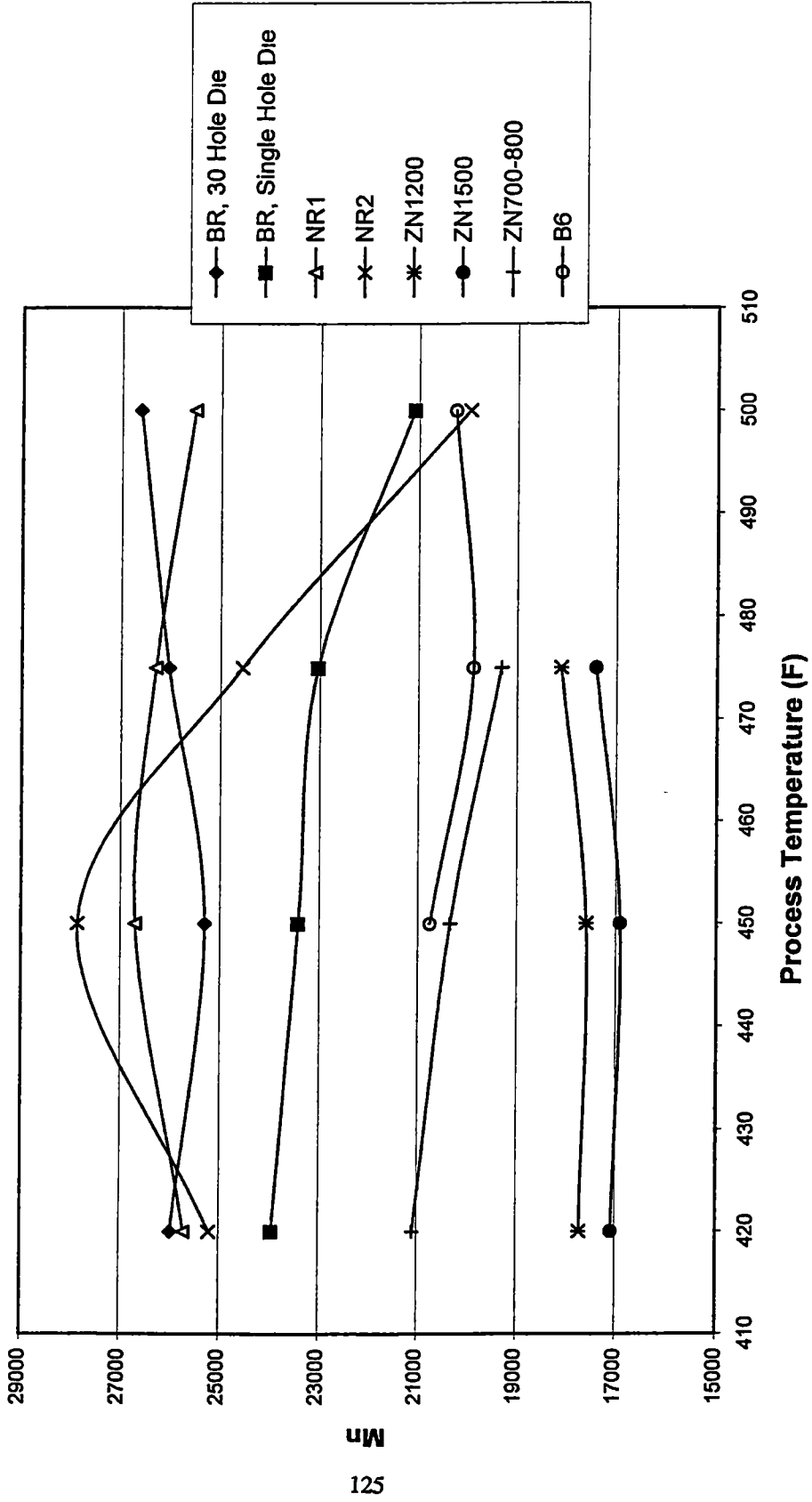


Figure 4.16 Number Average Molecular Weight
 (5 psig die pressure, 0.8 grams/min./hole, 16" DCD)

melt flow rates produced lower number average molecular weight fabrics, which can be attributed to the correlated changes between MFR, viscosity and molecular weight. The three curves in **Fig.4.16** of the base metallocene resin and the nucleated resins have comparable number average molecular weights. When comparing the effect of the number of die holes, **Fig.4.16** shows that the multi-hole (thirty- hole die) fabric has higher number average molecular weights than that of the single hole die fabric of the same resin. This is likely related to longer residence time at elevated temperature in the extruder resulting in greater degradation of the resin.

Figure 4.17 shows the weight average molecular weight versus the processing temperature, this figure shows similar trends as those shown in **Figure 4.16**, again the conventional resins are in the lower area of the plot and the metallocene resins in the higher area of the plot, showing that the conventional resins have lower weight average molecular weights than those of the same MFR metallocene resins. And again, the higher MFR Ziegler-Natta catalyzed resins have lower weight average molecular weights than the lower MFR ones. Comparing the effect of number of die holes, **Figure 4.17** shows the same trend of **Figure 4.16**, the 30 hole die fabrics have higher weight average molecular weights than those of the single hole fabrics.

The polydispersity, the ratio of the weight average molecular weight to the number average molecular weight, is shown in **Figure 4.18**. This figure shows that the conventional resin fabrics have higher polydispersities than those of the metallocene

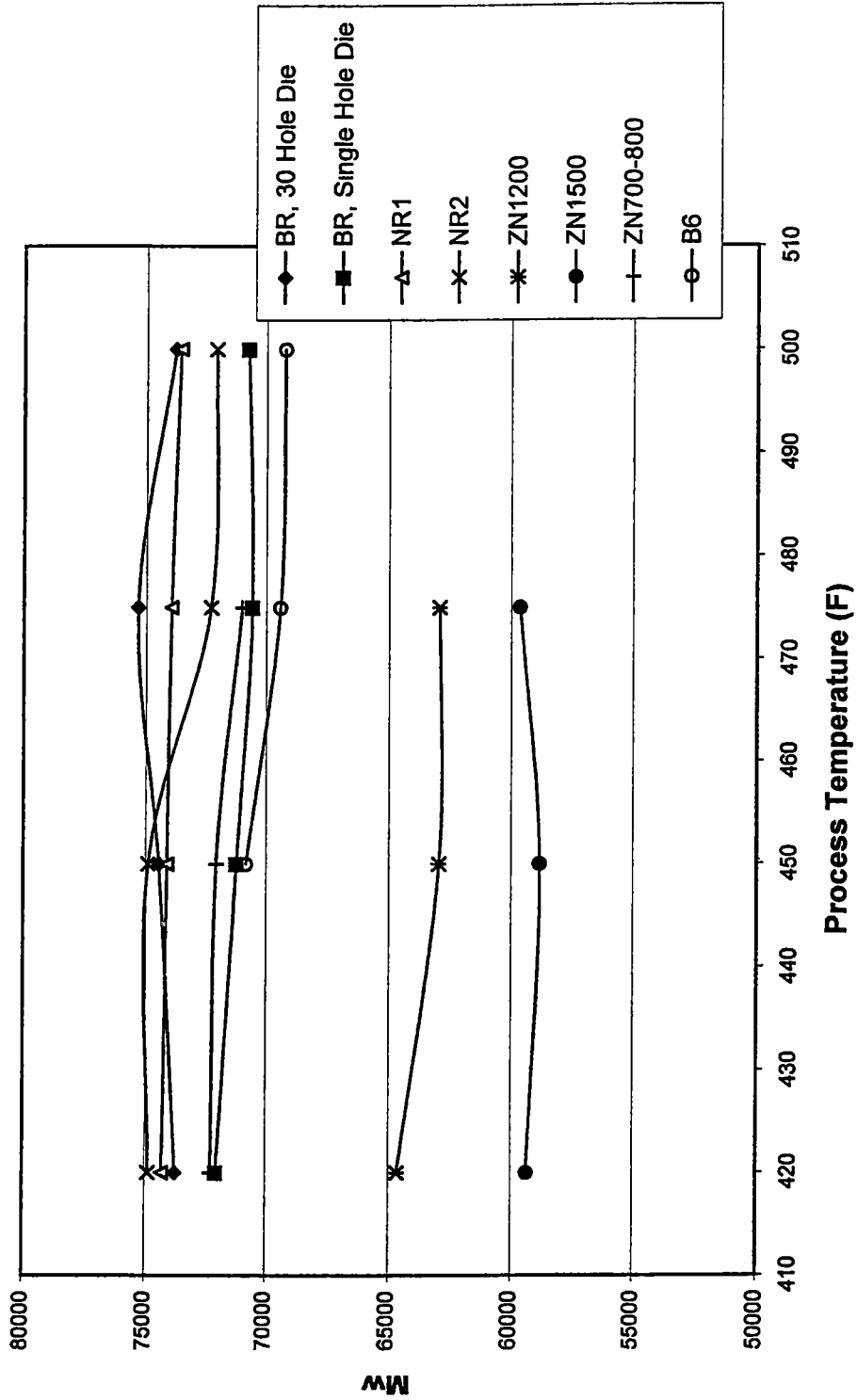


Figure 4.17 Weight Average Molecular Weight
 (5 psig die pressure, 0.8 grams/min./hole, 16" DCD)

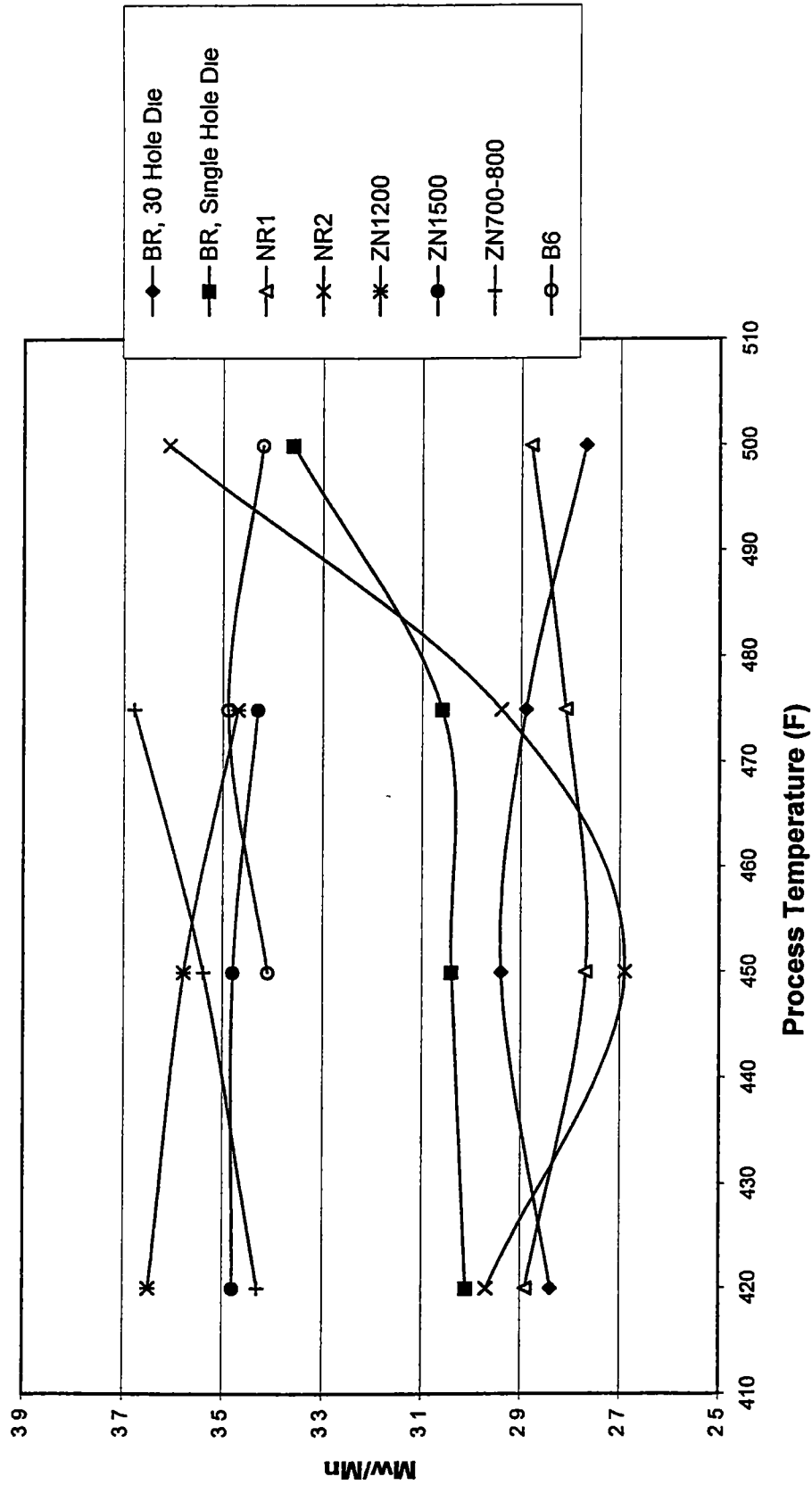


Figure 4.18 Polydispersity Or Molecular Weight Distribution
 (5 psig die pressure, 0.8 grams/min./hole, 16" DCD)

resin fabrics, which is expected because of the fact that conventional (Zeigler-Natta catalyzed) resins have broader molecular weight distributions than those of the metallocene catalyzed resins. The metallocene base resin and the nucleated resins have comparable polydispersities.

Previous work [50] was done on 300 MFR resin, the intrinsic viscosity, molecular weight, and polydispersity index of the resins and webs were measured. There was notable decrease in intrinsic viscosity, molecular weight, and polydispersity index between the resin and the webs. The decrease in molecular weight and intrinsic viscosity was about 22 to 25%. This indicated thermal breakdown or degradation of polymer chains. The decrease in polydispersity index indicated that the polymer molecular weight distribution became narrower after processing. This was anticipated because of the breakdown of longer polymer chains.

4.4 Molecular Orientation of the Fibers

The measured birefringence is an indicator of molecular orientation in the fibers. **Figure 4.19** shows the orientation or birefringence of the melt blown fibers vs fiber diameter, which is a good way to present birefringence in melt blown fibers, since we usually have a distribution of fiber diameters ranging from 2-5 μm in the melt blowing process. This figure shows that the birefringence of melt blown fibers is a function of fiber diameter; the orientation decreases as the diameter increases. It can also be seen

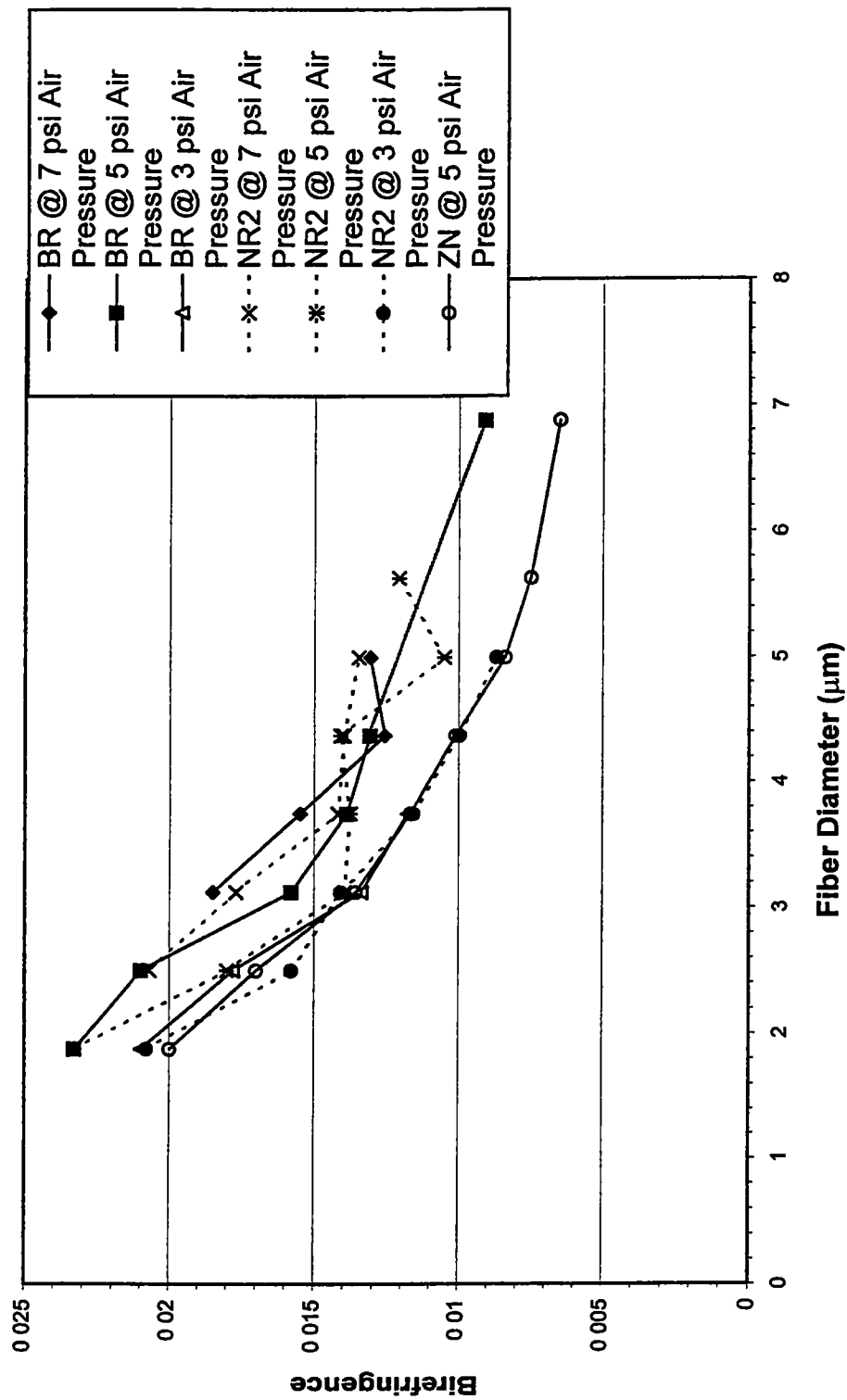


Figure 4.19 Birefringence vs. Fiber Diameter
 (30 hole die, 0.8 grams/ min./hole, 16 inches DCD)

that as the air pressure increases, the birefringence of the fibers increases. The nucleating agent does not seem to influence the orientation strongly, as **Figure 4.19** shows only a slight change of the orientation with the addition of the nucleating agent.

In addition to the above, **Figure 4.19** shows a comparison between the birefringence of melt blown fibers of the metallocene base resin and of a conventional Ziegler-Natta resin of similar MFR. The figure shows that the fibers made of the conventional resin have lower overall molecular orientation than those fibers melt blown from the metallocene resin. This is likely attributed to the formation of a bimodal crystalline structure in the broad molecular weight distribution fibers, commonly observed in polypropylenes crystallized in extensional flow. An earlier study [70] showed that metallocene catalyzed resins exhibited a lower tendency toward the formation of this bimodal texture.

Milligan [58], Malkan [50] measured the birefringence of melt blown fibers, and the values obtained were similar to those measured in this research. Malkan showed that the birefringence decreased as throughput rate increased for fibers processed at 75% air flow rate using standard orifice die. The birefringence values presented in this thesis were comparable to the values of regular melt spun fibers as reported by Lu and Spruiell [71]. Choi et al. [49] reported lower values than the values obtained in this study. The birefringence values certainly indicated that the melt blown fibers have

orientation, however, the mechanism and magnitude of forces involved in the molecular orientation of melt blown fibers is still not clear.

In the melt blowing process, the factors that are responsible for the final melt blown fiber diameter of 2 to 8 μm has perplexed earlier researchers. From the visual observation of the process, it seems intuitive that as soon as the polymer streams are extruded from the die orifices, the air continuously impinges on the polymer streams to form micro-fibers and carries them to the collector. The dependence of final fiber diameter observed in the previous figure on the air pressure is an indication of that. Other mechanisms may cause the attenuation of fibers. They include 1) the flapping motion of the fibers proposed by Milligan and co-workers [64,65]; and 2) drawing of fiber segments between entanglement points as fiber network is stressed during its flight, by Bresee and Wadsworth [72].

CHAPTER FIVE

CONCLUSIONS AND FUTURE WORK

5.1 Conclusions

The relation between shot production, average fiber diameter and processing conditions has been studied by a few researchers. The following first five conclusions are verification of previous experimental observations that have been concluded in the present study as well:

- 1- Shot production increases with increasing die air pressure (air velocity) for a constant process temperature and polymer throughput.
- 2- Shot production increases with increasing process temperature for a constant die air pressure and polymer throughput.
- 3- Average fiber diameter decreases with increasing die air pressure (air velocity) for a constant process temperature and polymer throughput.
- 4- Average fiber diameter decreases with increasing process temperature for a constant die air pressure and polymer throughput.

- 5- There is an inverse relationship between shot production and average fiber diameter processing trends. The same process parameter that produces small fiber diameters aid in the production of shot for constant polymer throughput.

In addition to the above conclusions, the following important items were also concluded in the present research:

- 6- The early generation commercial metallocene base resin used in this research produced more shot than the conventional Ziegler-Natta resin with all other parameters being constant. Therefore, it might be implied that the narrower molecular weight distribution of the metallocene resins used in this study does not produce less shot than that of the standard conventional broader molecular weight distribution resins.
- 7- Blending of the Ziegler-Natta resin with the metallocene resin tended to reduce the level of shot produced. The reduction occurred approximately in proportion to the amount of Ziegler-Natta resin added.
- 8- The addition of a nucleating agent has little effect on the number of shot, indicating that crystallization kinetics is probably not a very significant factor in causing the differences in shot formation between metallocene and Ziegler-Natta resins.

- 9- The nucleating agent had no appreciable effect on the birefringence of the melt-blown filaments.
- 10- Orientation increased slightly as a function of air pressure, and decreased as the fiber diameter increased.
- 11- The metallocene melt blown fibers had higher overall molecular orientation than those of the Ziegler-Natta fibers.
- 12- A smectic phase is observed in the melt blown fibers before the fibers reach the collector, and an α -crystalline phase is observed in the fabrics or fibers after being collected.
- 13- Average fiber diameter measurements performed with an optical microscope, scanning electron microscope and the WebPro diameter analysis were comparable in that the fiber diameter trends were the same for each procedure.
- 14- The WebPro shot analysis method worked very well for web samples that possessed fine fibers and were produced at an optically opaque basis weight. For a given basis weight the web samples with fine fibers were very dense optically and light would pass through any shot particle much easier than through the surrounding fine fibered web. This type of web would tend to produce very reliable and repeatable shot analysis results. However, webs with larger fibers would not be as optically dense

and allow much more light transmittance than that of the fine fibered webs. This light transmittance could be (and quite often is) interpreted by WebPro as a shot particle.

5.2 Future Work

- 1- Further investigation of the effects of molecular weight distribution on shot production and stress induced crystallization, an important fact that emanated from the study of the effect of blending metallocene and Ziegler-Natta resins on shot production.
- 2- On-line high speed image analysis of the shot formation and the motion of fibers in the melt blowing process. High speed image analysis is already underway in our labs using a high speed image analysis system on the pilot melt blowing line located at Dougherty engineering building.
- 3- Study of the die swell of the different resins and the different dies used in the melt blowing process and the correlation of die swell to average fiber diameter and possible implications on shot formation.
- 4- Further study of the crystal structure development in the melt blown fibers from the die to the collector.

- 5- Investigating the fiber temperature variation over DCD This will give an indication of the speed of the cooling process and the changes in the fiber temperature over DCD for the different resins and the different processing temperatures.
- 6- Study of the melt spinning behavior of the blend resins in a quest to have a better understanding of the process of melt blowing and shot formation, since the fiber spinning process is more controllable and understood. In order to do that, a smaller diameter die has to be used since the resins used in the melt blowing process are high melt flow rate resins and they drain in a capillary at relatively low temperatures.
- 7- Study of the rheology of the melt blowing resins, including the shear and elongational viscosity.
- 8- Study and develop techniques to study stress induced crystallization in the melt blowing process. As mentioned earlier, one of the obstacles faced in the melt blowing process is the disability of getting as-blown fibers before they are laid on the collector to form a web. Knowing the magnitude of forces experienced by the melt blown fibers in addition to the magnitude of stress induced crystallization in these fibers will be of great importance to understanding the process and the properties of the final products.

List of References

List of References

1. Malkan, S.R, ' A Review on Melt Blowing Technology', INB Nonwovens, 2/91, p.46.
2. Malkan, S.R., Nonwovens : An Advanced Tutorial, Turbak, A.F. and Vigo, T.L., Editors, Tappi Press, Atlanta, USA, 1989, p. 101-129.
3. Milligan, M.W. and Utsman, F., International Nonwovens Journal, 7(2)· 65 (1995).
4. Wentz, V.A., United States Department of Commerce, Office of Technical Services Report No. PB111437, NRL 4364, April 15, 1954.
5. Buntin, R.R. and Lohkamp, D.T.: Tappi, V. 56, No. 4, 1973, pp. 74-77.
6. Milligan, M.W. and Haynes, B.D., J. Nonwovens Research, V.3, 1991, pp. 20-25.
7. Malkan, ' Advancements in Polyolefin Resins for Polymer-laid Nonwovens', Hi-Per Fab, 96 conference, Singapore, April 24-26,1996.
8. Maria R. Ribero, ' Supported Metallocene Complex for Ethylene and Propylene Polymerization: Preparation and Activity', Industrial Engineering Chemistry Research, V36, 1997, p.1224.
9. Anonymous, Polypropylene will be next wave of Metallocene-catalyzed Polyolefins, Plastics Technology, Aug. 1994, p.19.
10. Porter, K., Physics in Technology, V. 8, No.9,1977, pp.204-212.
11. American Society for Testing and Materials : Annual Book of Standards, Philadelphia, Pennsylvania, 1989.
12. Hearle, J.W.S., Textile Institute and Industry. Volume 5, No. 8, 1967, pp. 232-261.
13. Dahlstorm, N., Melliand Textilberichte, Volume 68, No.6, 1987, pp. 381-383.
14. www.nonwovens.com, Miller Freeman Paper Newsgroup, San Fransisco, CA, July 1998.
15. Ahmed, M., Polypropylene Fibers Science and Technology, Elsevier Scientific Publishing Company, New York, 1982, pp. 434-448.

16. Till, D.E. : Modern Textiles Magazine, No.10, 1959, pp. 36-44.
17. Mansfield, R.G., Textile World, No.2, 1979, pp.83-84.
18. Newton, A. and Ford, J.E., Textile Progress, Volume 5, No.3, 1973, pp. 57-59.
19. Wadsworth, L.C. and McCulloch, W.J.G., Meltblown Technology Today, Miller Freeman Publications, San Francisco, 1989, pp.28-40.
20. Anonymous, Meltblown Technology Today, Miller Freeman Publications, San Francisco, 1989, pp.7-12.
21. Ahmed, K.Y.A., PhD Dissertation, University of Tennessee, Knoxville, 1993.
22. Jana, P., Masters thesis, University of Tennessee, Knoxville, 1998.
23. Frank Kuber, Dreams of the Perfect Plastic, New Scientist, Aug. 14, 1993, p 28-31.
24. McAlpin, A., Impact of Metallocene based Propylene Polymers on Nonwovens, Nonwovens World, Summer 1996, p 82.
25. Cheng, C.Y., ' Processing Characteristics of Metallocene Propylene Homopolymer', TANDEC conference, Knoxville, TN, 1997.
26. Brookman, R.S., Plastics Engineering, Oct. 97, p.35-37.
27. Ecstat, M., 'Metallocene- the new wave', chemical engineering, sept. 1996, p 92.
28. Morrow, D R., J. Macromolecular Science, Physics Edition, V. B3, No.1, 1969, pp. 53-65.
29. Lotz, B., Wittman, J., Lovinger, A., Polymer, 37, 4979 (1996).
30. Natta, G., Corrandini, P., Suppl. Nuovo Cimento, 15, 40 (1960).
31. Meille, S., Ferro, D., Bruckner, S., Lovinger, A., Padden, F., Macromolecules, 27, 2615 (1994).
32. Lovinger, A. Chua, J., Bryte, C., J. Polymer Sci. Phys., 15, 641, (1977).
33. Keith, H., Padden, F., Walter, N. Wychoff, H., J. Appl. Phys., 20, 1485 (1959).
34. Addink, E., Berentena, T., Polymer 2, 185 (1961).

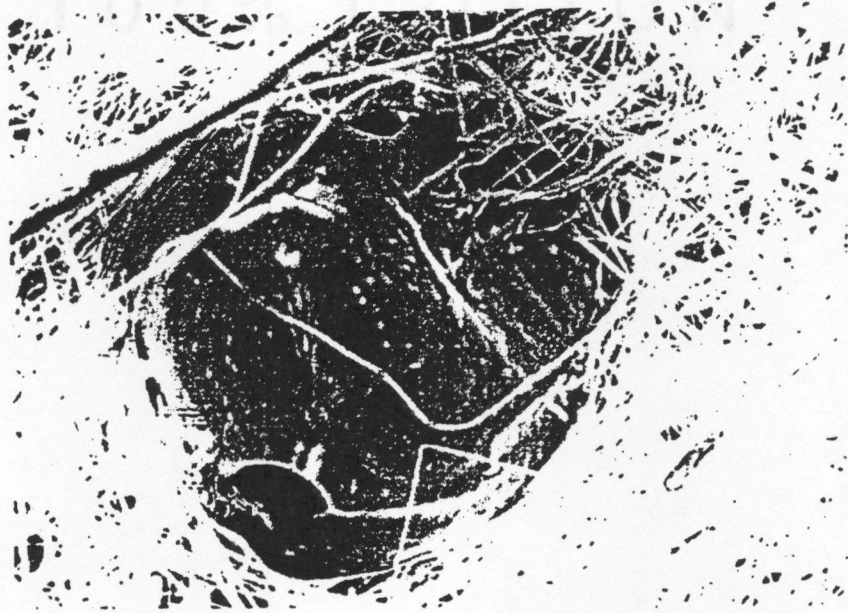
35. Turner-Jones, A., *Polymer* 12, 487, (1971).
36. Mezghani, K., Phillips, P., *Polymer*, 36, 2407 (1995).
37. Miller, R., *Polymer*, 1, 135 (1960).
38. Osawa, S., Porter, R., *Polymer*, 35, 545 (1994).
39. Wang, G.H., *Zeitschrift Fuer Physik. B. Condensed*, V. 65, No.3, 1987, pp. 347-351.
40. Bond, E.B., Spruiell, J.E., Lin, J.S., *J. Polymer Science, Part B, Polymer Physics*, V.37, 3050-3064 (1999)
41. Moore, G.K., *Meltblown Technology Today*, Miller Freeman Publications, San Francisco, 1989, pp. 150-158.
42. Wente, V.A., *Industrial and Engineering Chemistry, Volume 48*, 1956, pp.1342-1346.
43. Jones, A.M., *Book of Papers, fourth international conference on Polypropylene fibers and textiles*, Nottingham, England, Sept. 23-25, 1987, pp.47.1-47.10.
44. Wadsworth, L.C. and Jones, A.M., *Book of Papers, INDA-TEC*, Philadelphia, Pennsylvania, June 2-6, 1986, pp. 312-320.
45. Jones, A.M. and Wadsworth, L.C., *Tappi Proceedings*, Atlanta, Georgia, April 21-24, 1986, pp. 23-30.
46. Eaton, G.M., *Book of Papers, INDA-TEC*, Hilton Head, South Carolina, USA, May 18-21, 1987, pp.221-231.
47. Eaton G.M., *Book of Papers, The Pira Paper and Board Fibramerics Programme, Volume 1, International Conference on Nonwovens in Medical and Healthcare Applications*, Brighton, England, November 10-12, 1987, p. 1-19.
48. Wadsworth, L.C., *Book of Papers, INDA-TEC*, Philadelphia, Pennsylvania, USA, May 30-June 2, 1989, pp. 585-600.
49. Choi, K.H., Spruiell, J.E., Fellers, J.F. and Wadsworth L.C., *Polymer engineering and Science*, Volume 28, No.2, 1988, pp. 81-89.
50. Malkan S.R., PhD. Dissertation, University of Tennessee, Knoxville, p.12 (1990).

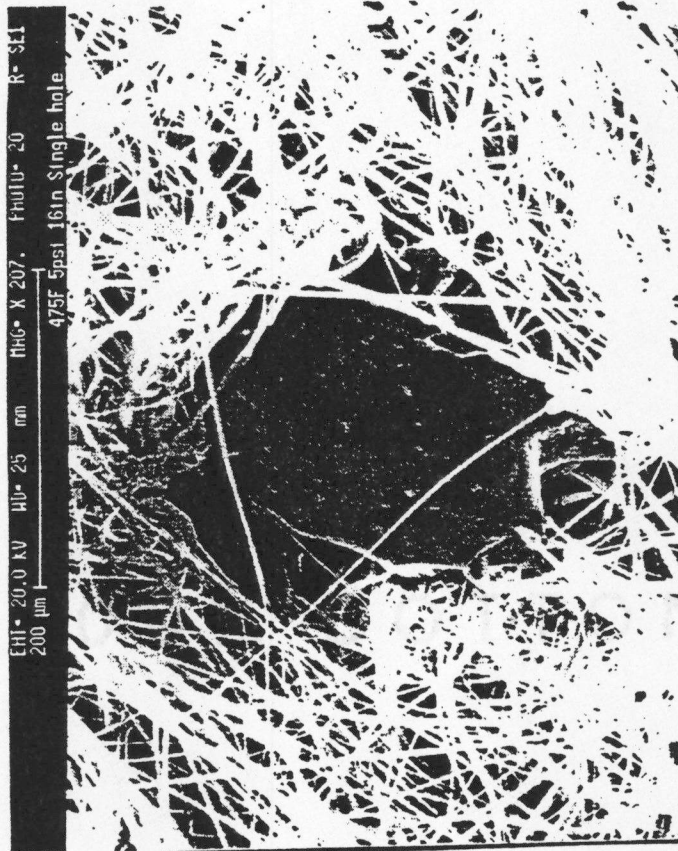
51. Bodaghi, H., Book of Papers, INDA-TEC, Philadelphia, Pennsylvania, USA, May 30-June 2, 1989, pp 535-571.
52. Narasimahan, K.M. and Shambaugh, R.L., Book of Papers, INDA-TEC, Hilton Head, South Carolina, USA, May 18-21, 1987, pp.189-205.
53. Shambaugh, R.L., Industrial Engineering Chemistry Research, Volume 27, No.12, 1988, pp. 2363-2372.
54. Shambaugh, R.L., Book of Papers, 58th Annual Meeting, Society of Rheology, Tulsa, Oklahoma, 1986.
55. Milligan, M.W., Nonwovens: An advanced Tutorial, Turbak, A.F. and Vigo, T.L., Editors, Tappi Press, Atlanta, USA, 1989, P. 101-129.
56. Milligan, M.W., Book of Papers, INDA-TEC., Philadelphia, Pennsylvania, USA, May 30-June 2, 1989, pp. 573-583.
57. Milligan, M.W., American Society of Mechanical Engineers, Volume 54, pp. 47-50.
58. Milligan, M.W., Lu, F., Buntin, R.R., and Wadsworth, L.C., J. Appl. Polym. Sci., V.44, 279-288 (1992).
59. Wadsworth, L.C., Book of Papers, INDA-TEC, Philadelphia, PA, May 30-June 2, 1989.
60. Straeffer, G. and Goswami, B C., Book of Papers, INDA-TEC 90, Association of Nonwoven Fabric Industry, Cary, NC, pp.385-419 (1990).
61. Warner, S.Z., Perkins, C.A., Abhraman, A.S., Melt blown PP fibers, INDA JNR, Volume 2, No.2, 1990, p33.
62. Wallen, J., Fellers, J.F., and Milligan, M.W., International Nonwovens Journal, 7(3): 51(1995).
63. Bresee, R.R. and Yan, Z., Journal of Textile institute, 1998, 89, Part I, No.2, pp.304-319.
64. Utsman, F., M. Master's thesis, University of Tennessee, Knoxville, 1995.
65. Haynes, B.D, Ph.D., Dissertation, University of Tennessee, Knoxville, 1991.
66. Spencer, E.G., Master's thesis, University of Tennessee, Knoxville, 1994.

67. Stein, R.S., Norris, F.H., J. Polymer Science, 21, 381 (1956).
68. Cullity, B.D., X-ray Diffraction, 2nd Edition, Addison Wesley, Reading 1977.
- 69 Bond, E.B., Ph.D. Dissertation, University of Tennessee, Knoxville, 1998.
70. Misra, S., Lu, F.M., Spruiell, J.E., and Richeson, G.C., J. Applied Polymer Science, V.56, 1761-1779 (1995).
71. Lu, F.M., Spruiell, J.E., J. Applied Polymer Science, V.34, 1521-1539 (1987); Ibid. pp 1541-1556.
72. Bresee, R.R. and Wadsworth, L.C., Books of Papers, Exxon Melt Blown Seminar, Baytown, Texas, September, 1988, pp 15-16.
73. Milligan, M.W., " A Model for Shot Formation in Meltblown Webs", TANDEC 1993, Conference Proceedings, Knoxville.

APPENDIX

SEM Images of Shot Particles and Melt Blown Fibers

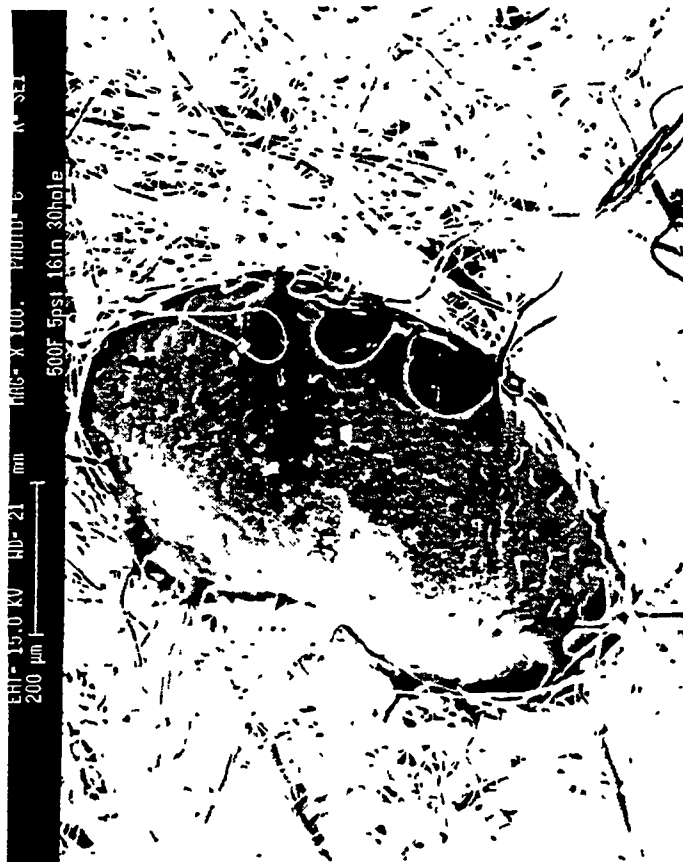


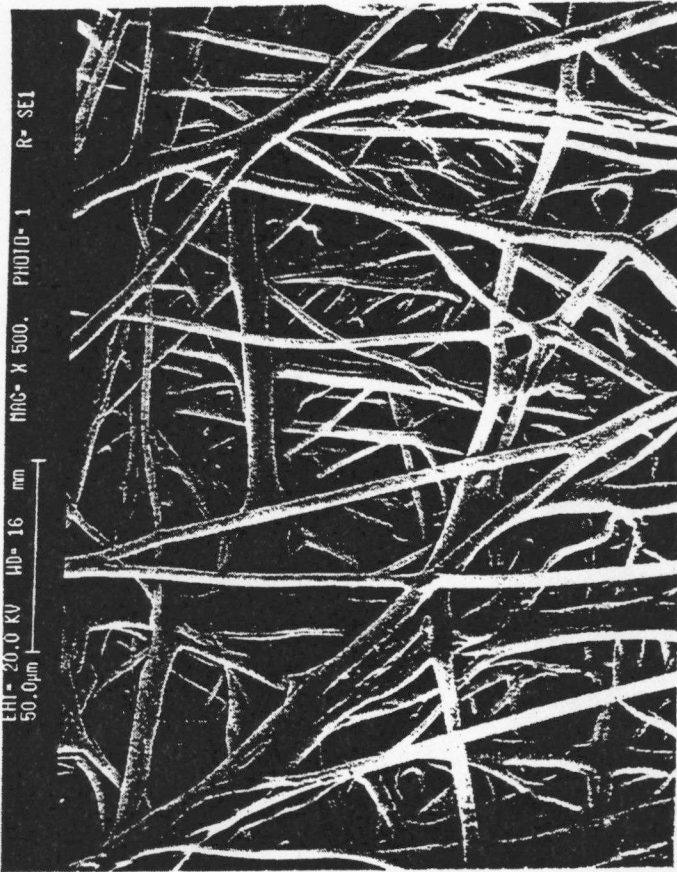


GILBERT

100% COTTON







VITA

Imad M. Qashou was born in Tripoli, Libya in January 1972. He attended Yarmouk University in Jordan where he received a Bachelor of Science in Physics and a Minor in Statistics in May 1992. In August, 1993, he joined the physics department at the University of Tennessee, Knoxville, and received a Master of Science in Physics in Dec. 1996. He continued his graduate studies at the department of material sciences and engineering at the University of Tennessee, Knoxville, and received a Master in Science in Polymer Engineering in May of 2000.